Current Status of Eutrophication in the Belgian Coastal Zone

Edited by
Rousseau V., Lancelot C. and D. Cox

Current Status of Eutrophication in the Belgian Coastal Zone

Edited by

Véronique Rousseau
Université Libre de Bruxelles, Belgium

Christiane Lancelot
Université Libre de Bruxelles, Belgium

David Cox
Belgian Science Policy

Presses Universitaires de Bruxelles
Avenue Paul Héger 42
1000 Bruxelles
Belgique

N° dépôt légal : D/2006/1191/45

Cover illustration:
Phaeocystis foam on beach, Oostende, May 1998, V. Rousseau

Contents

Acknowledgement

The authors of this book are indebted to the many people who contributed to improve their knowledge of the BCZ ecosystem. The captains and crew of R.V. Belgica and Zeeleeuw are warmly thanked for their help in many sampling occasions.

Fellow colleagues from marine institutions are acknowledged for fruitful collaboration, in particular F. Lantoine and M.-J. Chrétiennot-Dinet (Observatoire de Banyuls sur Mer, France) for microphotographs of *Phaeocystis* morphotypes; Yvette Spitz from Oregon State University at Corvallis (USA) for her contribution to the development of the ecological model MIRO during the AMORE I and II projects; Gilles Billen, Josette Garnier and Vincent Thieu for providing RIVERSTRAHLER simulations of Seine, Somme and Scheldt nutrient loads.

L. van Ijzerloo, P. van Rijswijk, D. Van Gansbeke, A. Van Kenhove, B. Beuselinck and D. Schram are thanked for technical assistance in research.

Introduction

The Belgian Coastal Zone (BCZ) located in the Southern Bight of the North Sea is largely eutrophied due to riverine, atmospheric and transboundary inputs of land-based nutrients which modify both quantitatively and qualitatively the coastal environment. As in many other marine coastal areas over the world, eutrophication in the BCZ results in the excessive development of undesirable phytoplankton species. These blooms affect negatively the marine ecosystem inducing structural changes in the planktonic foods webs and impacting the services and goods provided by the coastal ecosystem.

Since the seventies, the Belgian Science Policy has initiated and financed research programmes devoted to the study of the North Sea ecosystem. The goal of these programmes is to enhance the knowledge on this ecosystem and to stimulate its sustainable management and exploitation. In the frame of these successful programmes special attention was given amongst others to research activities on marine coastal eutrophication. In 2002, the Belgian Science Policy launched the "Second Scientific Support Plan for a Sustainable Development Policy - Sustainable Management of the North Sea" (SPSD-II-North Sea) for stimulating science-based political decisions with respect to the North Sea management. Marine eutrophication was considered as top priority and three projects, adressing each of them eutrophication-related questions, were funded for a four-year period. These were SISCO (Silica Retention in the Scheldt Continuum and its Impact on Coastal Eutrophication), AMORE (Advanced MOdelling and Research on Eutrophication) and CANOPY (Carbon, Nitrogen and Phosphorus biogeochemical cycling in the North Sea) investigating the Scheldt nutrient inputs to BCZ, algal blooms and their modeling in response to nutrient changes and biogeochemical cycles, respectively.

The cluster COMETS (COMmunicating advanced progress in coastal Eutrophication To Stake holders and the scientific community) was then built on these three projects as a joint effort for transferring new scientific knowledge towards the scientists, public authorities and policy makers.

As a product of the COMETS activities, the present book "Current Status of Eutrophication in the Belgian Coastal Zone" offers to scientists, public authorities and policy makers a synthesis of current knowledge on eutrophication mechanisms in the BCZ. The book is organized in chapters covering different aspects of eutrophication.

The first chapter summarizes the physical oceanography of the BCZ as relevant to eutrophication dynamics. It describes the meteorological conditions prevailing in the area and how they are constraining the water mass circulation including the feature of river plumes.

Chapter 2 identifies and quantifies the riverine and direct freshwater, atmospheric and river-enriched Southwesterly Atlantic nutrient fluxes delivered

to the BCZ, and resulting quantitative and qualitative changes of the BCZ nutrient environment.

Chapter 3 focuses on the spreading of phytoplankton blooms in the BCZ, explaining how the peculiar biology and eco-physiology of one species make it particularly well adapted to anthropogenic nutrient enrichment of the BCZ waters.

Chapter 4 examines to which extent the phytoplankton production stimulated by land-based sources of nutrients impact zooplankton dynamics and the trophic efficiency in the BCZ.

Chapter 5 investigates the response of the benthic organisms to sedimentation of phytoplankton-derived material by studying the biogeochemical patterns and processes prevailing in two contrasted types of sediments of the BCZ.

Chapter 6 shows how mechanistic mathematical models are useful to provide scientific support to decision makers for evaluating the impact of nutrient reductions on the spreading of algal blooms in the BCZ.

Finally, Chapter 7 focuses on the impact of eutrophication on the CO_2 dynamics in the BCZ and assesses the evolution of the system over the last 50 years owing to model reconstruction.

CHAPTER 1

Hydrodynamics and meteorology of the Belgian Coastal Zone

Kevin Ruddick and Geneviève Lacroix

Management Unit of the North Sea Mathematical Models (MUMM)
Royal Belgian Institute for Natural Sciences (RBINS), Gulledelle 100
B-1200 Brussels, Belgium.

1.1 Physical oceanography of the Belgian coastal zone: parameters, time and space scales

This chapter describes the physical environment of the Belgian coastal zone (BCZ) as the framework in which eutrophication processes may occur. In addition to the bathymetry, which provides the geometrical constraints for all physical and biological processes, the most relevant physical oceanographic parameters are:

- currents, which advect nutrients and phytoplankton, and turbulent diffusion, which mixes both dissolved and particulate constituents,
- light at the sea surface, and the diffuse attenuation of light in the water column, which control the rate of primary production and hence timing of the spring bloom,
- temperature, which controls the rate of many biological processes, and
- salinity, which does not influence eutrophication processes directly but is a useful diagnostic tracer for water masses, in particular for regions influenced by freshwater inputs.

All these oceanographic parameters are themselves influenced by meteorological processes (wind, clouds and other atmospheric constituents with optical or thermal properties, rain and evaporation) in addition to the tidal effects generated by astronomic gravitational fields. The chain of impacts from meteorology to physical oceanography to biology is illustrated in Figure 1.1.

Regarding time scales, this book focuses on eutrophication processes and hence is mainly concerned with the annual cycle of biology as driven by the annual cycle of light and heat. Interannual variability of this forcing and the associated wind and rainfall which modulate the annual cycle are of particular interest because observed interannual biological variability is thought to be

closely related to meteorologically-induced physical variability (Breton *et al.*, 2006). In addition to the long-term average and the interannual variability, higher frequency processes, such as tidal fluctuations and wind events, must also be considered insofar as they impact the long-term average.

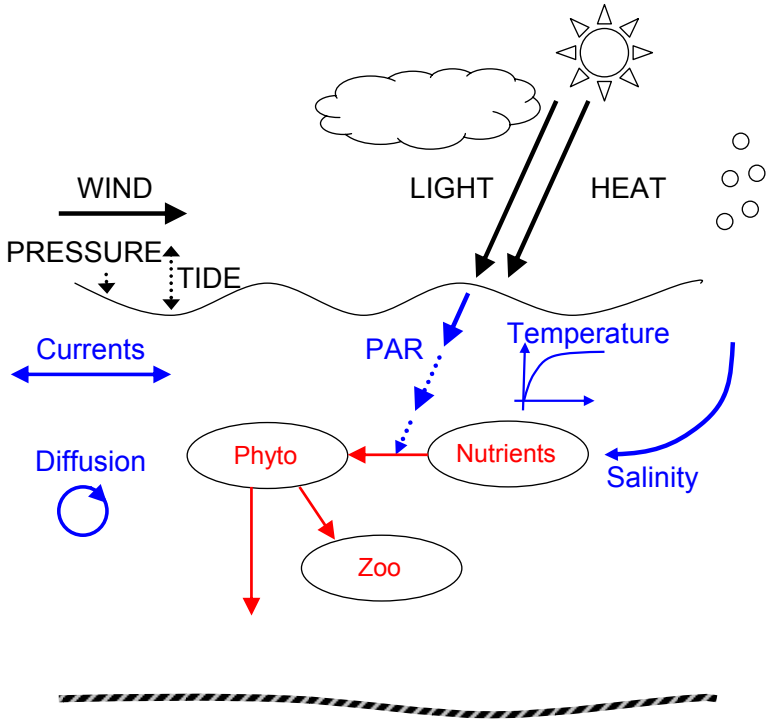

Figure 1.1. Scheme linking meteorological factors (black) with physical factors (blue), which influence the nutrient-phytoplankton-zooplankton cycle (red) by: a) currents and diffusion transporting dissolved and particulate constituents, b) temperature affecting most biological rates, c) PAR affecting photosynthetic rate, d) salinity as a tracer of nutrient-rich river water.

Regarding space scales, the focus is on the Belgian coastal waters. However, natural processes in the sea are obviously not constrained by political boundaries especially in this system with strong horizontal fluxes. This chapter will, therefore, consider also the adjacent sea areas of the Eastern Channel from 4°W and the Southern Bight of the North Sea up to 52.5°N, insofar as the larger area influences eutrophication processes in the Belgian coastal waters. This region, its bathymetry and main river discharges are shown in Figure 1.2. The focus is mainly on large scale processes, determining for example the spatial extent of eutrophication. Processes occurring at horizontal scales less than a few kilometers will not be considered in detail (and are relatively less well-known because of the lack of data and of suitable modeling tools).

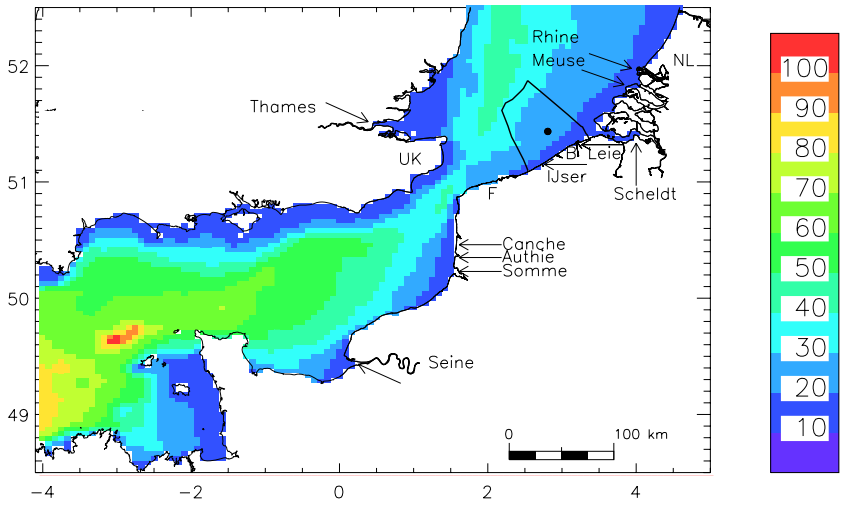

Figure 1.2. The Belgian coastal zone and adjacent marine areas, showing water depth (in metres, see colour scale), the boundaries of the Belgian coastal zone (dark lines) and the main river discharges (arrows). The monitoring station 330 is shown as a solid dot.

The Belgian coastal zone (BCZ) has a maximum alongshore width of about 65 km and extends about 87 km offshore with a surface area of about 3600 km^2. The average and maximum water depths are approximately 20 m and 45 m respectively (Maes *et al.*, 2005). In addition to the large scale gentle sloping of the sea bottom from the coast to offshore, the bathymetry is marked by many large and elongated submerged sandbanks, the Flemish Banks. These reach up to 15 km in length with crest to trough depth differences of up to 20 m, and are oriented approximately parallel to the coast (Ministerie van Openbare Werken, 1980).

1.2 Meteorology

Interannual variability of meteorological factors over the North Atlantic and Europe is highly correlated with the North Atlantic Oscillation index (NAO; Hurrell, 1995), which measures the large scale gradient between the Icelandic Low and the Azores High pressures (Fig. 1.3). This influences winds, precipitation, clouds and air temperatures. The NAO has a significant impact on the North Sea ecosystem via a number of different processes. In periods of high NAO Southwesterly winds are dominant, driving a stronger inflow of water from the Channel into the Southern North Sea (Breton *et al.*, 2006). The wind regime also affects the spreading of river plumes with Southwesterly winds (high NAO) inducing less cross-shore dispersion and greater North-Eastward dispersion of the Scheldt plume that Northeasterly winds (low NAO). High NAO is also positively correlated with rainfall over the Scheldt basin impacting the delivery of

diffuse nutrients to coastal waters (Breton *et al.*, 2006). The relationship between NAO and cloudiness has not been investigated. A long term decreasing trend has been identified in the NAO from the 1960's to the 1990's as a result of both natural variability and greenhouse gas forcing (Osborn, 2004).

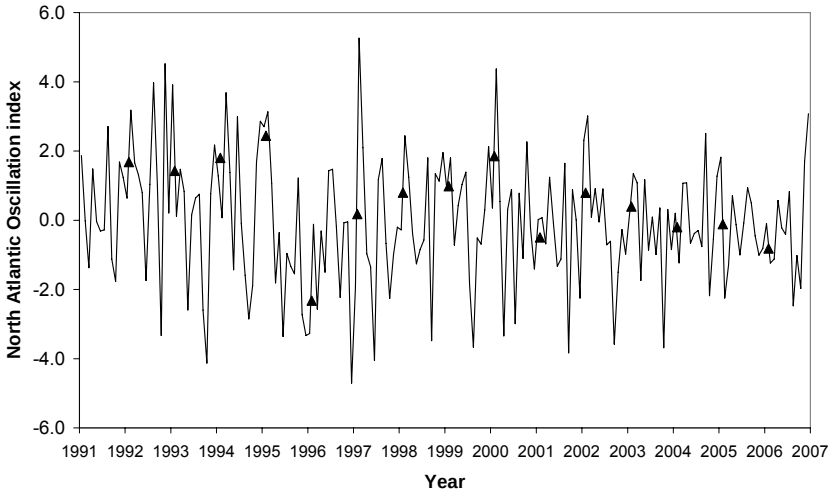

Figure 1.3. North Atlantic Oscillation index for the period 1991-2006 obtained from http://www.cru.uea.ac.uk/~timo/datapages/naoi.htm (Jones *et al.*, 1997; Osborn, 2006). Monthly mean data are given as a continuous line and the winter averages (December-March) are given as triangles.

Because of the shallow water depths in this region the impact of wind stress on currents is more significant than that of local atmospheric pressure gradients (De Vries *et al.*, 1995). Wind speed shows a significant variability at time scales of hours to days associated with the passage of low pressure atmospheric systems superimposed on an annual cycle with generally lower winds during summer (Fig. 1.4). Wind direction is also variable on similar time scales.

The Photosynthetically Available Radiation (PAR; spectral range 400-700 nm) reaching the sea surface (Fig. 1.5) varies over the annual cycle as function of sun elevation and photoperiod and at shorter time scales due to variability of clouds and, to a lesser extent, aerosols.

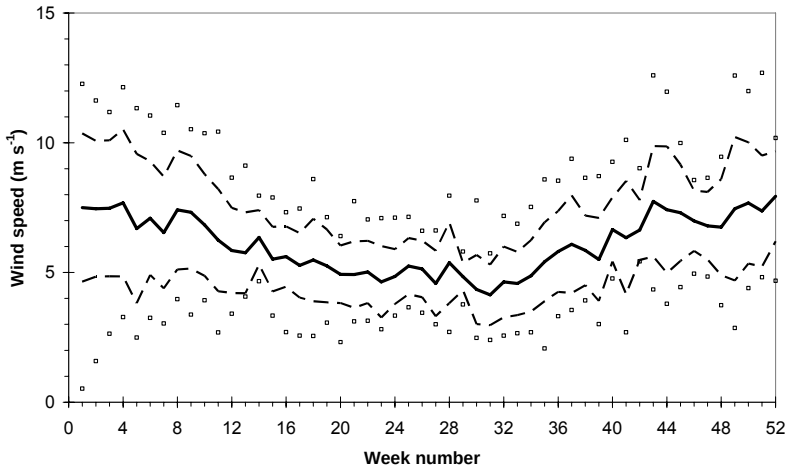

Figure 1.4. Wind speed at 10 m height above sea level at station 330 (51°26'N, 2°48.5'E) derived from data for the period 1991-2004 from UKMO model re-analysed forecasts at 6-hour resolution. Data are first averaged into 7-day bins for each year. The solid black line represents the mean average for all years. The dashed lines represent the interannual standard deviation between the 7-day average for each year and the full period average for the bin. The squares represent the maximum and minimum values of the 7-day average over the full period.

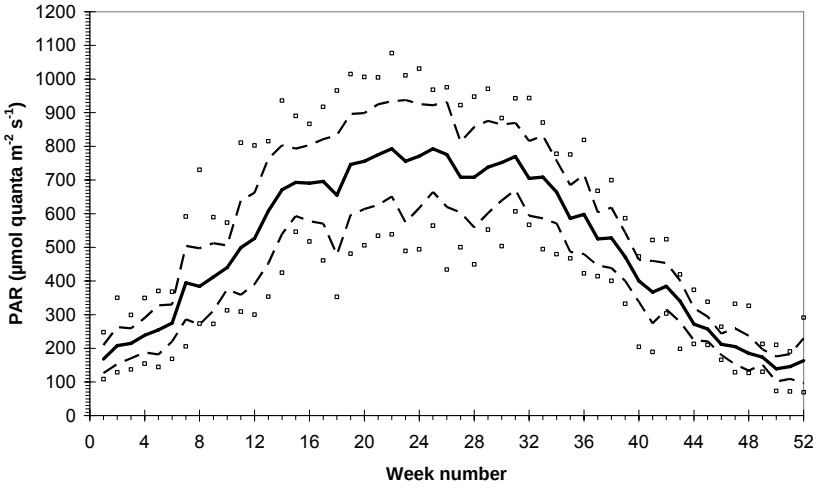

Figure 1.5. PAR averaged over the photoperiod just above the sea surface at station 330 derived from daily global solar radiation data of the Koninklijk Meteorologisch Instituut van België/Institut Royal Météorologique de Belgique for the period 1991-2004 using the empirical relationship described in Rousseau (2000). Labelling of points and lines is the same as for Figure 1.4.

The annual cycle of solar radiation and, to a lesser extent, wind speed (convective exchange and transport of Channel water) control the annual thermal cycle of the Southern North Sea and result in an annual cycle of sea surface temperature (see section 1.4).

Rainfall affects the ecosystem mainly via river discharge of freshwater and associated land-based. The main rivers in the area are, in order of importance (1991-2004 average discharge): the Rhine/Meuse (2059 $m^3 s^{-1}$), the Seine (524 $m^3 s^{-1}$) and the Scheldt (154 $m^3 s^{-1}$). The Thames does not significantly affect the BCZ (Lacroix *et al.*, 2004). The annual cycle of river discharge is characterized by higher discharge in winter and early spring (Fig. 1.6).

1.3 Currents and turbulent diffusion

The Southern North Sea is a region of strong tides with tidal currents reaching 1 m s^{-1} or more (Nihoul & Hecq, 1984; Otto *et al.*, 1990). The dominant semi-diurnal tides are modulated over the Springs-Neaps cycle by typically 10-30 %. Tidal current ellipses are elongated with the main component being alongshore, but with some changes in orientation caused by topographic features (Yang, 1998). The temporal average of tidal currents provides a net tidal residual current, typically of order about 0.01-0.1 m s^{-1}. Frequent wind events generate additional currents typically of order up to about 0.3 m s^{-1} and of duration of a few hours or days. Topographic steering orients these currents primarily alongshore (Yang, 1998). Except within river estuaries and the Rhine/Meuse plume, density gradients in this region are generally insufficient to generate significant density-driven currents.

The combination of tide- and wind-driven residual currents gives a net horizontal transport of salt, nutrients and plankton. In addition to this residual current, the horizontal dispersion caused by the oscillating tidal current is significant (Lacroix *et al.*, 2004). This dispersion is strongest in the alongshore direction and may transport salt, nutrients and plankton against the residual current.

Because of the lack of stratification and the relatively shallow water depths, the vertical variation of horizontal currents is limited as regards both direction and magnitude except within the bottom boundary layer. Vertical currents are determined primarily by topographic steering of horizontal currents, termed “upsloping” by Deleersnijder (1989), with no significant upwelling currents.

The combination of shallow water depths and strong tidal currents, enhanced by wind events, gives strong turbulent diffusion with typical modelled vertical diffusion coefficients of order 10^{-2} $m^2 s^{-1}$ or more.

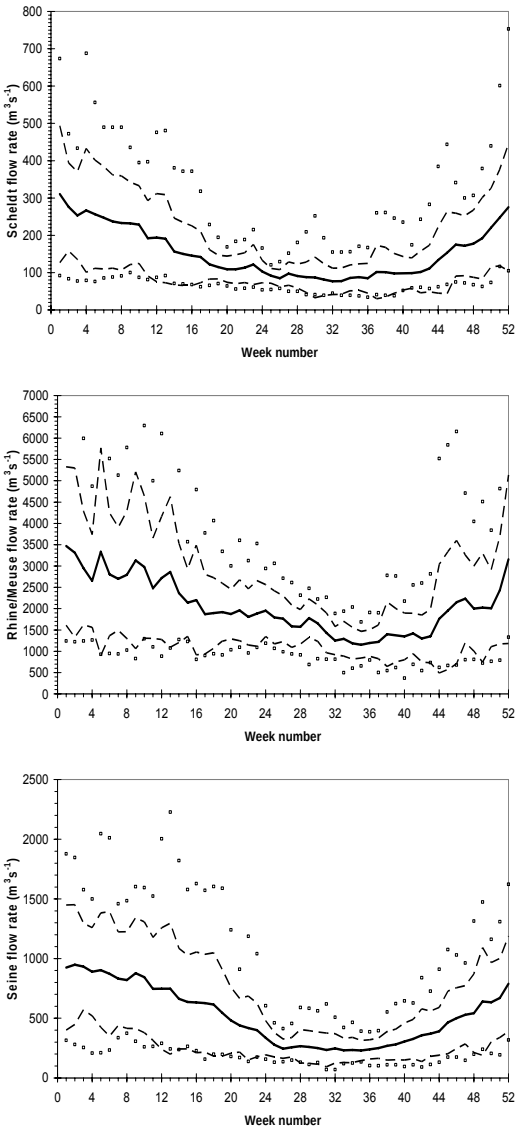

Figure 1.6. River discharge (m^3 s^{-1}) for the Rhine/Meuse, Seine and Scheldt, for the period 1991-2004. Data for the Scheldt were downloaded as 10-day averages at Schaar van ouden Doel from www.waterbase.nl courtesy of RIZA and from Administratie Waterwegen en Zeewegen. Rhine data were downloaded as daily averages from www.waterbase.nl courtesy of Rijksinstituut voor Integraal Zoetwaterbeheer en Afvalwaterbehandeling (RIZA) for Hoek van Holland (1997-2004) or estimated from the Maassluis flow (1991-1996). They were added to data from the Meuse which were downloaded from www.waterbase.nl courtesy of RIZA for Haringvlietsluizen (1997-2004) or estimated from Tiel Waal (1991-1996). Data for the Seine were downloaded as daily averages at Poses from http://seine-aval.crihan.fr (1994-2004) courtesy of Cellule anti-pollution DDE and by email from Ifremer. Labelling of points and lines is the same as for Figure 1.4

1.4 Temperature

The main source of variability of sea surface temperature (SST; Fig. 1.7), is the annual cycle of solar radiation. Interannual variability of SST is closely correlated with the NAO index (Tsimplis *et al.*, 2006). This large interannual variability (1-3° C) makes it difficult to establish a long-term trend.

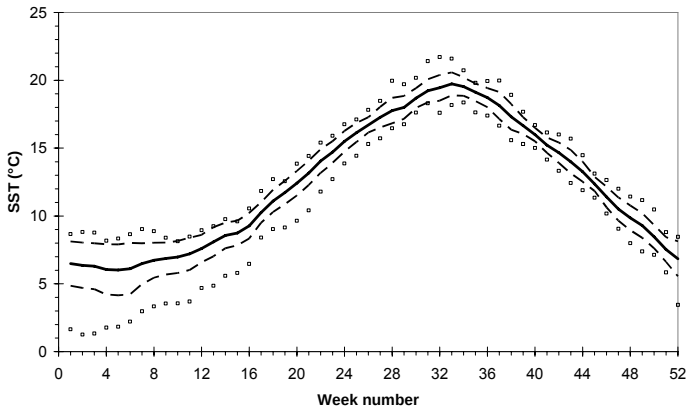

Figure 1.7. Sea Surface Temperature (SST) at station 330 for the period 1991-2004. Data originate from the Bundesamt für Seeschiffahrt & Hydrographie composite analysis of weekly ship and station data at 20 km spatial resolution (Loewe, 2003). Labelling of points and lines is the same as for Figure 1.4.

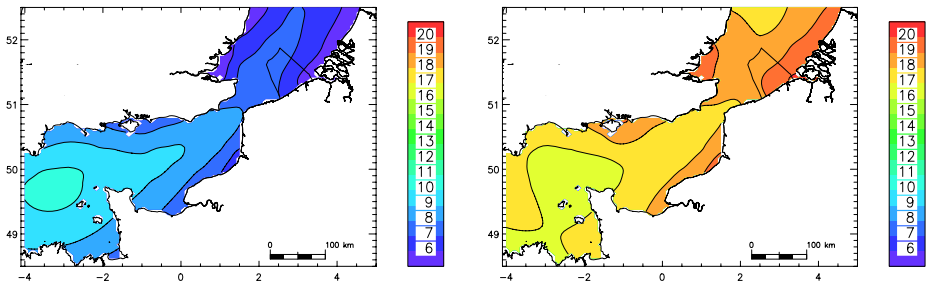

Figure 1.8. Monthly mean Sea Surface Temperature for the period 1993-2003. Left: February. Right: Augustus. Data originate from the Bundesamt für Seeschiffahrt & Hydrographie composite analysis of weekly ship and station data at 20 km spatial resolution (Loewe, 2003). For latitudes below 49°41'N, data have been extrapolated.

At shorter time scales, wind events, coupled with variations in air temperature give basin-scale modulations of this annual cycle. Some horizontal variability, of order 1-3°C, arises from the inflow of Atlantic/Channel water, which forms a tongue of warmer water in the centre of the Southern Bight in winter, and from faster heating of the shallower, coastal areas in summer (Fig. 1.8).

Because of the strong vertical diffusion, vertical variability of temperature is generally limited (less than 1°C) except within estuaries and the Rhine/Meuse plume, where salinity gradients may cause stratification, and in deeper parts of the Channel.

1.5 Salinity

Except for the fact that certain plankton species which are adapted to waters of certain salinity range, the direct impact of salinity on eutrophication dynamics is negligible. However, salinity distributions provide an excellent tracer for studying the dispersion of freshwater from rivers. At the scale of the Southern North Sea air-sea fluxes of freshwater (evaporation/precipitation) are negligible and there are no internal sources/sinks of salt so that salinity is a conserved parameter at all times.

The main variability of salinity is horizontal with lower salinity plumes forming from the mouths of the main estuaries. In particular, a band of lower salinity continental coastal water is found along the coast of North-East France, Belgium and the Netherlands (continuing into the German Bight) resulting from the discharges of the Seine, Scheldt, Rhine/Meuse and other smaller rivers (Fig. 1.2; Fig. 1.9). Cross-shore gradients of salinity are strong within this continental coastal water. Typical cross-shore variations of salinity of about 3-10 occur over a distance of 10-40 km. The continental coastal water is often bounded by a sharp, meandering front in Dutch waters while weaker fronts can be found in the vicinity of smaller rivers.

This long-term salinity distribution (Fig. 1.9) is modulated by wind events which may push the coastal water further offshore/onshore or deflect the plumes of individual rivers alongshore. The annual cycle of wind and river discharge causes a seasonal trend in salinity in Belgian waters (Fig. 1.10).

Because of the strong vertical diffusion, vertical variability of salinity is generally limited (less than 0.2) and transient in the BCZ. Haline stratification can be more significant (*e.g.* 1-4) in the Rhine/Meuse plume and in the Scheldt Estuary.

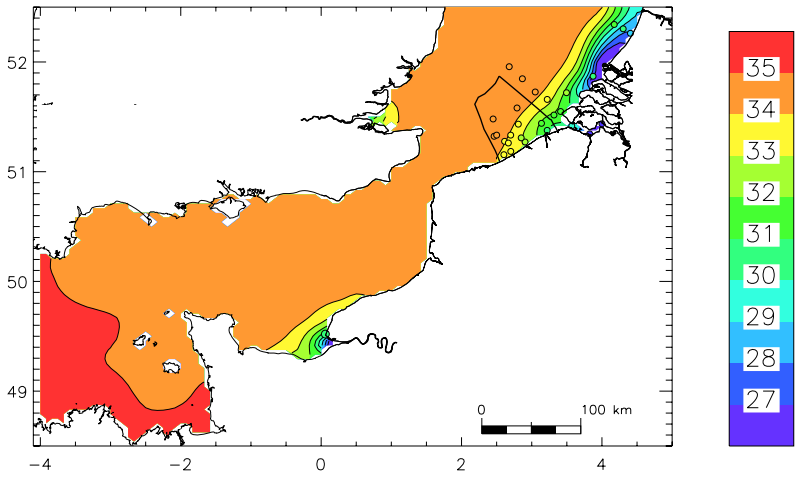

Figure 1.9. Long-term surface salinity distribution modeled for the period 1993-2002 (background coloring) together with in situ measurements superimposed as colored circles. Adapted from Lacroix *et al.* (2004).

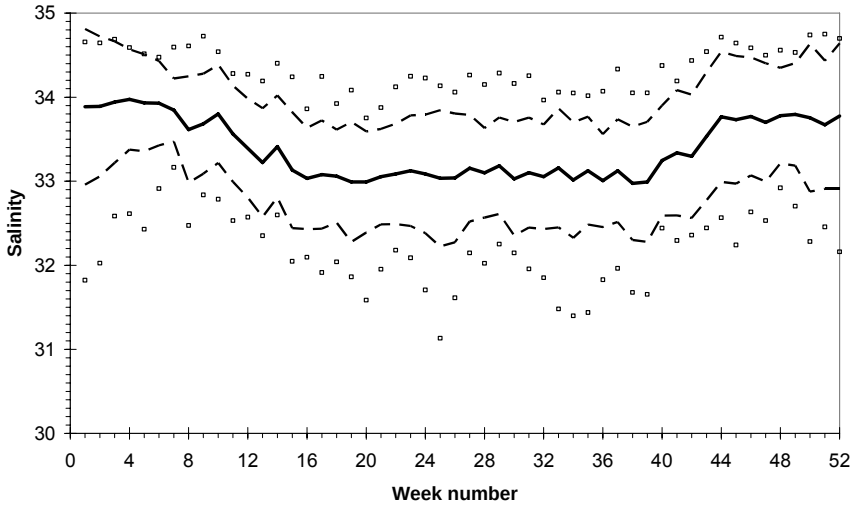

Figure 1.10. Surface salinity at station 330 for the period 1993-2004. Results were obtained from the model of Lacroix *et al.* (2004). Labelling of points and lines is the same as for Figure 1.4

1.6 Water masses

Model simulations (Lacroix *et al.*, 2004) show that the inflow of Atlantic water via the Channel is the dominant water mass in the BCZ, contributing to some 95.5% of the total water mass at station 330. Continental rivers supply most of the remaining water mass with contributions from the Rhine/Meuse, Scheldt and Seine estimated to 1.9%, 1.3% and 0.8% respectively for the long-term averages but with considerable interannual and high frequency variability. The horizontal distribution of these water masses is shown in Figure 1.11.

The residual circulation has been shown previously (*e.g.* Nihoul & Ronday, 1976; Delhez & Martin, 1992). However, the residual circulation, *e.g.* from the long-term averaged Eulerian currents, does not explain entirely the transport of biogechemical parameters since horizontal mixing is also important and can lead to dispersion of dissolved constituents in other directions.

Mean residence times have been calculated for the Southern North Sea region for water entering via the Dover straits (Delhez *et al.*, 2004). While useful for identifying regions where dissolved constituents may be retained, the concept of water age or residence time must be carefully defined (Deleersnijder *et al.*, 2001) and should not be confused with simplified approximations of transport used in some biogeochemical models (Lancelot *et al.*, 2005).

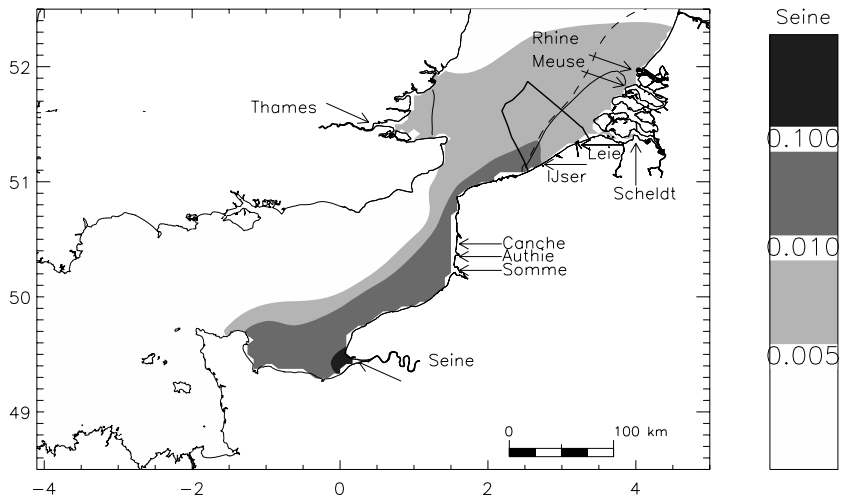

Figure 1.11. Modeled average horizontal distribution of water masses in the Channel and the Southern Bight of the North Sea for the period 1993-2003. Fractions of water from the Seine (and small French rivers) are indicated as grey scale colour map (0.5%, 1%, 10%), from the Scheldt, Leie, IJser and Thames water as superimposed solid line (1 %), from the Rhine/Meuse water as superimposed dashed line (1%). The BCZ is delimited by the continuous line. Adapted from Lacroix *et al.* (2004).

1.7 Light attenuation

The vertical attenuation of Photosynthetically Available Radiation (PAR) within the water column is generally more important than the intensity of abovewater PAR in controlling primary production (Behrenfeld & Falkowski, 1997). There is significant horizontal variability of PAR attenuation over the BCZ and Southern North Sea (Figure 1.12) because of variability in organic and inorganic suspended particulate matter and in colored dissolved organic matter (CDOM). Thus, the shallow waters close to the Belgian coast, over the Flemish Banks and around the Thames estuary are very turbid with total suspended matter concentrations ranging typically from 1-100 g m^{-3} or higher. Corresponding Secchi depths range typically from about 10 cm to a few meters. Further offshore in deeper water (30-40 m) clearer water is found with Secchi depths in the range 5-15 m. In general the euphotic depth is less than the total water depth and phytobenthos is found only in very limited areas such as tidal flats.

Temporal variability of PAR attenuation is linked essentially to the resuspension and advection of suspended particulate matter, itself modulated by the tide and by wind events over time scales of days to hours. The higher winds encountered in winter generate also a seasonal cycle with higher PAR attenuation during winter. The settling of suspended matter during calmer periods in spring may even influence the timing of spring phytoplankton blooms (Peperzak *et al.*, 1998; Rousseau *et al.*, 2008). Further temporal variability of PAR attenuation may be related to advection of CDOM of riverine origin and to self-shading during phytoplankton blooms.

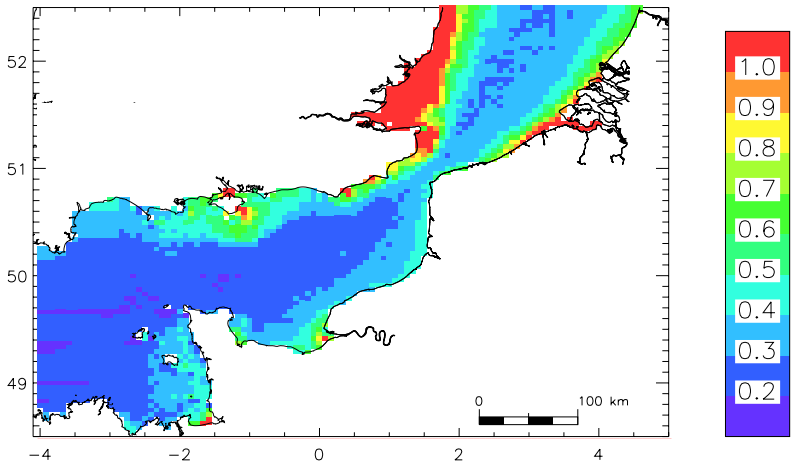

Figure 1.12. Annual (2003) average distribution of PAR attenuation coefficient (m^{-1}) in the Southern North Sea and Eastern Channel calculated from and used by the 3D-MIRO&CO model (Lacroix *et al.*, 2007b) based on the following inputs: TSM maps compiled from SeaWiFS, CDOM deduced from the modelled salinity and CHL deduced from the modelled phytoplankton biomasses. Reproduced from Ruddick *et al.* (2008).

1.8 Summary and future perspectives

This chapter summarizes the physical oceanography of the BCZ as relevant to eutrophication dynamics. The meteorological forcing, which is correlated with the NAO, is analysed in terms of the mean annual cycle of wind, PAR and river discharge and considers the range of their interannual variability. This meteorological forcing, combined with the astronomical tidal forces, drives variability of currents and turbulent diffusion, temperature, salinity (a proxy for dispersion of river water) and light availability in the water column, each of them influencing in turn nutrient and phytoplankton variability. Spatial variability of salinity and light availability are significant because of the lateral inputs of river water and the horizontal variability of water depth (and hence resuspended sediments).

This characterization of spatial and temporal variability of these parameters provides a reasonably complete description of the physical environment for the purposes of understanding eutrophication. It forms the basis for the MIRO&CO-3D ecosystem model of the region (Lacroix *et al.*, 2007a; Lacroix *et al.*, 2007b; Lancelot *et al.,* 2008). However, improvements in this understanding of the physical environment and in the capability to model it can be expected in the future, with priority on the following points:

- The spatial and temporal variability of underwater PAR is thought to be important in controlling the timing of the spring phytoplankton bloom. However, information on the high frequency variability of this parameter throughout the region is not yet available, particularly as regards PAR attenuation by suspended particles which vary at sub-diurnal time scales because of resuspension by tides and winds. The combination of satellite imagery (Doron *et al.*, 2005) and correlations obtained from high frequency data of PAR attenuation and suspended sediments (Greenwood *et al.*, 2006) could fill this gap in knowledge.
- The identification of long-term trends in physical parameters, particularly SST, their relation to anthropogenic forcing (greenhouse gases) and their impact on eutrophication are an important theme for future research. However, distinguishing long-term trends from the large interannual variability shown here remains a challenge. NAO is thought to characterize much of the large scale meteorology, although the direct links with the various physical factors (wind, rainfall/river discharge and possibly abovewater PAR) have not yet been clearly elucidated.
- The present review considers spatial scales from about 4 km to the scale of the Channel and Southern North Sea. Some extra spatial variability can be expected at smaller spatial scales, controlled by bathymetric features such as the Flemish Banks and by the coastline in very nearshore and estuarine waters. Finer resolution for hydrodynamic modeling will provide information on such processes.
- Incremental improvements should be expected in the validation and the quality of simulation of most physical parameters as more and better

forcing and validation data becomes available. For model studies, the river discharge data and the representation of estuarine processes are probably the most critical aspects requiring improvement.

1.9 References

Behrenfeld M. J. and P. G. Falkowski. 1997. A consumer's guide to phytoplankton primary productivity models. Limnology and Oceanography 42: 1479-1491

Breton E., Rousseau V., Parent J.-Y., Ozer J. and C. Lancelot. 2006. Hydroclimatic modulation of the diatom/*Phaeocystis* blooms in the nutrient-enriched Belgian coastal waters (North Sea). Limnology and Oceanography 51: 1-14

De Vries H., Breton M., Mulder T. D., Krestenitis Y., Ozer J., Proctor R. , Ruddick K. , Salomon J. C. and A. Voorrips. 1995. A comparison of 2D storm surge models applied to three shallow European seas. Environmental Software 10: 23-42

Deleersnijder E. 1989. Upwelling and upsloping in three-dimensional marine models. Applied Mathematical Modelling 13: 462-467

Deleersnijder E., Campin J.-M. and E. J. M. Delhez. 2001. The concept of age in marine modelling I. Theory and preliminary results. Journal of Marine Systems 28: 229-267

Delhez E. J. M., Heemink A. W. and E. Deleersnijder. 2004. Residence time in a semi-enclosed domain from the solution of an adjoint problem. Estuarine, Coastal and Shelf Science 61: 691-702

Delhez E. J. M. and G. Martin. 1992. Preliminary results of 3D baroclinic numerical models of the mesoscale and macroscale circulations on the North-Western European Continental Shelf. Journal of Marine Systems 3: 423-440

Doron M., Babin M., Mangin A. and O. Fanton D'andon. 2005. Retrieval of the penetration of light and horizontal visibility in coastal waters from ocean color remote sensing data, p. 85-94. In: R. J. Frouin, M. Babin and S. Sathyendranath (Eds), Remote Sensing of the Coastal Oceanic Environment. SPIE.

Greenwood N., Mills D. K. , Howarth M. J. , Proctor R., Pearce D. J., Sivyer D. B., Cutchey S. J. and O. Andres. 2006. High frequency monitoring in Liverpool Bay: variability of suspended matter, nutrients and phytoplankton. In: H. Dahlin, N. C. Flemming, P. Marchand and S. E. Petersson (Eds), European operational oceanography: present and future. European Commission.

Hurrell J. W. 1995. Decadal trends in the North Atlantic Oscillation: regional temperatures and precipitation. Science 269: 676-679

Jones P. D., Jonsson T. and D. Wheeler. 1997. Extension to the North Atlantic Oscillation using early instrumental pressure observations from Gibraltar and South-West Iceland. International Journal Climatology 17: 1433-1450

Lacroix G., Ruddick K. G. , Ozer J. and C. Lancelot. 2004. Modelling the impact of the Scheldt and Rhine/Meuse plumes on the salinity distribution in Belgian waters (southern North Sea). Journal of Sea Research 52: 149-163

Lacroix G., Ruddick K., Gypens N. and C. Lancelot. 2007a. Modelling the relative impact of rivers (Scheldt/Rhine/Seine) and Channel water on the nutrient and diatoms/*Phaeocystis* distributions in Belgian waters (Southern North Sea). Continental Shelf Research 27: 1422-1446

Lacroix G., Ruddick K., Park Y., Gypens N. and C. Lancelot. 2007b. Validation of the 3D biogeochemical model MIRO&CO with field nutrient and phytoplankton data and MERIS-derived surface chlorophyll a images. Journal of Marine Systems 64: 66-88

Lancelot C., Spitz, Y., Gypens, N., Ruddick, K., Becquevort, S., Rousseau, V., Lacroix, G. and G. Billen. 2005. Modelling diatom and *Phaeocystis* blooms and nutrient cycles in the Southern Bight of the North Sea: the MIRO model. Marine Ecology Progress Series 289: 63-78

Lancelot C., Lacroix G., Gypens N. and K. Ruddick. 2008. Ecological modeling as a scientific tool for assessing eutrophication and mitigation strategies for Belgian coastal waters. In: Current Status of Eutrophication in the Belgian Coastal Zone. V. Rousseau, C. Lancelot and D. Cox (Eds). Presses Universitaires de Bruxelles, Bruxelles, pp. 91-110

Loewe P. 2003. Weekly North Sea SST Analyses since 1968. In O. d. a. h. b. B. f. S. u. Hydrographie (Ed.)

Maes F. *et al.* 2005. A flood of space: towards a spatial structure plan for sustainable management of the North Sea. Gaufre Project. Belgian Science Policy

Ministerie van Openbare Werken. 1980. Vlaamse Banken bathymetric map D11

Mulligan D., Bouraoui F., Grizzetti D., Aloe A. and J. Dursaut. 2006. An Atlas of pan-European data for investigating the fate of agrochemicals in terrestrial ecosystems, p. 52. Joint Research Centre, European Commission

Nihoul J.C.J. and J.H. Hecq. 1984. Influence of the residual circulation on the physico-chemical characteristics of water masses and the dynamics of ecosystems in the Belgian coastal zone. Continental Shelf Research 3 (2): 167-174

Nihoul J.C.J. and F.C. Ronday. 1976. Modèles hydrodynamiques. Projet Mer. Final Report volume 3

Osborn T. J. 2004. Simulating the winter North Atlnatic Oscillation: the roles of internal variability and greenhouse gas forcing. Climate Dynamics 22: 605-623

Osborn T. J. 2006. Recent variations in the winter North Atlantic Oscillation. Weather 61: 353-355

Otto L., Zimmerman, J.T.F., Furnes, G.K., Mork, M., Saetre, R. and G. Becker. 1990. Physical Oceanography of the North Sea. Netherlands Journal of Sea Research 26: 161-238

Peperzak L., Colijn F., Gieskes W. W. C. and J. C. H. Peters. 1998. Development of the diatom-*Phaeocystis* spring bloom in the Dutch coatal zone of the North Sea: the silicon depletion versus the daily irradiance threshold hypothesis. Journal of Plankton Research 20: 517-537.

Rousseau V. 2000. Dynamics of *Phaeocystis* and diatom blooms in the eutrophicated coastal waters of the Southern Bight of the North Sea. PhD Thesis. Université Libre de Bruxelles, 205 Pp.

Ruddick K., Lacroix G., Lancelot C., Nechad B., Park Y., Peters S. and B. van Mol. 2008. Optical remote sensing of the North Sea. In: V. Barale and M. Gade (Eds.), Remote sensing of the European Seas. Springer-Verlag, pp. 79-90

Tsimplis M. N., Shaw A. G. P. , Flather R. A. and D. K. Woolf. 2006. The influence of the North Atlantic Oscillation on the sea-level around the northern European coasts reconsidered: the thermosteric effects. Philosophical Transactions of the Royal Society A 364: 845-856

Yang L. 1998. Modelling of hydrodynamic processes in the Belgian coastal zone. Faculteit Wetenschappen. Katholieke Universiteit Leuven. 214 pp.

CHAPTER 2

Nutrient loads to the Belgian Coastal Zone

Natacha Brion[1], Siegrid Jans[2], Lei Chou[3] and Véronique Rousseau[4]

[1] Vrij Universiteit Brussel (VUB), Analytical and Environmental Chemistry (ANCH), Pleinlaan 2, B-1050 Brussels, Belgium
[2] Management Unit of the North Sea Mathematical Models (MUMM), Royal Belgian Institute for Natural Sciences (RBINS), Gulledelle 100, B-1200 Brussels, Belgium
[3] Université Libre de Bruxelles (ULB), Océanographie chimique et Géochimie des Eaux (LOCGE), CP208, boulevard du Triomphe, B-1050 Brussels, Belgium
[4] Université Libre de Bruxelles (ULB), Ecologie des Systèmes Aquatiques (ESA), CP221, boulevard du Triomphe, B-1050 Brussels, Belgium

2.1 Introduction

Anthropogenic eutrophication in coastal environment results from increased delivery of land-based nutrients considerably enriched in nitrogen (N) and phosphorus (P) compared to silicon (Si). These nutrient inputs strongly modify the nutrient balance N:P:Si of coastal waters with respect to phytoplankton stoechiometry, *i.e.* N:P=16 for marine phytoplankton (Redfield *et al.*, 1963) and N:Si=1 for coastal diatoms (Bzrezinski, 1985). This in turn modifies the composition of the phytoplankton community characterized by a dominance of opportunistic non-siliceous species (*e.g.* Officer & Ryther, 1980; Billen *et al.*, 1991).

Coastal waters are enriched by nutrients delivered by rivers and canals, coastal tributaries, atmospheric deposition, and advection from adjacent areas (Fig. 2.1). River nutrient loads are largely influenced by human activity and depend on the population density in the watershed but also on environmental drivers such as land use and agriculture practices, industrialization, and waste water treatment management (Fig. 2.1). Nutrients are released to surface waters from point sources as domestic and industrial effluents (mainly NH_4^+ and PO_4^{3-}), and diffuse sources through soil leaching and ground water contamination by fertilizers and manure spreading (mainly NO_3^- and $Si(OH)_4$). Once released in the river system, nutrients are involved in physico-chemical and biological processes leading to their transformation, retention or elimination during their transfer along the aquatic continuum (Fig. 2.1; Billen *et al.*, 1991). Atmospheric deposition occurs mostly as N oxide (NO, N_2O, NO_2) originating from industrial and traffic combustion processes and as ammoniac (NH_3) resulting of animal breeding and manure spreading. Once in the atmosphere these gasses are

transformed and transported with the air masses before their wet or dry deposition onto coastal areas (Spokes & Jickells, 2005).

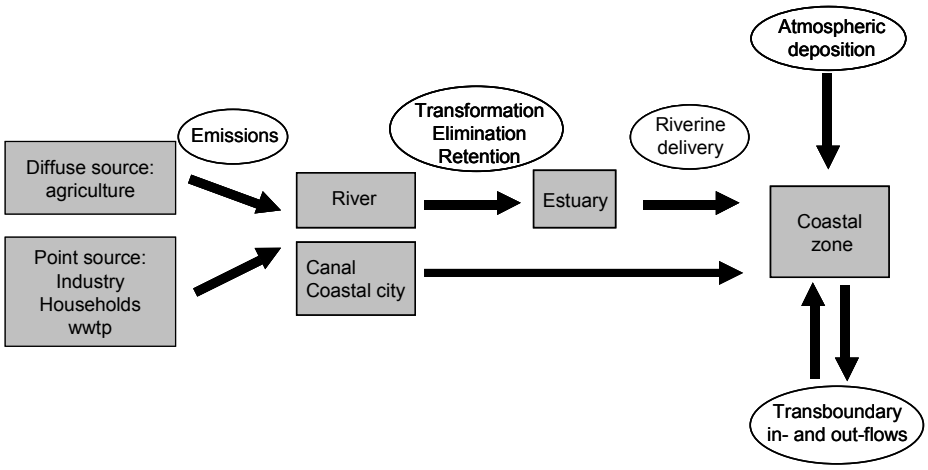

Figure 2.1. Schematic representation of nutrient delivery to coastal water including river, canal and coastal tributaries, atmospheric deposition and transboundary in- and out-flows. Riverine loads of nutrients result from nutrient emissions from point and diffuse sources in the watershed. They can be directly delivered to coastal waters or transformed, retained and/or eliminated during their transfer along the aquatic continuum before reaching the coastal area.

Nutrient enrichment of the Belgian coastal zone (BCZ; Fig. 2.2) results from local riverine inputs of the Scheldt, the IJzer and the coastal tributaries, from atmospheric deposition and from transboundary fluxes brought by the Southwesterly Atlantic waters enriched by the rivers Seine, Somme, Authie and Canche, and Rhine (Lacroix *et al.*, 2004). The relative importance of these different nutrient sources varies depending on change in human activity in the watersheds and on the North Atlantic Oscillation (NAO) which determines the weather conditions over North-western Europe and the hydrological budget of BCZ (Breton *et al.*, 2006).

This chapter synthesizes the information on N, P and Si delivery to the BCZ and resulting enrichment of coastal waters. It compares the present situation with available historical data in order to evaluate their long term changes. Quantitative changes in riverine loads are analysed in relationship with human pressure and biogeochemical transformations within the aquatic continuum. Qualitative changes in nutrients are also considered, in particular changes in the N:P:Si molar ratio determining the limiting element for phytoplankton growth and triggering harmful algal blooms (Billen & Garnier, 1997; 2007).

2.2 Freshwater nutrient loads

2.2.1 The BCZ watershed

The BCZ watershed is here defined as the catchment area of watercourses discharging directly in the BCZ but also indirectly through a significant influence of river plume. As such, the BCZ watershed includes the sub-basins of the IJzer, the coastal tributaries in the northeastern part of Belgium and the Scheldt considered here upstream the Belgian-Dutch border (Fig. 2.2). It covers a total area of 24 010 km^2, distributed in the northwestern France (30%) and Belgium (70%).

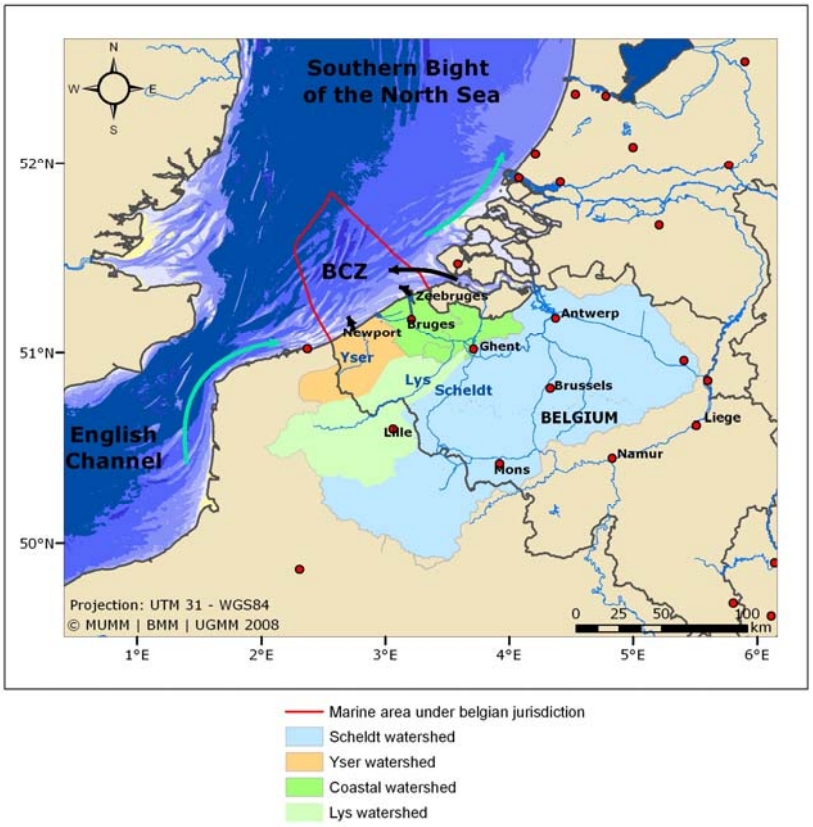

Figure 2.2. The Belgian Coastal Zone (BCZ) in the Southern Bight of the North Sea and its watershed including the Scheldt, the IJzer and the Coastal sub-basins. The Leie watershed is also indicated. Source: Map (MUMM-BMDC, 2008); bathymetry (Maes *et al.*, 2005); hydrology in Belgium and The Netherlands (DGRNE - Scaldit) and BD-CARTO (copyright IGN-PARIS-2000), BD-CARTHAGE (copyright IGN-PARIS-2000), AGENCE DE L'EAU ARTOIS-PICARDIE, DIREN NORD PAS DE CALAIS in France. Arrows indicates the riverine (black) and transboundary (blue) nutrient fluxes.

The river Scheldt is a lowland river, with a total length of 355 km. Its main affluents are the Haine, Dender and Rupel with its confluents the rivers Zenne, Dijle, Grote and Kleine Nete (Fig. 2.3). The course of one of its tributary, the river Leie, has been deviated directly to the sea through several canals (Van Geystellen *et al.*, 1980) so that the Leie sub-basin (4344 km^2) will be here included in the Coast watershed (Fig. 2.2). Contrarily to the tributaries of the Coast and IJzer watersheds which discharge directly freshwater to marine waters, the river Scheldt has a tidal estuary, the Westerschelde, showing large seasonal fluctuations of the freshwater discharge (20-350 $m^3 s^{-1}$). High water velocities and bottom friction are sufficient to mix efficiently the water column so that little or no vertical stratification of solutes occurs. This estuary is 100 km long. Salt intrusion in the brackish estuary occurs up to Hemiksem, *i.e.* downstream the confluence of the main rivers at about 85 km from the mouth but tidal limits are located more upstream in the main affluents (Fig. 2.3). The residence time of Scheldt freshwater may reach 2 to 3 months during the summer but about 1 month during the high flood period in winter and early spring. The long residence time and the fluctuations of the water composition within the estuary are very favorable conditions for the occurrence of physical, chemical and biological transformations, which may significantly modify the nutrient fluxes to the BCZ.

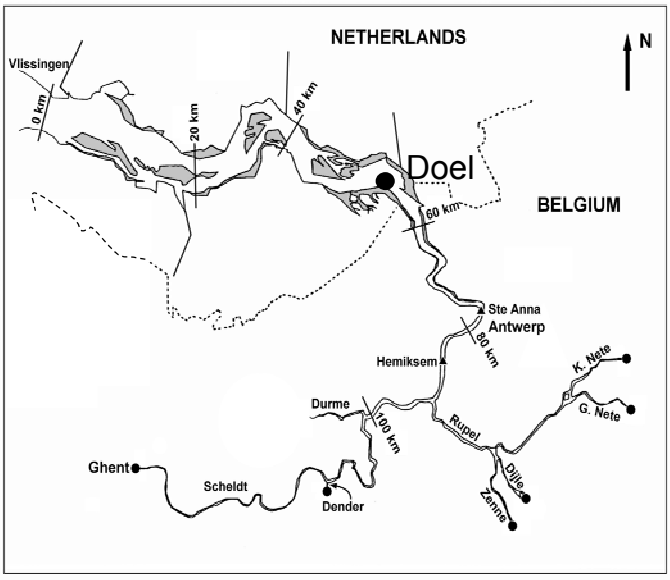

Figure 2.3. The Scheldt estuary. Upstream tidal intrusion occurs up to Hemiksem while the limits of tidal influence are located in the rivers Scheldt, Dender, Zenne, Dijle, Grote Nete and Kleine Nete (solid circles). The location of Doel, at the Belgian-dutch border is also indicated.

The IJzer watershed (1749 km^2) drains the western coastal area of Belgium (Fig. 2.2). Its hydrographic system receives mainly polder effluents. The Coast watershed (1914 km^2; Fig. 2.2) drains the maritime plain in the northeastern part of the BCZ watershed. Its main watercourse consists of canals that mainly receive polder drainage and flow seaward via harbour channels (Gent-Oostend, Leopold, Schipdonk and Gent-Terneuzen canals).

The population density differs considerably between the three river basins with 522, 417 and 227 inhab km^{-2} for the Scheldt, Coast and IJzer watersheds respectively. The higher population density in the Scheldt basin is mainly due to the presence of the large cities Antwerp, Brussels and Ghent (Fig. 2.2). Agricultural practices differ also considerably from one sub-basin to another with very intensive cattle, pig and poultry farming in the IJzer and Coast watersheds. Pig farming is very significant in the IJzer watershed with animal density being eight-fold that of the Scheldt (Rousseau *et al.*, 2004). High population density, intensive agriculture and industrialization (mainly in the northern watershed), make of the Scheldt one of the most heavily polluted rivers in Europe (Billen *et al.*, 2005).

2.2.2 N and P emissions in the BCZ watershed in 2000

2.2.2.1 N and P emissions to surface waters of the Scheldt, IJzer and Coast watersheds

Domestic, industrial and agricultural N and P emissions to surface waters of the Scheldt, IJzer and Coast watersheds were estimated for the year 2000 from data reported in the last exhaustive inventory of human activities and land use by Federal Institutes and by the Regions (see details in Rousseau *et al.*, 2004). Domestic emissions of N and P were calculated on basis of the watershed population, a per capita load of 10 g N and 1.8 g P $inhab^{-1}$ d^{-1} specific for western european countries in the late nineties (Billen *et al.*, 1999; Servais *et al.*, 1999), the wastewater treatment capacity in each watershed and a rate of N and P elimination by wastewater treatment specific to each watershed. Industrial emissions of N and P were estimated based on a census of industry and a specific release rate of N and P to surface waters and to public waste water treatment plants. The transfer of N and P from agricultural sources to surface water was estimated using the semi-empirical model SENTWA (System for the Evaluation of Nutrient Transport to WAter, Ministry of Small Enterprises, Traders and Agriculture). This model is based on reliable statistical data on land use, livestock density, spreading of animal manure and fertilizers taking into account lithology, nutrient species and meteorology. It also calculates N and P fluxes to surface water resulting from atmospheric deposit, direct flow, drainage, groundwater overflow, excess fertilizer or manure use, erosion and run-off.

This detailed census estimated the total N and P emissions to surface waters of the BCZ watershed in 2000 to 65.2 kt N (Fig. 2.4a) and 6.6 kt P (Fig. 2.4c) respectively. The Scheldt watershed was the main source of nutrients, contributing to 69% of N and 73% P of the total emissions. The Coast watershed was responsible for some 20% of N and P discharge while the IJzer

contributed to only 10% of N and 7% of P total emissions. Nutrient sources varied according to the different watersheds. Agriculture was indeed the major source of N (81%) and P (54%) in the IJzer watershed while domestic emissions in the Scheldt watershed are responsible for most N (52%) and P (75%) emissions. The Coast watershed shows an intermediate situation with agriculture as the main source of N (60%) but a major household contribution (52%) to P emissions.

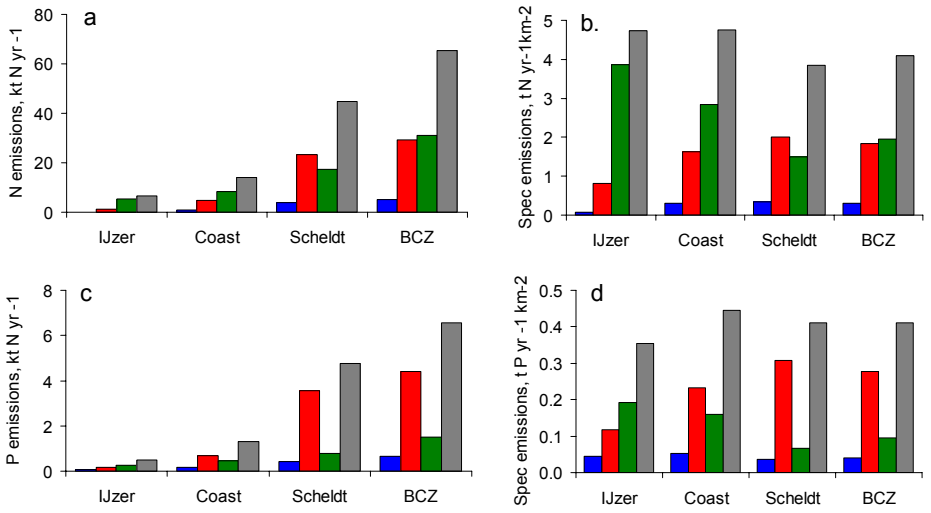

Figure 2.4. N (a) and P (c) emissions and N (b) and P (d) specific emissions to surface water of the IJzer, Coast, Scheldt and BCZ watersheds. Agriculture (green), domestic (red), industry (blue) and Total (grey) nutrient emissions are indicated.

These differences reflect contrasted land use in the three watersheds as shown by the specific emissions of N (Fig. 2.4b) and P (Fig. 2.4d), *i.e.* emissions related to the respective area of each watershed. In the densely populated Scheldt watershed, specific emissions of N and P from domestic activities are dominant. Specific agricultural emissions of N and P dominate all other emissions in the IJzer and Coast catchment basins due to the intensive agricultural practices developed in these watersheds, in particular the cattle, pig and poultry manure production and spreading on fields.

2.2.2.2 N and P loads from IJzer, Coast and Scheldt watersheds

Annual N and P loads for 2000 were estimated at the outlet of each sub-watershed (Fig. 2.5). Scheldt nutrient loads were computed from nutrient concentrations measured at Doel and runoffs available at station Schelle. Nutrient loads from the IJzer and Coast watersheds were estimated from nutrient concentrations and runoffs available at downstream monitoring stations

(see details for calculations and data source in Rousseau *et al.*, 2004). These N and P loads can be considered as the nutrient delivered to the BCZ. In total, some 56.8 kt N (Fig. 2.5a) and 4.4 kt P (Fig. 2.5b) were delivered by the 3 watersheds in 2000 with the Scheldt being by far the major contributor to N and P total loads. Coastal tributaries discharged about one third of N and P loads while the river IJzer contributed to only 5% of both N and P loads.

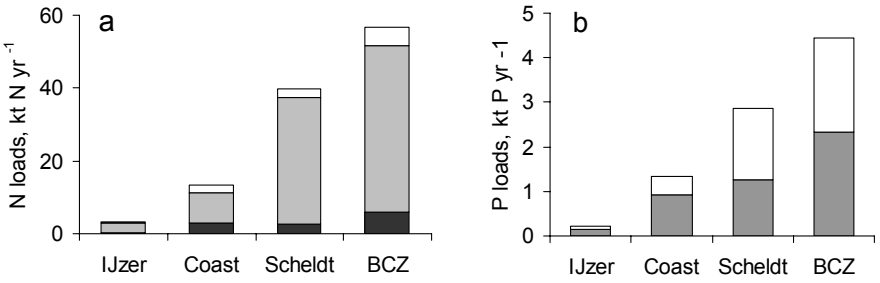

Figure 2.5. N (a) and P (b) riverine loads discharged to the BCZ by the IJzer, Coast and Scheldt watersheds in 2000. N forms represented as NH_4^+ (black), NO_3^-+NO_2^- (grey), Total N – DIN (white) and P forms as PO_4^{3-} (grey), Total P-PO_4^{3-} (white). Data compiled as described in Rousseau *et al.* 2004.

Dissolved inorganic nitrogen (DIN) loads represented a large part (in average 90%) of the N delivered to the BCZ with oxidized N forms (NO_3^-+NO_2^-) contributing to some 80% (Fig. 2.5a). NH_4^+ loads from the IJzer and Coast watersheds were the highest. Globally half of the P riverine load was delivered as PO_4^{3-} but with contrasted situation in the different basins. In the IJzer and Coast watersheds, PO_4^{3-} contributes to about two thirds of P loads but 44% in the Scheldt watershed (Fig. 2.5b).

Comparison between nutrient loads and emissions in 2000 (Table 2.1) indicates that the efficiency of nutrient retention varied among watersheds. Nutrient retention was the highest in the IJzer watershed where half of the N and P emitted to surface waters was retained in the aquatic environment. In contrast, nutrient retention was not significant in the Coast watershed where a very slight P production occurred. In the Scheldt watershed, some 11% of N and 40% of P were retained. Globally, some 13% N and 32% of P emitted in the BCZ watershed are retained in the aquatic continuum. However, as the uncertainty on emissions may be large, retention should be considered with care.

Table 2.1: Nutrient retention in the IJzer, Coast, Scheldt and BCZ watersheds in 2000

kt N yr^{-1}	IJzer	Coast	Scheldt	BCZ
Emissions	6.47	13.94	44.83	65.24
Loads	3.31	13.50	39.94	56.75
Retention (%)	49	3	11	13
kt P yr^{-1}	IJzer	Coast	Scheldt	BCZ
Emissions	0.48	1.30	4.77	6.55
Loads	0.23	1.34	2.87	4.44
Retention (%)	52	-3	40	32

2.2.3 Nutrient emissions, transformations and loads in the Scheldt estuary

The link between anthropogenic emissions of nutrients, their riverine loads, their delivery to the coastal waters and the biogeochemical processes leading to their transformation and elimination are the best known for the Scheldt watershed.

2.2.3.1 Changes in nutrient emissions in the Scheldt watershed between 1950 and 2000

Human activities and land use with resulting nutrient emissions to surface- and ground-water of the Scheldt watershed have considerably varied between 1950 and 2000 (Fig. 2.6; Billen *et al.*, 2005). Point sources of nutrients were at their maximum in the seventies when domestic and industrial emissions were discharged without treatment into surface water of the Scheldt and its tributaries. Domestic loading into surface waters increased dramatically between 1950 and 1975 mainly due to the connection of the population, whose rate increased from 15 to 90%, to sewer systems with however a low water treatment capacity at that time (Fig. 2.6a). Secondary waste water treatment was implemented in the Scheldt watershed from the early seventies with a capacity progressively increasing from 1 to 5 M eqinhab between 1970 and 2000 (Fig. 2.6a; van Damme *et al.*, 1995; Billen *et al.*, 2005). Nutrient emissions by industries (mainly chemistry and food) increased considerably following the post-world war development up before being very efficiently reduced (some 90%) by the implementation of waste water treatment plants from the mid-seventies (Fig. 2.6b). Also, the use of polyphosphate-containing detergents for domestic and industrial purposes in the seventies and eighties was responsible for increase of P emissions to rivers. These polyphosphate-containing detergents were progressively ban in the early nineties (Billen *et al.*, 1999; 2001). Agricultural practices, with large-scale use of fertilizers and intensive cattle-farming (Fig. 2.6c), have also considerably evolved over this fifty years

period impacting both point and diffuse nutrient sources (Billen *et al.*, 2005). As an example, Billen *et al.* (2005) estimate that groundwater nitrate concentrations in the aquifers of the Scheldt watershed were increasing from 2 to 10 mg N L^{-1} between 1950 and 2000.

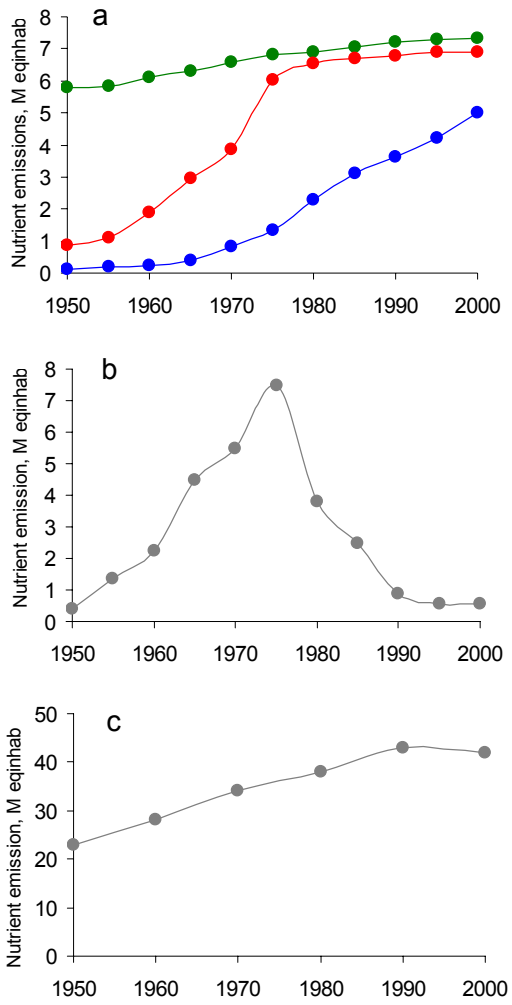

Figure 2.6. Evolution during the period 1950-2000 of nutrient emissions (expressed in terms of M inhabeq) in the Scheldt watershed of domestic loads by the population (green), by population connected to a sewer system (red) and to wastewater treatment plant (blue) (a); net industrial loads (b) and cattle waste (c). Redrawn from Billen *et al.*, 2005.

2.2.3.2 Nutrient filtering capacity of the Scheldt estuary

Once released in the aquatic environment, nutrients undergo biogeochemical transformations which depend on the physico-chemical conditions prevailing along the aquatic continuum. These transformations are especially important in the estuary. By determining light availability in the water column, turbidity is an important factor governing phytoplankton growth. In the uppermost freshwater tidal reaches of the Scheldt estuary where light and residence time are sufficient, summer phytoplankton blooms reaching up to up to 160 µg chl *a* L^{-1} are responsible for significant nutrient removal (Billen *et al.*, 1986, Muylaert *et al.*, 2001). Downstream, in the brackish and salt estuary, phytoplankton blooms occur from April to September but are much less pronounced than in the river due to higher turbidity (Baeyens *et al.*, 1998; Muylaert *et al.*, 2000) except in the most marine part where summer blooms of marine species are recorded.

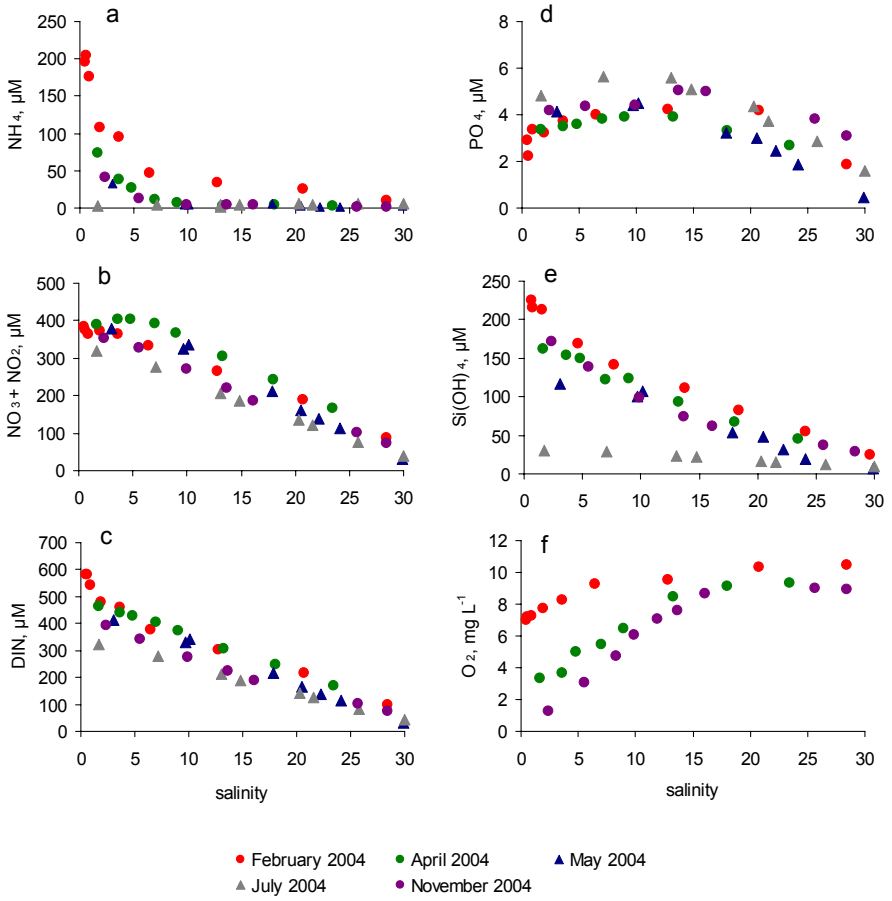

Figure 2.7. Longitudinal profiles of NH_4^+ (a), NO_3^-+NO_2^- (b), DIN (c), PO_4^{3-} (d), $Si(OH)_4$ or DSi (e), and O_2 (f) as a function of salinity at different seasons in 2004 in the brackish Scheldt estuary. Data compiled from MUMM (Monitoring the Belgian Continental Shelf and the Scheldt estuary, dots) and SISCO (Silica retention in the Scheldt continuum and its impact on coastal eutrophication, triangles).

The oxygen status of riverine and estuarine waters, largely dependant on the organic matter load, is another important factor governing the biogeochemical transformations of nutrients. During the seventies, complete oxygen depletion resulting from the aerobic respiration of the organic matter from anthropogenic origin especially in summer months was the rule in many rivers of the Scheldt watershed (Soetaert & Herman, 1995; Billen *et al.*, 2005). From the eighties, the water quality has considerably improved owing to wastewater treatment policies but anoxia is still present in summer in the Rupel (Billen *et al.*, 2005).

Nitrogen biogeochemistry. The major microbiological processes affecting N in aquatic systems are ammonification (production of NH_4^+ by the mineralization of organic matter), nitrification (transformation of NH_4^+ into NO_3^-) and denitrification (elimination of NO_3^- in anaerobic zones through its transformation into gaseous N_2). They are particularly significant in both the freshwater and brackish Scheldt estuary (van Damme *et al.*, 1995; Herman & Heip, 1999; Soetaert *et al.*, 2006; van der Zee *et al.*, 2007; Brion *et al.*, 2008). In the freshwater estuary, mass balance calculations of N fluxes measured in the productive period of 2003 (May-September) showed that nitrification dominated the most upper part of the freshwater estuary (420 t of $N\text{-}NH_4^+$ converted to $N\text{-}NO_3^-$) while the more downstream section was dominated by ammonification with a net production of 42 t $N\text{-}NH_4^+$ and denitrification with a net consumption of 270 t $N\text{-}NO_3^-$ (van der Zee *et al.*, 2007). Globally, the freshwater estuary acts as a sink for N (180 t N or 10% of incoming N). In the brackish estuary, the occurrence of nitrification is visible on the longitudinal profiles of N species, showing a significant decrease of NH_4^+ (Fig. 2.7a) concomitant to a NO_3^-+NO_2^- increase particularly evident in April (Fig. 2.7b) and resulting in conservative DIN profiles (Fig. 2.7c). Additionally, the importance of ammonification and nitrification processes was demonstrated by direct process measurements (Table 2.2). Nitrification has considerably intensified in the Scheldt as a result of the implementation of secondary waste water treatment in the mid-seventies and subsequent improvement of the oxygenation status of the Scheldt tributaries and estuary (Billen *et al.*, 2005; Soetaert *et al.*, 2006). This intensification is coupled to an upstream migration of the nitrification key site from the mid-estuary in the seventies to its freshwater part since the nineties (Soetaert & Herman, 1995; Soetaert *et al.*, 2006). Reversely, the water quality improvement negatively impacts the importance of denitrification. During the seventies and eighties, this process was responsible for the complete elimination of NO_3^- in the upper Scheldt estuary under summer anoxic conditions (Billen *et al.*, 2005). The reduction of riparian denitrification due to agricultural drainage also contributes to the decrease of NO_3^- elimination in the watershed (Billen *et al.*, 2005). In the late seventies, riparian and in-stream denitrification was indeed responsible for the elimination of some 65% (48 kt N yr^{-1}) of the total N loading to the Scheldt river system while 25 years later, some 50% (35 kt N yr^{-1}) of N emissions were eliminated (Billen *et al.,* 2005). Above salinity 10 in the brackish estuary, dilution is the main process affecting N dynamics as shown by the conservative behaviour of NH_4^+, NO_3^-+NO_2^- and DIN (Fig. 2.7a-c). Their concentrations vary however seasonally with lower values during summer. The NH_4^+ decrease is particularly significant with complete depletion of this nutrient during summer (Fig. 2.7a).

Table 2.2. Daily N fluxes associated with pelagic ammonification and nitrification in the Scheldt estuary between Rupelmonde and Breskens in 2003 (Brion *et al.*, 2008)

tN d^{-1}	Ammonification	Nitrification
January	215	30
April	25	150
July	140	20
October	40	40

Phosphorus biogeochemistry. The P biogeochemistry is complex and displays a strong seasonal variability. P retention due to sorptive removal of PO_4^{3-} on suspended iron hydroxides in oxygenated water with further aggregation and precipitation onto the bottom sediments and planktonic algal uptake, is very efficient in the freshwater part of the Scheldt estuary (Zwolman, 1994; Billen *et al.*, 2005). Mass balance calculations of P fluxes measured from March 2003 to February 2004 estimates that some 0.45 kt P-PO_4^{3-} and 0.57 ktP-TP corresponding respectively to 53% of PO_4^{3-} and 25% of TP entering the Scheldt affluents at the tidal limits, were retained in the freshwater tidal estuary (Van der Zee *et al.*, 2007). Under the low oxygen conditions prevailing at the fresh-brackish interface during spring and summer, increase of PO_4^{3-} concentrations has been attributed to the remobilization from reducing fluvial sediments (Zwolman, 1994). In the brackish estuary, a production of PO_4^{3-} is observed along year in the salinity range 0-15 before it is conservatively diluted up to marine waters (Fig. 2.7d). This source would result from the desorption of PO_4^{3-} from iron hydroxides due to lower stability of iron-bound P when pH increase along the salinity gradient (Zwolman, 1994). This production can be significant, acting as an important source of PO_4^{3-} to the BCZ where this nutrient can be limiting for phytoplankton growth in spring (Van der Zee & Chou 2005; Lancelot *et al.*, 2005; Gypens *et al.*, 2007). As an example, Van der Zee *et al.* (2007) estimated that in May 2004, about 51% of the PO_4^{3-} flux exported to the coastal marine waters originated from PO_4^{3-} desorption and would correspond to 75% of the PO_4^{3-} retained in the freshwater tidal estuary. Over the period 1990-2005, the maximum PO_4^{3-} concentrations in the Scheldt profile decrease from 15 µM in 1992 to about 5 µM in 2005. Both increasing PO_4^{3-} retention due to precipitation in the re-oxygenated Scheldt estuary (Zwolman 1994; Van Damme *et al.*, 1995; Van der Zee *et al.*, 2007) and decreasing P emissions could have contributed to this significant decrease of PO_4^{3-} concentrations.

Silicon biogeochemistry. The main process affecting Si dynamics in the Scheldt is its retention due to diatom uptake and sedimentation. While not important in the river, Si uptake by diatoms might be significant in the upper freshwater and marine Scheldt estuary in summer (Fig. 2.7e; Muylaert *et al.*, 2005; Chou & Wollast, 2006; Lionard *et al.*, 2008). These blooms can be responsible for the retention of one third of the riverine dissolved silicate (DSi or $Si(OH)_4$; Carbonell *et al.*, in prep). From October to April, DSi behaves as a conservative element in the brackish Scheldt estuary with concentrations of some 250 µM at the

freshwater end-member (Fig. 2.7e). The nowadays situation with both freshwater and estuarine diatom blooms consuming DSi contrasts with that reported in the late sixties when these only occur in the brackish estuary depleting DSi around salinity 20. The lack of diatom blooms in the freshwater estuary was due to the prevailing high turbidity preventing diatom growth at that time (Wollast & De Broeu, 1971).

2.2.3.3 Long-term changes in the Scheldt N, P and Si loads to the BCZ

Quantitative trends. Long-term trends of nutrient loads integrate changes in both nutrient emissions in the Scheldt watershed (section 2.3.1) and their biogeochemical transformations along the aquatic continuum (section 2.3.2). Scheldt N, P and Si loads were estimated at station Doel, at the Belgian-Dutch border in the brackish estuary (Fig. 2.3) from which nutrients behave nearly conservatively up to the coastal zone. Nutrient loads were calculated as described in Rousseau *et al.* (2004) based on available nutrient concentrations (source: RIKZ, http://www.waterbase.nl) and Scheldt runoff at Schelle (source: AWZ, Administratie Waterwegen en Zeewezen of the Ministry of Flemish Community) available for the period 1965-2005.

N, P and Si loads show marked variations during this period each however with a different timing and amplitude (Fig. 2.8). Nutrients originating mainly from point source as NH_4^+ (Fig. 2.8a) and PO_4^{3-} (Fig. 2.8f) show a marked decreasing long term trend in their loads. However nutrients of diffuse origin are mainly modulated by fluctuations of the Scheldt runoff (NO_3^-+NO_2^- ; Fig. 2.8 b,h; r=0.88 and DSi; Fig. 2.8 e,h; r=0.69).

After a two-fold increase between 1966 and the early seventies resulting from the increasing rate of sewage collection and industrial activity with a low capacity of waste water treatment, NH_4^+ loads decrease by some 93% from the early seventies up to 2005 (Fig. 2.8a). This drop is explained by nutrient retention during waste water treatment and the intensification of estuarine nitrification resulting from the net improvement of the oxygenation of the Scheldt river system following the implementation of secondary waste water treatment (sections 2.3.1 & 2.3.2). The decline of PO_4^{3-} loads over the same period shows a two-step trend, being first sharp between 1966 and 1983 and then more gradual up to reaching in 2005 lower levels than those prevailing in the early seventies (0.6 kt P; Fig. 2.8f). Such a decrease is also visible in the Tot P loads which drop by some 86% between 1974 and 2005 (Fig. 2.8g). The considerable increase of P Scheldt loads observed in the seventies has been related to the intensive domestic and industrial use of polyphosphate-containing detergents (Billen *et al.*, 1999; 2001). Their further decrease during the last twenty years is explained by the progressive ban of PO_4^{3-} from detergents, the increased wastewater treatment capacity implemented in the early eighties but also higher P retention due to the co-precipitation of PO_4^{3-} with Fe(oxy)hydroxydes in the re-oxygenated freshwater tidal Scheldt estuary (Zwolman 1994; Billen *et al.*, 2001; Van der Zee *et al.* 2007; sections 2.3.1 & 2.3.2).

Despite the fluctuations related to hydrological conditions, NO_3^-+NO_2^- loads show a global increase since the mid-seventies (Fig. 2.8b) reflecting not only the evolution of diffuse sources of nitrate through leaching of agricultural soils

but also the improvement of the oxygen status of the river, which reduced denitrification but increased the nitrification of the ammonium load (Billen *et al.*, 2005). Altogether this was caused by the intensification of agricultural practices, in particular the large-scale use of fertilizers and the intensive cattle-farming (Fig. 2.6) but also enhanced nitrification and decreasing denitrification due to a better oxygenation of Scheldt tributaries and estuary (section 2.3.2; Billen *et al.* 2005). As a result of NH_4^+ and NO_3^-+NO_2^- load fluctuations, DIN (Fig. 2.8c) and Tot N (Fig. 2.8d) loads show a slight decreasing trend from the early eighties up to 2005. The contribution of NO_3^-+NO_2^- and NH_4^+ to DIN loads was however completely reversed with NH_4^+ representing 60% in 1976 but less than 10% in 2005. DSi loads decreased by about 26% between 1975 and 2005 (Fig. 2.8e) explained by a higher diatom uptake in the upstream courses of the drainage network (Chou & Wollast, 2006).

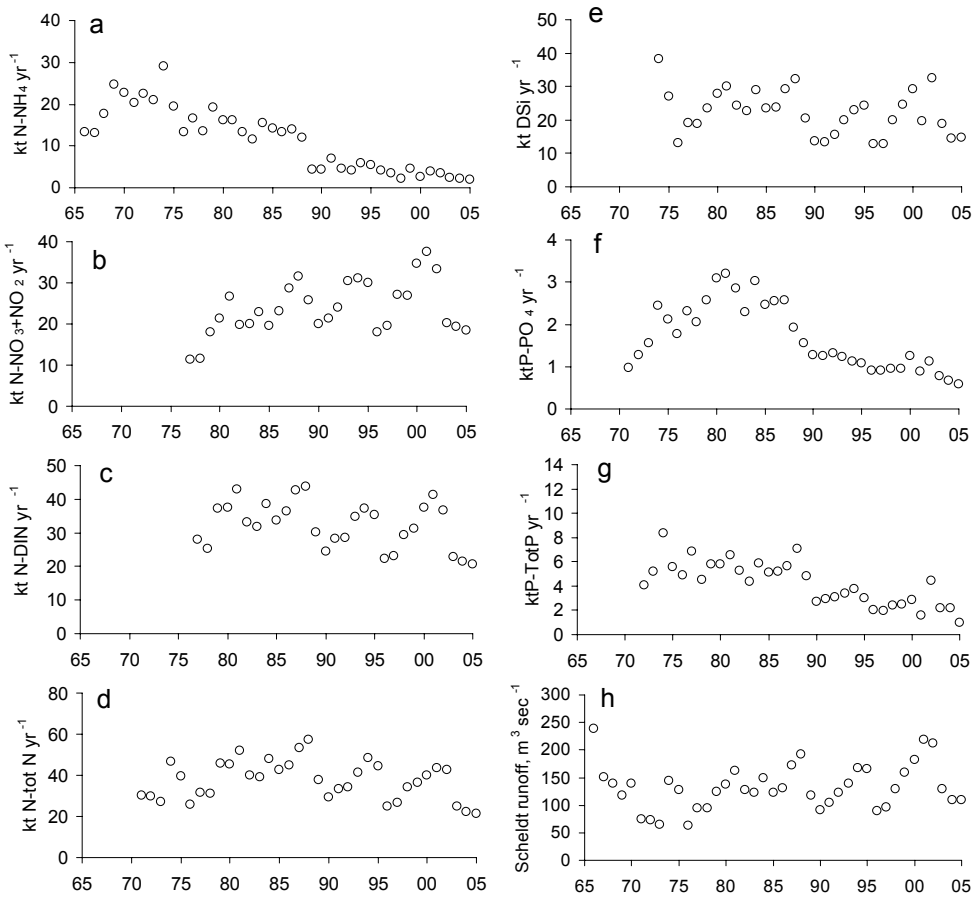

Figure 2.8. Inter-annual variations between 1966 and 2005 of Scheldt loads of NH_4^+ (a); NO_3^-+NO_2^- (b); DIN (c); Tot N (d); DSi (e); PO_4^{3-} (f); Total P (g) and mean yearly runoff (h). Loads were calculated based on nutrient concentration data at Schaar van ouden Doel from www.waterbase.nl courtesy of RIZA and Scheldt runoff available at Schelle (Courtesy of Administratie Waterwegen en Zeewegen).

Qualitative trends. The long-term changes observed in the annual Scheldt loads modify substantially the N:P:Si balance of nutrients discharged to the BCZ since the three last decades (Fig. 2.9). Major shifts occurred in the late eighties when the molar TN:TP ratio increased from values close to the Redfield's ratio in the 1970-1990 period to values higher than 30 in the present-day (Fig. 2.9a). This shift is much more pronounced for the DIN: PO_4^{3-} ratio, which amounted 30 in the mid-seventies and increased by more than a factor 2 (Fig. 2.9a). This shift, stressing a dramatic excess of N over P, is mainly caused by the significant reduction of PO_4^{3-} (Fig. 2.8f) compared to DIN loads (Fig. 2.8c; Soetaert *et al.*, 2006). Compared to the N:Si stoechiometry of diatoms, N largely exceeds Si (DIN:DSi ~ 3) since the mid-70's (Fig. 2.9b). This excess is exacerbated in the 1990's although slightly relieved during the last years. Molar ratios of DSi:PO_4^{3-} present value close to 10 from mid-70's up to mid-80's, lower than the diatom Si:P (*i.e.* 16) indicating a deficit of DSi for diatom growth. This situation reversed in the late eighties when DSi: PO_4^{3-} ratios increase up to 25 indicating at that time a potential PO_4^{3-} limitation for diatom growth (Fig. 2.9c).

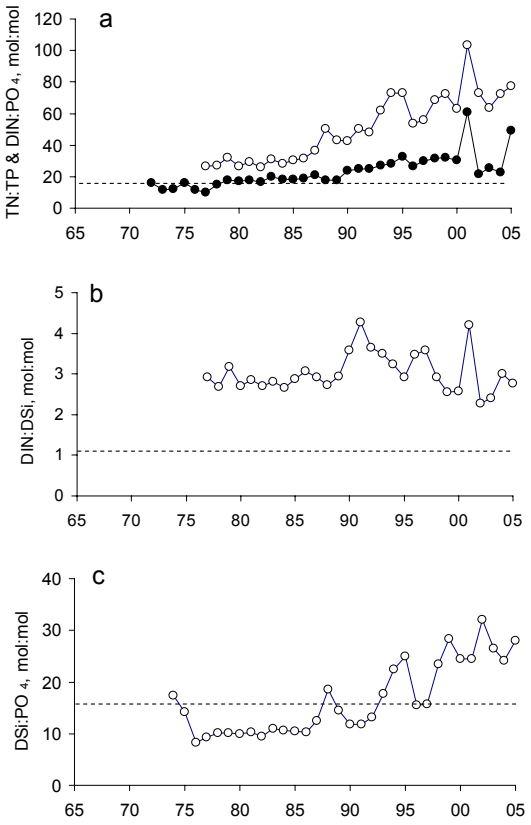

Figure 2.9. Interannual variations (1972-2005) of Scheldt load molar ratios DIN:PO_4^{3-} (open dots) and TN:TP (filled dots) (a); DIN:DSi (b); DSi:PO_4^{3-} (c) compared to phytoplankton N:P (Redfield *et al.*, 1963) and diatom N:Si and Si:P (Brzezinski, 1985) stoechiometry (hatched lines).

2.3 Atmospheric nitrogen deposition

The tropospheric environment of the North Sea and more particularly of the Southern Bight of the North Sea is surrounded by industrialised countries which are important sources of atmospheric nitrogen. Atmospheric inputs are delivered to surface waters through dry deposition of gases and aerosol particles and in wet deposition. Nitrogen deposition is influenced by wind speed and direction, wave size and frequency, and precipitation with the highest deposition occurring during strong winds, high and frequent waves and abundant precipitation events during winter and summer storms (Spokes & Jickells, 2005 and references therein).

2.3.1 Emissions of gaseous nitrogen by adjacent countries of BCZ

BCZ, as adjacent coastal areas, is submitted to reactive N gasses originating from Belgium, France, Germany, the Netherlands and the United Kingdom, but also from the intense ship traffic occurring in the North Sea and adjacent Atlantic Ocean (OSPAR, 2005). These N emissions to the atmosphere have been estimated to some 3 216 kt N yr^{-1} in 2001 among which 51% as NO_x (Fig. 2.10a) and 49% as NH_y (Fig. 2.10b). Emissions of NO_x have decreased by some 35% between 1990 and 2001, especially in France, Germany and UK (Fig. 2.10a). NH_y emissions also decreased in the same period but to a smaller extent (12%; Fig. 2.10b).

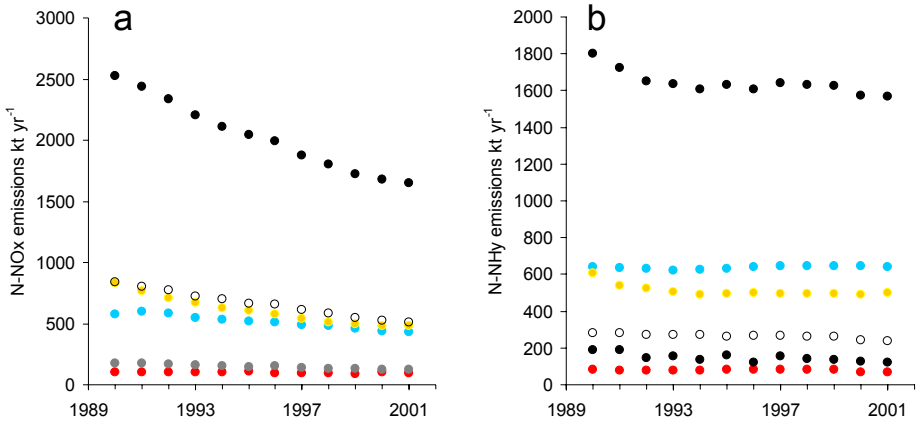

Figure 2.10. Inter-annual variation of annual N emission as N-NO_x (a) and N-NH_y (b) in Belgium (red), France (blue), Germany (yellow), The Netherlands (grey), the United Kingdom (white) and total (black). Source: OSPAR data (OSPAR, 2005).

2.3.2 Atmospheric deposition of N and P into BCZ

N deposition to the BCZ has been quantified using the Unified EMEP model simulating atmospheric transport and deposition of acidifying and euthrophying compounds in Europe (Simpson *et al.*, 2003; OSPAR, 2005). Results indicate

little variations in N deposition between 1991 and 2001 (Fig. 2.11) amounting in average to 1 t N $km^{-2}yr^{-1}$ from which 55% as NO_x and 45% as NH_y. This result is in very good agreement with the value estimated by Rousseau *et al.* (2004) based on literature data on measurements and/or modelling available for the Southern North Sea (Nelissen & Stefels, 1988; Rendell *et al.*, 1993). This synthesis estimates a specific N deposition flux varying between 0.96 and 1.04 t N km^{-2} yr^{-1}. N deposition into BCZ is therefore estimated for the BCZ superficy (3600 km^2) to 3.6 kt N yr^{-1}, corresponding to 0.1 % of the total N emissions by bordering countries of the Southern Bight of the North Sea.

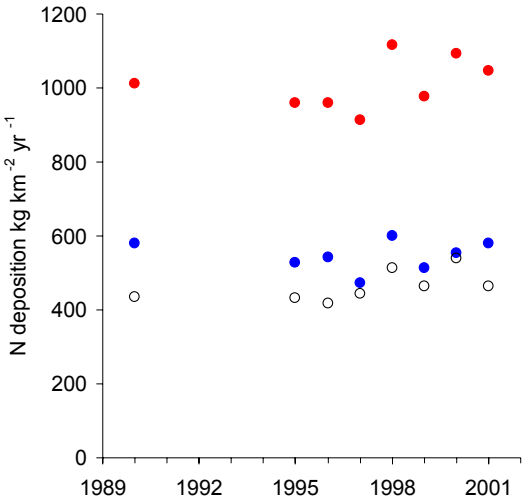

Figure 2.11. Inter-annual variation of annual N deposition (NO_x in white, NH_y in blue, total in red) in BCZ. Source : OSPAR data (OSPAR, 2005).

N emissions originating from France and UK, located upstream BCZ with respect to dominant winds, contributed to 46 % of N deposition in BCZ, Belgium and the Netherlands to 27% and the rest (26%) from ship traffic and other bordering countries such as Germany (OSPAR, 2005).

2.4 Transboundary fluxes

Transboundary nutrient fluxes between BCZ and the adjacent marine areas of France and the Netherlands are those associated with the Southwesterly Atlantic water fluxes enriched by the nutrients brought by the rivers Seine, Somme, Authie and Canche, and Rhine (Lacroix *et al.*, 2004; Fig. 1.2 in Ruddick and Lacroix, 2008). It is commonly admitted that residual currents flow parallel to the coast and that lateral advective fluxes are negligible. The water inflow from the Channel into the Southern North sea is highly variable and

depends on the wind regime with stronger inflow driven by dominant southwesterly winds themselves related to NAO (Breton *et al.*, 2006; Ruddick & Lacroix, 2008). Quantifying nutrient exchange between BCZ and adjacent areas is therefore very complex and requires modeling.

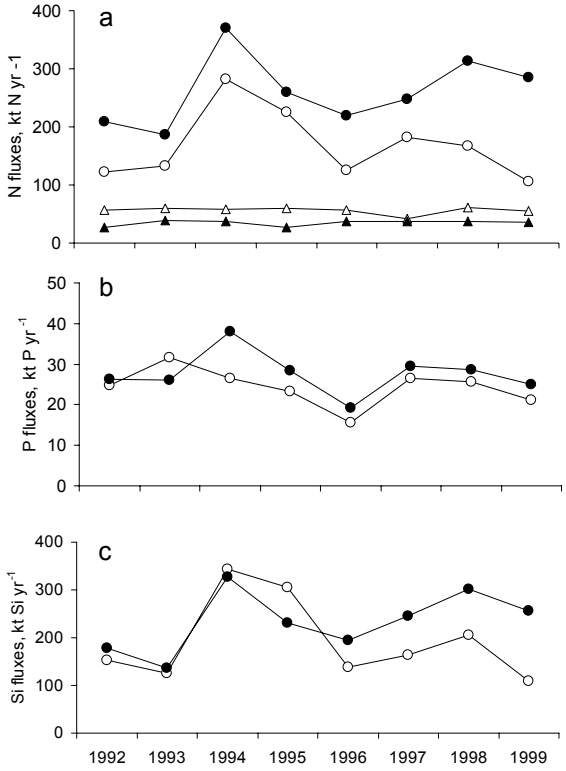

Figure 2.12. Transboundary fluxes of NO_3^-+NO_2^- (dots) and NH_4^+ (triangles) (a); PO_4^{3-} (b) and DSi (c) across the southwestern (Open symbols) and northeastern (filled symbols) borders of BCZ.

Estimations of transboundary fluxes of NO_3^-+NO_2^-, NH_4^+, PO_4^{3-} and DSi were calculated on a monthly basis for the period 1992-1999 as the product of modeled water fluxes and nutrient concentrations measured along the BCZ southwestern (French-Belgian) and northeastern (Belgian-Dutch) bordering transects (see details in Rousseau *et al.*, 2004). The Southwesterly Atlantic water fluxes across the BCZ were calculated using a vertically integrated, 2D

"shallow water wave equation" model (J. Ozer, unpublished). These calculations show that the annual nutrient fluxes across the southwestern and northeastern borders of BCZ are highly variable from one year to another (Fig. 2.12). These fluxes are one order of magnitude higher than the Scheldt nutrient loads (section 2.3.3). The significant fluxes of 1994 correspond to a particularly high intrusion of the Southwesterly Atlantic water into BCZ due to dominant southwesterly winds related to high NAO (Breton *et al.*, 2006).

On an annual basis, there is a net export of NO_3^-+NO_2^- from the BCZ to the North (Fig. 2.12). This is also generally the case for PO_4^{3-} and DSi although some years retention of these nutrients occurs in the BCZ. On the contrary, BCZ acts as a sink for NH_4^+ (Fig. 2.12).

2.5 Nutrient enrichment of BCZ

2.5.1 Spatial distribution of winter nutrients

Nutrient enrichment of BCZ results from the nutrient loads associated to freshwater discharges, atmospheric deposition and Southwesterly Atlantic water inflow (see sections 2.2-2.4). The contribution of these nutrient sources varies with meteorological and hydrological conditions (Breton *et al.*, 2006) resulting in a strong variability of the spatial distribution of nutrient concentrations (Rousseau *et al.*, 2004). High nutrient concentrations associated to low salinity field on BCZ are prevalent when the Scheldt plume spreading is high and the Southwesterly Atlantic water intrusion is moderate. In contrast, a weak extent of the Scheldt plume associated to a large intrusion of Atlantic water into BCZ under persistent strong southwesterly winds result in higher salinities and lower nutrient concentrations.

The enrichment of BCZ is illustrated by the distribution of nutrients and salinity in winter 2003 (Fig. 2.13). As shown by salinity distribution, the Scheldt plume extended on the Southeastern part of BCZ (Fig. 2.13a). Nutrients show a clear gradient from the Scheldt mouth to offshore with higher concentrations close to river and canal mouths indicating the major role of the Scheldt as nutrient source in BCZ but also local effects of the IJzer and coastal tributaries. DIN concentrations (mostly as NO_2^-+NO_3^-) higher than 80 µM are recorded nearby the Scheldt mouth and along the coast decreasing progressively to the northwest where concentrations between 10 and 20 µM, *i.e.* higher than the signature of Atlantic waters (8 µM), are still measured (Fig. 2.13b-d). More than half of the southern BCZ area is characterized by PO_4^{3-} concentrations higher than 1 µM with maximum PO_4^{3-} concentrations (1.5-2 µM) offshore Zeebrugge and Ostend harbours (Fig. 2.13f). The distribution of DSi is similar with concentrations higher than 20 µM prevailing over half of the southern BCZ area (Fig. 2.13e).

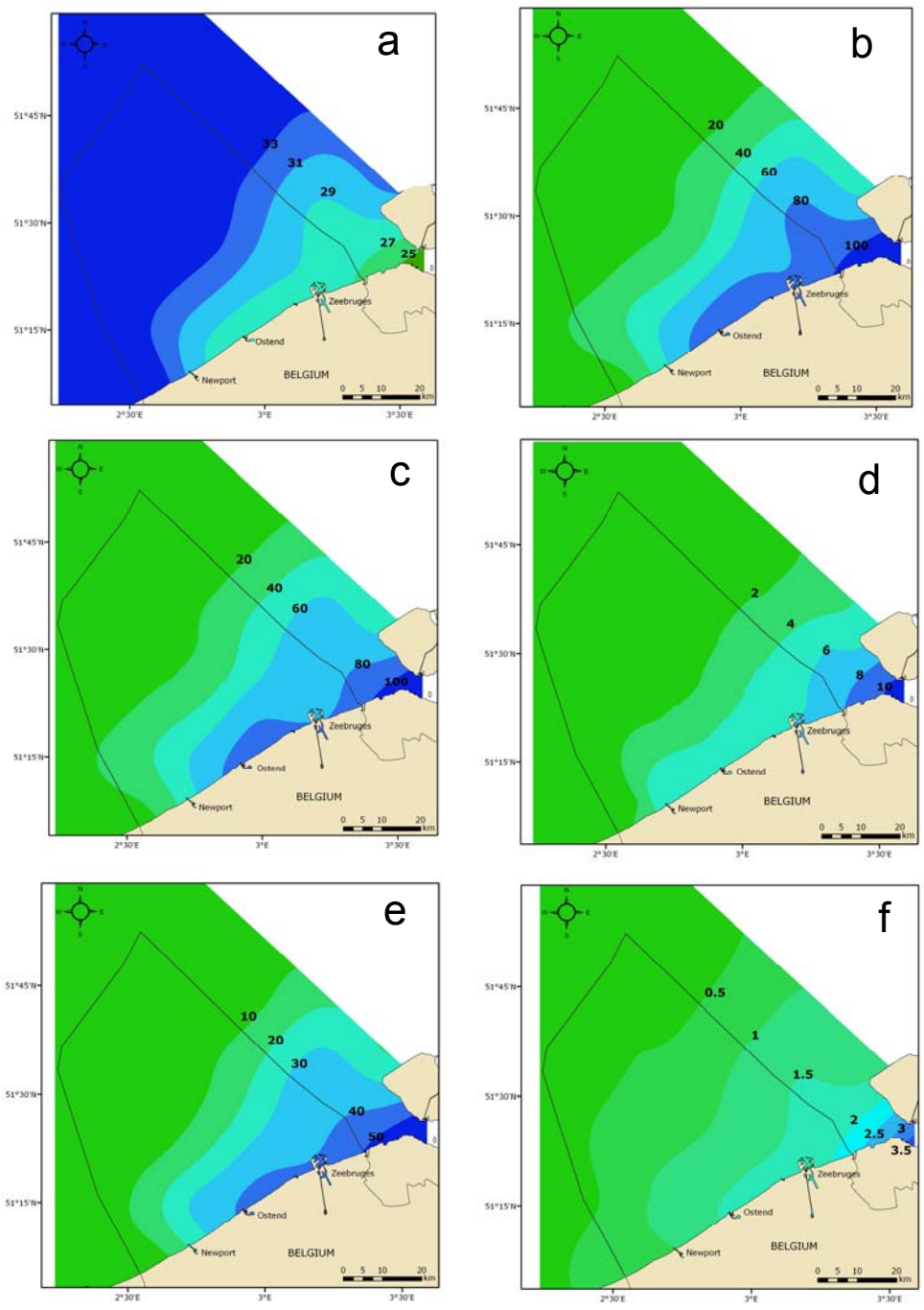

Figure 2.13. Spatial distribution of salinity (a); DIN (b); NO_3^-+NO_2^- (c), NH_4^+ (d), DSi (e) and PO_4^{3-} (f) concentrations (µM) in January 2003 in BCZ.

2.5.2 Long term changes in the enrichment of the BCZ

The average enrichment of the BCZ and its long term evolution were estimated using winter nutrient concentrations and salinity available for the period 1974-2005. In order to encompass hydrological variability, the average nutrient enrichment was computed as the nutrient concentration interpolated at the BCZ salinity of 33.5 as described in Rousseau *et al.* (2004). Both NH_4^+ (Fig. 2.14a) and PO_4^{3-} (Fig. 2.14c) concentrations decrease markedly during this three decade period, reaching values respectively lower than 1.5 and 1 µM in 2005. Such a trend is not observed for NO_3^-+NO_2^- (Fig. 2.14b) and DSi (Fig. 2.14d) in spite of high fluctuations. A long term average of 12 and 27 µM Si and N respectively is calculated. The contribution of NO_3^-+NO_2^- to inorganic N is significant and increases from 90% in the seventies to 95-97% in 2000-2005 (Fig. 2.14a,b). As a result, DIN concentrations do not show significant changes during the 1974-2005 period (not show). These long term changes in the global nutrient enrichment of BCZ reflect the evolution of Scheldt nutrient loads (Fig. 2.8). This is particularly evident for point source NH_4^+ and PO_4^{3-} whose decrease at sea corresponds to the marked drop in Scheldt loads during the late eighties (Fig. 2.8). The PO_4^{3-} decrease is however much less pronounced at sea than in the Scheldt estuary.due to the larger P inputs by inflowing Southwestern Atlantic waters (Lancelot *et al.*, 2005; 2007).

As a result of PO_4^{3-} winter concentration decrease, the N:P:Si balance of winter nutrients is significantly modified over the 1974-2005 period when compared to nutrient requirements of coastal phytoplankton (Redfield *et al.*, 1963) and diatoms (Brzezinski, 1985). Both N:P (Fig. 2.14e) and Si:P (Fig. 2.14g) winter molar ratios show a marked shift in the mid-eighties. The former evolves from values closed to Redfield ratio during the 1972-1985 period to high N excess conditions after the mid-1980's, with a most significant change during the nineties when it increased from 20 to more than 35 (Fig. 2.14e). The evolution of Si:P clearly indicates that the coastal ecosystem evolved from a Si limitation between 1974 and 1990 to a much balanced situation in terms of Si and PO_4^{3-} availability (Fig. 2.14g). N:Si molar ratios fluctuating between 2 and 5 indicates that DIN availability largely exceeded the Si requirement of diatom during the whole period (Fig. 2.14f).

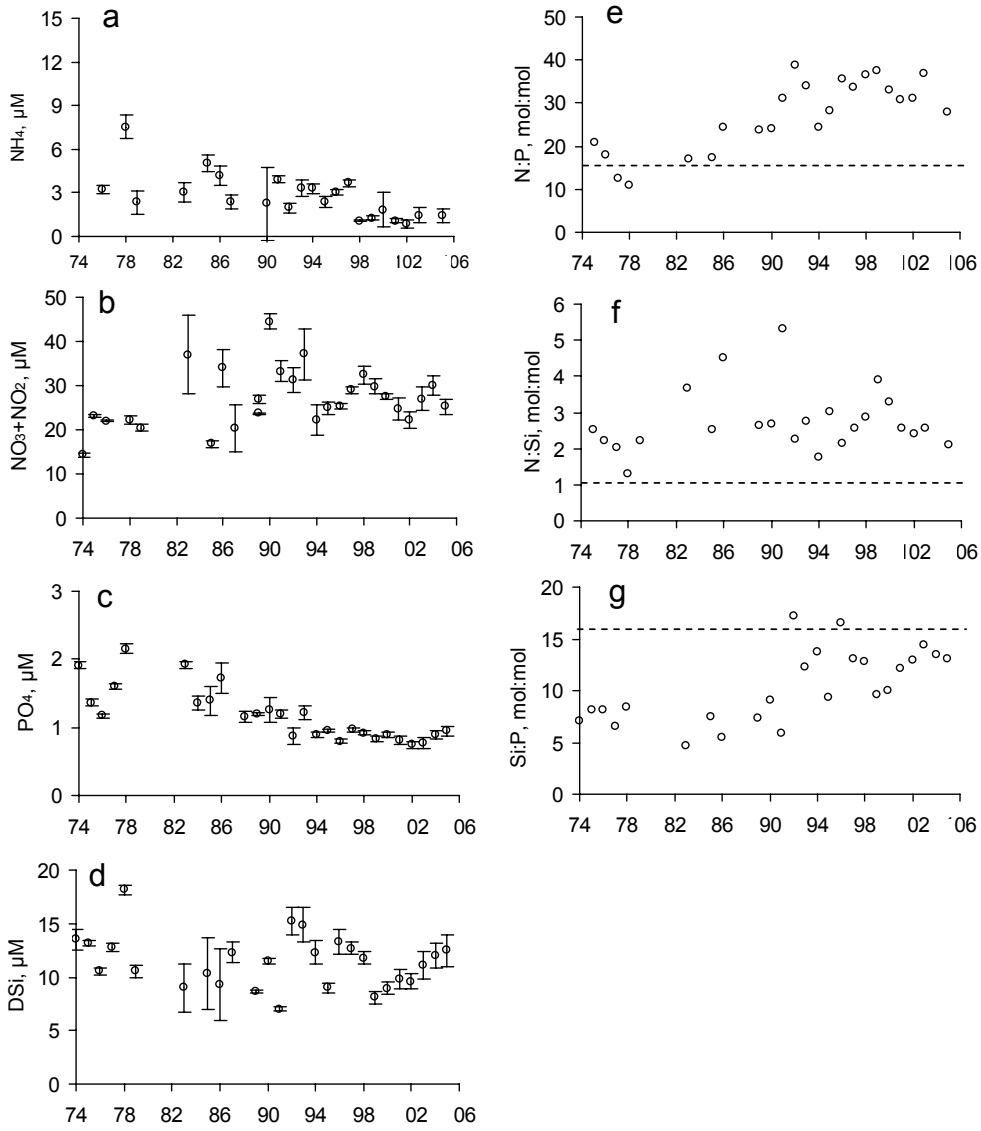

Figure 2.14. 1974-2005 evolution in BCZ of NH_4 (a), NO_3+NO_2 (b), PO_4 (c) and DSi (d) average concentrations and N:P (e), N:Si (f), Si:P (g) winter molar ratios. Hatched line indicates phytoplankton N:P (Redfield *et al.*, 1963) and diatom N:Si and Si:P (Brzezinski, 1985) stoichiometry.

2.6 Conclusions and perspectives

Nutrient enrichment of the BCZ, at the base of eutrophication problems, results from local riverine inputs of the Scheldt, the IJzer and the coastal tributaries, from atmospheric nutrient and from transboundary fluxes brought by the river-enriched Southwesterly Atlantic waters (Lacroix *et al.*, 2004).

2.6.1 Nutrient emissions and loads

The major nutrient loads to the BCZ are the river-enriched transboundary fluxes which are submitted to important interannual fluctuations. These fluxes are in average one order of magnitude larger than riverine and coastal tributary loads while atmospheric deposition is of minor importance.

Emissions of nutrients in the BCZ watershed are strongly correlated to economic development and environmental policy. As illustrated for the Scheldt basin, nutrient emissions varied considerably between 1950 and 2000. Development of demography and economic needs following the WW-II period has resulted in the increase of point and diffuse sources of N and P due to untreated sewage effluents and intensification of agriculture. From the 70's on, ecological considerations were translated in more restrictive environmental policy rules that resulted in a progressive reduction of nutrient point sources thanks to the implementation of waste water treatment and the banishment of polyphosphate-containing detergents. However, agricultural practices, with large-scale use of fertilizers and intensive cattle-farming proved to be, politically, much more difficult to control and diffuse nutrient sources continued to increase until the 2000's. Nutrient loads to the BCZ partly reflect this economical and environmental evolution but are also strongly dependant on complex biogeochemical transformations occurring in the watershed. For example, although N point sources decreased since the 70's, N loads did not significantly decrease probably because of the still important diffuse sources and the restoration of better oxygen levels in streams, reducing the self purification (denitrification) of the N load. On the contrary, phosphorus loads strongly decreased since the 70's as a direct result of reduced emissions combined to increased in-stream retention processes thanks to higher oxygen levels. The link between nutrient emissions and loads to the BCZ is thus complex to understand and to predict. Comprehensive tools such as mathematical models describing the complex ecological interactions between the nutrients and the environment are needed to predict such changes. Their development and implementation should be considered as priority research field in the future (see Lancelot *et al.*, 2008).

2.6.2 Nutrient budget in the BCZ

An annual budget of inorganic nutrients in the BCZ has been established based on estimations of riverine inputs (section 2.2, Rousseau *et al.*, 2004), atmospheric deposition (section 2.3) and transboundary fluxes (section 2.4). This budget has been established as an average for the period 1990-2000.

Table 2.3. Average annual N and P budgets in the BCZ for the period 1990-2000. Average riverine loads have been estimated from Rousseau *et al.* (2004). OUT-IN represents the difference between nutrient inputs and outputs.

kt N yr^{-1}	BCZ
Loads from the BCZ watershed	43
Loads from atmosphere (DIN only)	3.5
Net loads to Northeastern area (DIN only)	72
OUT-IN	+ 25.5

kt P yr^{-1}	BCZ
Loads from the BCZ watershed	2.7
Net loads to Northeastern area	4.5
OUT-IN	+ 1.8

The difference between nutrient inputs (riverine loads, atmospheric deposition) and outputs (net average export of DIN and P for the period; section 2.4), OUT-IN, indicates a net average annual export of both DIN and P (Table 2.3). This suggests the existence of an important nutrient source within the BCZ. The DIN and P source could well originate from organic matter mineralization processes occurring in both the water column and/or sediments. Organic forms of nutrients are not considered in this budget which is limited to inorganic forms of N and P. Data on organic nutrients are hardly available so that their significance is not currently quantifiable. According to Brion *et al.* (2008), organic N could represent between 30% (winter) and 90% (summer) of the total N pool in Channel waters, and between 20% (winter) and 40% (summer) in Scheldt plume waters. Additionally, Cornell *et al.* (1995) reports DON concentrations in rainwater over the sea twice as high as the DIN concentrations. Diaconu (2008) showed that NH_4^+ regeneration rates through the mineralization of organic matter were intensive in the water column of the Southern Bight of the North Sea, and more or less equalled inorganic N uptake on an annual scale. A nutrient budget established on basis of both inorganic and organic nutrients would thus lead to different conclusions. Lancelot *et al.* (2005) have estimated a global N and P annual budget, including organic nutrient forms, for the BCZ area under influence of the Scheldt (1500 km^2) based on simulations with the ecological MIRO model of nutrient uptake and remineralization. These authors concluded that nowadays this area retained annually 2 and 4% of the respective total N and total P inputs to the BCZ. Nitrogen transformations in the BCZ are suggested to decrease inorganic and organic N forms flowing out of the area by respectively 3 and 1 %, respectively, compared to inflows. Altogether the model

calculates an increased export of NH_4 and PO_4 towards the North Sea (Dutch coastal zone).

Owing to their presumed importance in the BCZ, measurements of organic nutrient pools and dynamics in the BCZ constitute then a priority for future research. Accordingly organic nutrient concentration measurements should be included in future monitoring programmes.

2.7 References

Baeyens W., Van Eck B., Lambert C., Wollast R. and L. Goeyens. 1998. General description of the Schedlt estuary. Hydrobiologia 366: 1-14

Billen G. and J. Garnier. 1997. The Phison River plume: coastal eutrophication in response to changes in land use and water management in the watershed. Aquatic Microbial Ecology 13(1): 3-17

Billen G., Garnier J. and V. Rousseau. 2005. Nutrient fluxes and water quality in the drainage network of the Scheldt basin over the last 50 years. Hydrobiol. 540: 47-67

Billen G., Garnier J., Deligne C. and C. Billen. 1999. Estimates of early industrial inputs of nutrients to river systems : implication for coastal eutrophication. The Science of the Total Environment 243/244: 43-52

Billen G., Garnier J., Ficht A. and C. Cun. 2001. Modeling the response of water quality in the Seine river estuary to human activity in its watershed over the last 50 years. Estuaries, 24(6B): 977-993

Billen G., Lancelot C. and M. Meybeck. 1991. N, P and Si retention along the Aquatic Continuum from Land to Ocean. In: R.F.C. Mantoura, J.-M. Martin and R. Wollast [eds.], Ocean Margin Processes in Global Change. John Wiley & Sons, Ltd, p 19-44

Billen G., Lancelot C, Debecker E and P. Servais. 1986. the terrestrial-marine interface: modeling nitrogen transformations during its transfer through the Scheldt rver system and its estuarine zone. In: Marine Itefaces Ecohydrodynamics (Nihoul J.C. J., ed). Elsevier, Amsterdam, pp. 429-452

Breton E., Rousseau V., Parent J.-Y., Ozer J. and C. Lancelot. 2006. Hydroclimatic modulation of diatom/*Phaeocystis* blooms in the nutrient-enriched Belgian coastal waters (north sea). Limnology and Oceanography 51(3): 1401-1409

Brion N., Andersson M.G I., Elskens M., Diaconu C., Baeyens W., Dehairs F., and J. Middelburg. 2008. Nitrogen cycling, retention and export in an eutrophic temperate macrotidal estuary. Marine Ecology Progress Series 357: 87-99

Brzezinski M.A. 1985. The Si:C:N ratio of marine diatoms: interspecific variability and the effect of some environmental variables. Journal of Phycology 21: 347-357

Brion N., Elskens M., De Galan S., Diaconu C., Baeyens W;, Chou L., van der Zee C., Roevros N., Borges A. V., Schiettecatte L.-S, Delille B., Frankignoulle M., Laane R. W. P. M. and T. van Engeland. 2008. Biogeochemical cycling of carbon, nitrogen and phosphorus in the North Sea (CANOPY). Final report. Belgian Science Policy Publication - SPSDII Research contract n° EV20

Chou L. and R. Wollast. 2006. Estuarine Silicon dynamics. In: the silicon cycle, human perturbations and impacts on aqutic systems. In: Ittekot V., Ungr D., Humborg C. and Tac An N. (Eds). Island press, pp. 93-120

Cornell S., Rendell A. and T. Jickells. 1995. Atmospheric inputs of dissolved organic nitrogen to the Oceans. Nature 376: 243-246

Diaconu C. 2008. Nitrogen dynamics in estuarine and coastal marine ecosystems. Case study: the Scheldt estuary and Southern Bight of the North Sea. PhD Sciences, Vrije Universiteit Brussel. 266 pp.

Herman P.M.J. and C.H.R. Heip. 1999. Biogeochemistry of the Maximum TURbidity Zone of Estuaries (MATURE): some conclusions. Journal Marine Systems 22: 89-104

Lacroix, G., Ruddick K., Ozer J. and C. Lancelot. 2004. Modelling the impact of the Scheldt and Rhine/Meuse plumes on the salnity distribution in Belgian waters (southern North Sea). Journal Sea Research 52: 149-163

Lancelot C. 1995. The mucilage phenomenon in the continental coastal waters of the North Sea. The Science of the Total Environment 165: 83-102

Lionard M., Muylaert K., Tackx M., and W. Vyverman. 2008. Evaluation of the performance of HPLC-CHEMTAX analysis for determining phytoplankton biomass and composition in a turbid estuary (Schelde, Belgium). Estuarine Coastal and shelf Science 76(4): 809-817

Maes F. *et al.* 2005. A flood of space: towards a spatial structure plan for sustainable management of the North Sea. Gaufre Project. Belgian Science Policy

Muylaert K., Van Wichelen J., Sabbe K. and W. Vyverman. 2001. Effects of freshets on phytoplankton dynamics in a freshwater tidal estuary (Schelde, Belgium). Archiv fur Hydrobiologie 150(2): 269-288

Muylaert K., Tackx M. and W. Vyverman. 2005. Phytoplankton growth rates in the freshwater tidal reaches of the Scheldt estuary (Belgium) estimated using a simple light-limited primary production model. Hydrobiologica 540: 127-140.

Nelissen, P.H.M. and J. Stefels. 1988. Eutrophication of the North Sea. Nederlands Instituut voor Onderzoek der Zee. Report 1988-4 100 pp.

Officer C.B. and J.H. Ryther. 1980. The possible importance of silicon in marine eutrophication. Marine Ecology Progress Series 3: 83-91

OSPAR. 2005. Common Procedure for the Identification of the Eutrophication Status of the OSPAR maritime area, OSPAR agreement 2005-3

Redfield A.C., Ketchum B.H. and F.A. Richards. 1963. The influence of organisms on the composition of sea-water. In M.N. Hill [ed], The Sea. John Wiley & sons. NY pp 12-37

Rendell A.R., Ottley C.J., Jickells T.D. and Harrison R.M. 1993. The atmospheric input of nitrogen species to the North Sea. Tellus 45B: 53-63

Rousseau V., Breton E., De Wachter B., Beji A., Deconinck M., Huijgh J., Bolsens T., Leroy D., Jans S. and C. Lancelot. 2004. Identification of Belgian maritime zones affected by eutrophication (IZEUT). Towards the establishment of ecological criteria for the implementation of the OSPAR Common Procedure to combat eutrophication. Belgian Science Policy Publications, Brussels, D/2004/1191/28, 77 pp

Rousseau V., Park Y., Ruddick K., Vyverman W., Jans S. and C. Lancelot. 2008. Phytoplankton blooms in response to nutrient enrichment. In: Current Status of Eutrophication in the Belgian Coastal Zone. Rousseau V., Lancelot C. and D. Cox (Eds). Presses Universitaires de Bruxelles, Bruxelles, pp. 45-59

Ruddick K. and G. Lacroix. 2008. Hydrodynamics and meteorology of the Belgian coastal zone. In: Current Status of Eutrophication in the Belgian Coastal Zone. Rousseau V., Lancelot C. and D. Cox (Eds). Presses Universitaires de Bruxelles, Bruxelles, pp. 1-15

Servais P., Garnier J., Demarteau N., Brion N. and G. Billen. 1999. Supply of organic matter and bacteria to aquatic ecosystems through waste water effluents. Water Research 33: 3521-3531

Simpson D., Tuovinen J.P., Emberson L., Ashmore M.R. 2003. Characteristics of an ozone deposition module II: Sensitivity analysis. Water, air and soil Pollution 143(1-4): 123-137

Soetaert, K. and P.M.J Herman. 1995. Nitrogen dynamics in the Westerschelde Estuary (SW Netherlands) estimated by means of the ecosystem model MOSES. Hydrobiologia 311: 225-246

Soetaert K., Middelburg J.J., Heip C., Meire P., van Damme S. and T. Maris. 2006. Long-term change in dissolved inorganic nutrients in the heterotrophic Scheldt estuary (Belgium, The Netherlands). Limnology and Oceanography 51(1): 409-423

Spokes L.J. and T.D. Jickells. 2005. Is the atmosphere really an important source of reactive nitrogen to coastal waters? Continental Shelf Research 25: 2022-2035

van Bennekom A.J. and F.J. Wetsteijn. 1990. The winter distribution of nutrients in the Southern Bight of the North Sea (1961-1978) and in the estuaries of the Scheldt and the Rhine/Meuse. Netherlands Journal of Sea Research 25: 75-87

Van Damme S., Meire P., Maeckelberghe H., Verdievel M., Bourgoing L., Taverniers E., Ysebaert T. and G. Wattel. 1995. De waterkwaliteit van de Zeeschelde: evolutie in de voorbije dertig jaar. Water 85: 244-256

Van der Zee C. and L. Chou 2005. Seasonal cycling of phosphorus in the Southern Bight of the North Sea. Biogeosciences Discussions 1: 681-707

van der Zee C., Roevros N. and L. Chou. 2007. Phosphorus speciation, transformation and retention in the Scheldt estuary (Belgium/The Netherlands) from the freshwater tidal limits to the North Sea. Marine Chemistry 106(1-2): 76-91

Van Geystelen L., D. Verhoeve and H. De Schepper. 1980. De waterqualiteit van de Schelde (vanaf de Freanse grens tot Antwerpen), periode 1977-1978. Report. Inst. V. Hygiene en Epidemiologie. Ministerie van Volksgezondheid en van het Gezin. Brussels.

Wollast R. and F. De Broeu F. 1971. Study of behaviour of dissolved silica in the estuary of the Scheldt. Geochim. Cosmochim. Acta 35:613-620

Zwolman J.J.G. 1994. Seasonal variability and biogeochemistry of phosphorus in the Scheldt estuary, South-west Netherlands. Estuarine Coastal Shelf Science 39: 227-248

CHAPTER 3

Phytoplankton blooms in response to nutrient enrichment

Véronique Rousseau[1], Youngje Park[2], Kevin Ruddick[2], Wim Vyverman[3], Jean-Yves Parent[1] and Christiane Lancelot[1]

[1] Université Libre de Bruxelles (ULB), Ecologie des Systèmes Aquatiques (ESA), CP221, boulevard du Triomphe, B-1050 Brussels, Belgium
[2] Management Unit of the North Sea Mathematical Models (MUMM), Royal Belgian Institute for Natural Sciences, Gulledelle 100, B-1200 Brussels, Belgium
[3] Universiteit Gent (UG), Protistologie en Aquatische Ecologie, Krijgslaan 281 S8, B-9000 Gent, Belgium

3.1. Phytoplankton blooms in the eutrophied Belgian Coastal Zone

Delivery of continental nutrients to coastal waters generally results in phytoplankton blooms characterized by high biomass levels. Such is the case in the Belgian Coastal Zone (BCZ) where satellite images recurrently detect high Chl *a* concentrations (Fig. 3.1) particularly in the coastal waters influenced by the nutrient-enriched freshwater of the Scheldt and coastal tributaries (see Fig. 2.13 in Brion *et al.*, 2008). These phytoplankton blooms are particularly significant in April and May, when Chl *a* concentrations higher than 10 and locally 25 mg m^{-3} are reached in Belgian and Dutch nearshore waters (Fig. 3.1). Phytoplankton blooms start in average in March, in the clearest Southwestern coastal waters (Fig. 3.1; Borges & Frankignoulle, 2002; Muylaert *et al.*, 2006), and propagate in April-May in the almost entire BCZ and adjacent waters (Fig. 3.1). During summer and fall, moderate Chl *a* concentrations, *i.e.* 3-10 mg m^{-3}, are still detected but are restricted to the very nearshore region (Fig. 3.1), presumably due to the local influence of nutrient enrichment at that time of the year.

Satellite time series Chl *a* data retrieved for stations 230, 330 and 435 along an in-offshore transect (Fig. 3.1) reproduce well the phytoplankton bloom dynamics in the BCZ, highlighting a major spring bloom at all 3 stations but significant summer blooms at the coastal station 230 only (Fig. 3.2). The time series data show the transient nature of the phytoplankton blooms as well as a significant interannual variability in their magnitude and timing (Fig. 3.2).

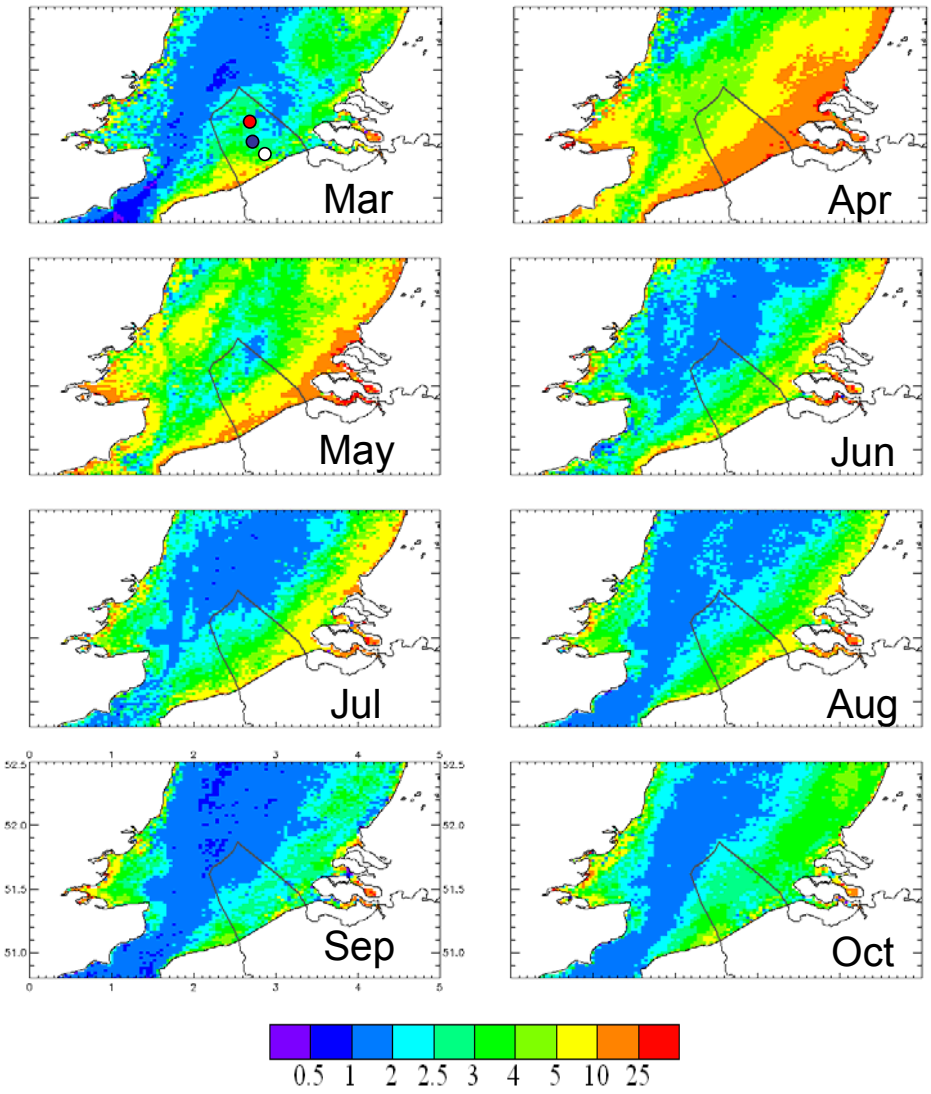

Figure 3.1. Monthly means of MERIS chl *a* concentration (mg m^{-3}) for the period 2003-2007 derived from the MERIS sensor using processor version 5.02 and 5.04 with data quality screened by use of the product confidence flag. The Belgian continental shelf is indicated by solid black lines. White, blue and red dots indicate stations 230, 330 and 435 respectively. Data provided by the European Space Agency in the framework of Envisat AOID 3443 and processed in the BELCOLOUR-2 project.

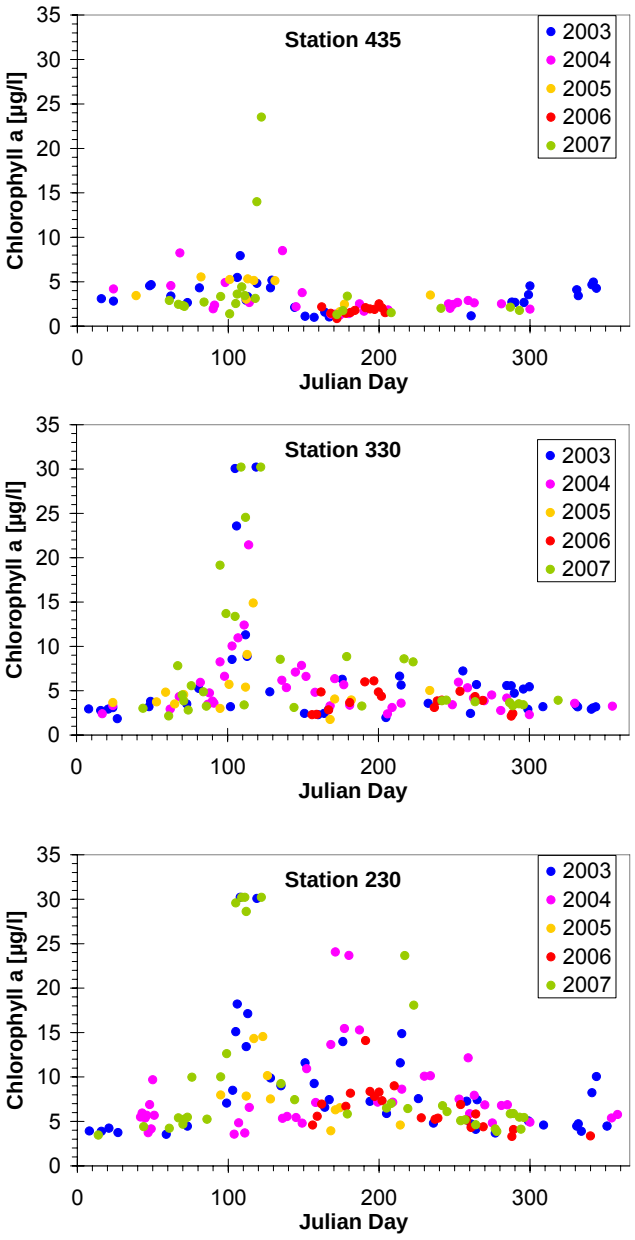

Figure 3.2. Time series of MERIS chlorophyll *a* concentration for the period 2003-2007, except September 2005-June 2006. Location of stations 230, 330 and 435 is shown in Figure 3.1. Satellite data source and processing as in Figure 3.1.

3.2. *Phaeocystis* and diatom blooms in the BCZ

Analysis of phytoplankton composition indicates that two major taxa, the diatoms and the colonial haptophyte *Phaeocystis globosa*, are contributing to the bulk Chl *a*. Other phytoplankton groups such as cyanobacteria, euglenophytes, cryptophytes, chlorophytes or dinoflagellates are also present but as very minor contributors (Muylaert *et al.*, 2006). The phenology of diatoms and *Phaeocystis* blooms has been intensively investigated during 13 years (1988-2000) at station 330 (see location in Fig. 3.1), chosen because it represents the average physico-chemical conditions prevailing in the BCZ (Rousseau, 2000). This phytoplankton time series data show that diatoms are present during the whole vegetative season while *Phaeocystis* colonies occur only as a single spring event lasting between 4 and 13 weeks (Fig. 3.3; Breton *et al.*, 2006).

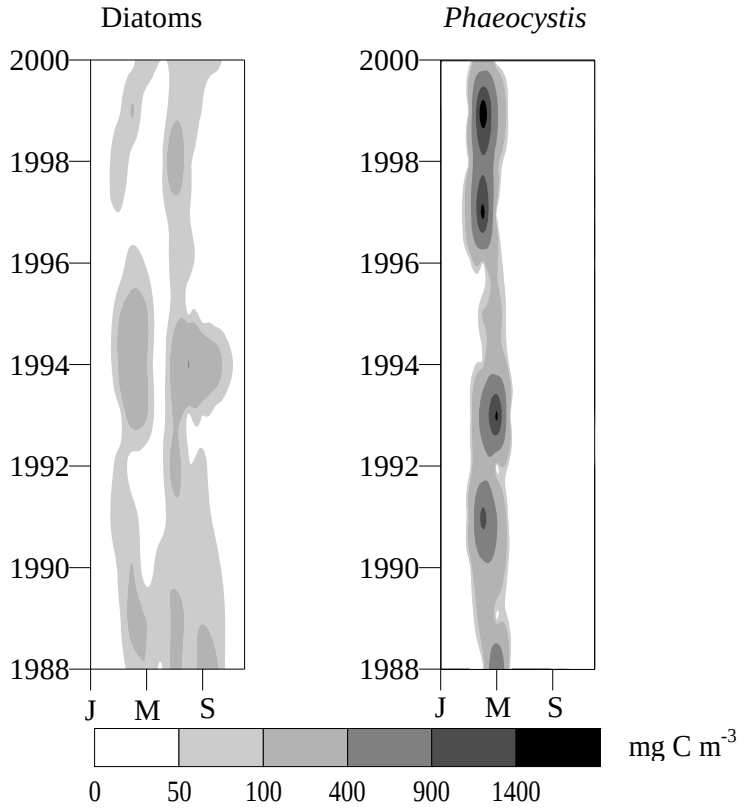

Figure 3.3. Seasonal pattern of diatom and *Phaeocystis* colony biomass (mg C m^{-3}) at station 330 from 1988 to 2000 (JMS: January, May, September). From Breton *et al.* (2006). Copyright (2008) by the American Society of Limnology and Oceanography, Inc.

Contrary to diatoms which constitute the major phytoplankton group in well balanced N:P:Si enriched waters, the spring proliferation of *Phaeocystis* colonies is the eutrophication-related event in the BCZ and the Southern Bight of the North Sea. When blooming, *Phaeocystis* cell density can reach 50-120 10^6 cells L^{-1} and represent some 70 % of the spring net primary production (Rousseau *et al.*, 2000). These high biomasses are related to the ability of *Phaeocystis* to rapidly form gelatinous colonies containing several thousands of cells (Fig. 3.4), whose size makes them unpalatable for mesozooplankton (Daro *et al.*, 2008). Ungrazed colonies are responsible for the deposit of thick layers of odorous foam on the beaches resulting from food chain disruption (Fig. 3.4; Lancelot, 1995). These undesirable colony blooms are not recent as demonstrated by model reconstruction of Seine and Scheldt watersheds, showing that *Phaeocystis* colonies were already blooming in pristine time (Lancelot *et al.*, 2008). At that time, *Phaeocystis* colonies were present under grazable forms efficiently transferred to higher trophic levels.

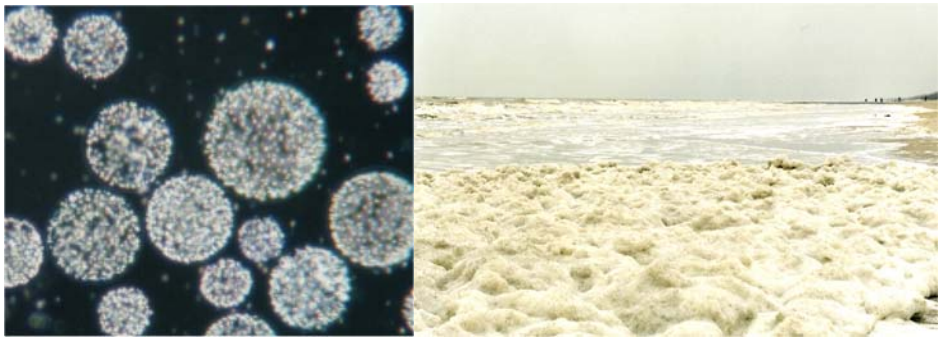

Figure 3.4. Eutrophication-related event in the BCZ; *Phaeocystis globosa* spherical colonies (left)*;* foam accumulation on the beach of Oostend in May 1998 (right).

3.2.1. Present-day variability of the magnitude of diatoms and *Phaeocystis* blooms

Diatom and *Phaeocystis* blooms at station 330 present significant interannual fluctuations in their magnitude with most of the years dominated by *Phaeocystis* but a few by diatoms (Fig. 3.3). This year to year variability results from the combined effects of hydro-climatic variability and human activities via the Scheldt nutrient loads (Fig. 3.5; Breton *et al.*, 2006). Hydro-climatic variability is driven by the North Atlantic Oscillation (NAO) which governs meteorological conditions, *i.e.* local wind dominance and rainfall, over the Northwestern Europe (Hurrell, 1995). Wind and rainfall, in turn, determine the hydrodynamical features of the BCZ with a higher propagation of English Channel waters and higher Scheldt water and nutrient discharge under southwesterly wind dominance and high rainfall in the Scheldt watershed (Fig. 3.5). Wind direction also influences the spreading of the Scheldt plume at station 330 with lower freshwater influence under southwesterly wind dominance (Fig. 3.5). On this

basis, Breton *et al.* (2006) demonstrated that diatom biomass variability at station 330 is mostly related to a change in hydrodynamics, *i.e.* the balance between English Channel Water Inflow and Scheldt freshwater inputs in the BCZ, while *Phaeocystis* bloom variability results from the NAO modulation of Scheldt freshwater and nutrient discharge on the one hand, and their spreading in the BCZ on the other hand (Fig. 3.5).

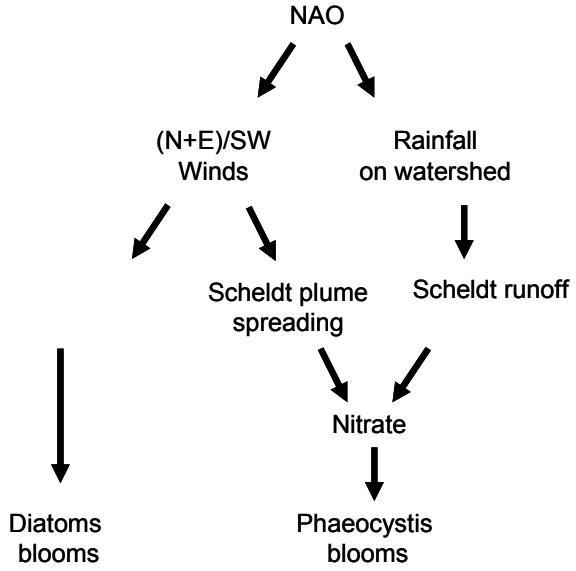

Figure 3.5. Mechanisms linking NAO, meteorological, hydrodynamical, physico-chemical characteristics and diatom and *Phaeocystis* spring blooms at station 330. Redrawn from Breton *et al.* (2006). (N+E)/SW represents the ratio between northern and eastern to southwesterly winds.

3.2.2. Present-day interannual variability of succession, timing and duration of diatoms and *Phaeocystis* blooms

A hierarchical classification of phytoplankton observed at station 330 identified a recurrent successional pattern of three diatom communities and *Phaeocystis* (Fig. 3.6; Rousseau *et al.*, 2002; Rousseau *et al.*, in preparation). These assemblages of euryhalin and eurytherm species are typical of the non-stratified Southern Bight of the North Sea. The phytoplankton spring succession is invariably initiated in late winter-early spring by bentho-pelagic diatom species *Paralia sulcata*, *Thalassionema nitzschioides*, *Asterionellopsis glacialis*, *Plagiogramma brockmannii*, *Thalassiosira spp.* and *Skeletonema costatum.* This first assemblage is progressively replaced by a community of *Chaetoceros* and then large-sized diatoms, mainly *Guinardia delicatula*, *G. striata* and *Rhizosolenia shrubsolei* and *Phaeocystis* colonies. In the late phase of the spring bloom, *Phaeocystis, G. delicatula*, *G. striata* and *R. shrubsolei* are the more often co-occurrent before completely disappearing in late spring-early

summer (Fig. 3.6). Later in summer, the large diatoms constitutes the bulk of phytoplankton with *Chaetoceros* and small diatoms succeeding in summer or/and in fall, in a reverse sequence of the spring succession. The presence of *Pseudonitzschia* spp. has also been reported during late spring (Muylaert *et al.*, 2006). A different timing of this succession is observed in the different parts of the BCZ with early spring diatoms blooming one month earlier in the Southwestern than in the Northeastern part (Muylaert *et al.*, 2006).

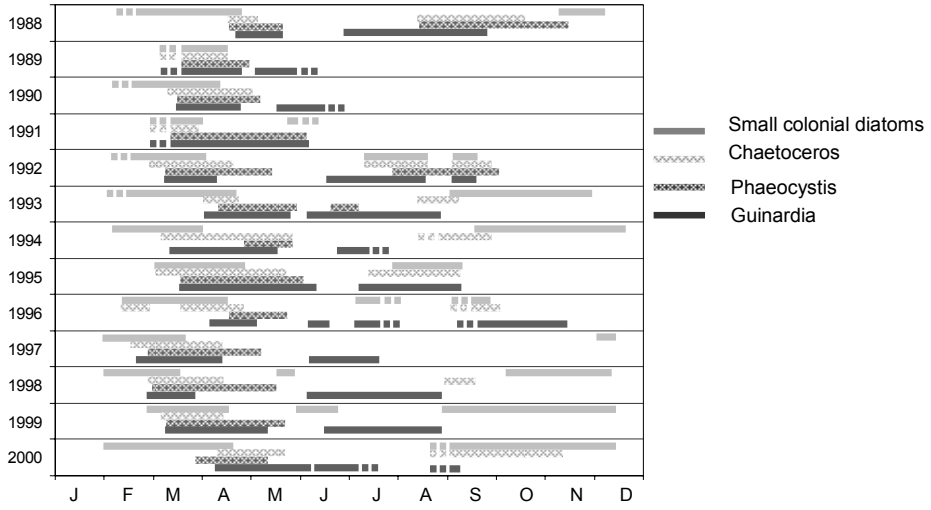

Figure 3.6. Successional pattern of diatoms and *Phaeocystis* between 1988 and 2000. The three diatom communities were identified on based of a hierarchical classification (Rousseau *et al.*, in preparation).

While the phytoplankton succession is remarkably repeated, the onset time and duration of the phytoplankton communities are variable from year to year (Fig. 3.6). The onset of the spring succession varies indeed from early February to early March, being driven by a light threshold of 12 µmol quanta m^{-2} s^{-1} in the water column which is primarily determined by the load of suspended matter of the coastal waters (Rousseau, 2000). The onset time of *Phaeocystis* is invariably associated to that of *Chaetoceros*, taking place between early-March and mid-April (Fig. 3.6).

The control of the successional phytoplankton pattern is multifactorial and consists in a complex interaction between autecological properties of species (regulation of growth by temperature, light and nutrients), potential allelopathic effects and grazing. The ecological preference of the three diatom communities and *Phaeocystis* identified at station 330 are surprisingly similar. The environmental conditions prevailing during their respective growth period encompass indeed a wide and overlapping range of salinity, temperature, nutrients and light (Rousseau *et al.*, in preparation). A better adaptation to low water column irradiance (Meyer *et al.*, 2000; Rousseau, 2000) and temperature

(Lancelot *et al.*, 1998) prevailing in late winter-early spring could however not be excluded to explain the initiation of the diatom-*Phaeocystis* succession by the small colonial diatom community. Once initiated, the diatom succession is shaped by the adaptation of the diatom communities to ambient dissolved silicate (Rousseau *et al.*, 2002). A higher sensitivity of the G*uinardia-Rhizosolenia* community to the grazing by the dinoflagellate *Noctiluca* could well explain phytoplankton disappearance from the water column during summer (Daro *et al.*, 2008).

3.3. Understanding the *Phaeocystis* phenomenon

3.3.1 The taxonomy and biology of *Phaeocystis*

The genus *Phaeocystis* sp. belongs to the class of Haptophyceae (synonym Prymnesiophyceae Hibberd), order Phaeocystales Medlin, family of Phaeocystaceae Lagerheim (Edvardsen *et al.*, 2000). Up to now, six species have been formally described within this genus, among which four form colonies (Zingone *et al.*, 1999). Recent molecular and morphological data suggest however that the number of species in the genus is underestimated (Medlin & Zingone, 2007). The *Phaeocystis* species forming large blooms during spring in the Southern Bight of the North Sea has been identified as *P. globosa*. This identification is based on colony morphology, i.e., its globular shape (Sournia, 1990), physiological and biochemical properties (Baumann *et al.,* 1994; Jahnke & Baumann, 1987; Vaulot *et al.,* 1994) and more recently on the SSU rDNA full-length sequence of the strain BCZ99 isolated from the BCZ (Rousseau, Le Gall & Rodriguez, unpublished data).

P. globosa is characterized by a heteromorphic life cycle which alternates colonies of diploid cells and nano-sized haploid free-living cells (Rousseau *et al.*, 2007). The ability of both haploid and diploid morphotypes to divide by mitosis supports the existence of a haploid-diploid life cycle in *P. globosa* (Rousseau *et al.,* 2007). In the natural environment, haploid flagellates persist in the water column between blooms of diploid colonial cells, suggesting that colony bloom initiation and termination involve sexual processes (Fig. 3.7). The vegetative reproduction of the diploid stage occurs through two distinct pathways: (i) the mitotic division of colonial cells within the colony, *i.e.* colony growth, and (ii) the formation of new colonies from diploid short-living flagellates originating from the transformation of colonial cells when released in the ambient water (Fig. 3.7). However, the significance of this latter process in the natural environment is probably reduced (Rousseau *et al.*, 2007).

The factors responsible for the transition between *P. globosa* life cycle stages are still not understood. The vernal growth of diatoms and a sufficient light intensity have been suggested to induce colony formation from haploid flagellates (Kornmann, 1955; Peperzak, 1993; Rousseau *et al.*, 1994). Alternatively, a possible allelopathic relationship between small *Phaeocystis* colonies and *Chaetoceros* spp. cannot be excluded (section 3.2.2). The formation of haploid flagellates at the end of a *P. globosa* colony bloom has

been related to nutrient depletion (Verity *et al.* 1988; Escaravage *et al.*, 1995), light limitation associated to the sinking of healthy colonies in low light conditions (Peperzak *et al.*, 1998).

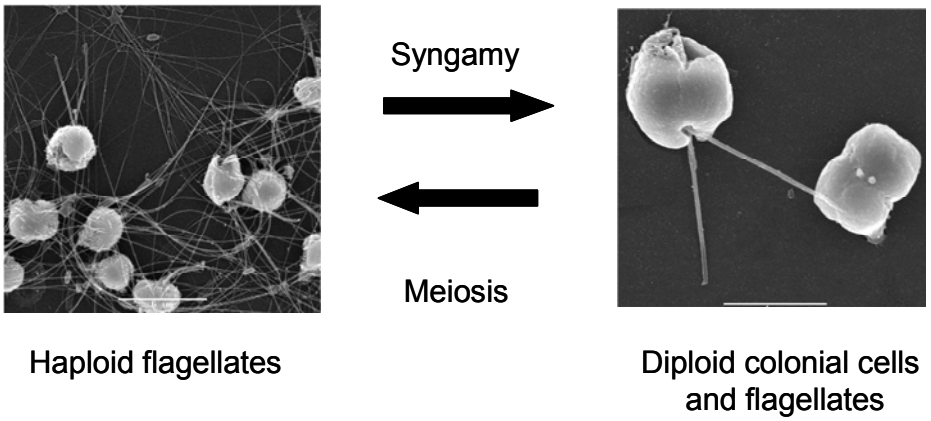

Figure 3.7. The haploid-diploid life cycle of *P. globosa* illustrated with electron microscope photographs of morphotypes present in strain BCZ99 isolated from the BCZ. The haploid flagellates in the size range 3.6-5.8 µm, possess stars, filaments and a cell coverage of scales. Colonial cells and diploid flagellates have the same size range, i.e. 5.8-10.4 µm, and lack the stars, filaments and scales. Colonial cells bear two short appendages on their apical side while diploid flagellates have two flagella and a haptonema. Photographs: Francois Lantoine (Observatoire biologique de Banyuls sur Mer, France).

3.3.2. The physiology and ecology of *Phaeocystis* colonies

The success of *P. globosa* as blooming species has been related to the specific physiology and ecology of its colonial stage (Lancelot & Rousseau, 1994; Lancelot *et al.,* 2002). The colony matrix composed of exopolysaccaride embedding the cells acts as energy and nutrient storage (Lancelot & Rousseau, 1994), allowing higher growth rates to colonial cells (Veldhuis *et al.*, 2005). The higher energetic supply also confers a competitive advantage to *Phaeocystis* colonies to utilize nitrate as nitrogen source (Riegman *et al.*, 1992; Lancelot & Rousseau, 1994). Besides, the ability to use organically-bound phosphorus owing to phosphatase provides *Phaeocystis* colonies with an additional competitive advantage when phosphate is depleted (van Boekel & Veldhuis, 1990; van Boekel, 1991; Lancelot *et al.*, 2007).

In addition, the colonial form precludes an efficient top-down control of its biomass. *P. globosa* colonies with a size higher than 400 µm (Weisse *et al.*, 1994) are indeed generally not, or insignificantly, grazed by mesozooplankton, in particular by *Temora longicornis*, the dominant spring copepod species (Daro *et al.*, 2008). As a consequence, most of *Phaeocystis*-derived production escapes the linear food chain and is mainly remineralised in the water column by intense bacterial activity (Rousseau *et al.*, 2000). Part of this production is

however resuming the classical food-web through mesozooplankton feeding activity on protozoa, leading to complex planktonic food-webs with low trophic efficiency (Hansen *et al.*, 1993; Rousseau *et al.*, 2000; Daro *et al.*, 2008). Moreover, the colony skin constitutes a physical barrier, protecting cells against grazers, virus and bacterial infection (Hamm, 2000; Brussaard *et al.,* 2005). High acrylate accumulation inside the *Phaeocystis* colonies could in addition have antimicrobial effects (Noordkamp *et al.*, 2000).

3.4. Linking *Phaeocystis* colony blooms to nutrient enrichment of the BCZ

As in many other coastal regions, eutrophication in the BCZ appears as a shift in the phytoplankton community composition with the spring proliferation of a non-siliceous species, *P. globosa*. This shift results from unbalanced delivery of nutrients compared to phytoplankton N:P:Si requirements (e.g. Billen *et al.*, 1991). The nowadays nutrient enrichment of the BCZ is characterized by a large excess of dissolved inorganic nitrogen, mainly nitrate, compared to phosphate and silicate (Brion *et al.*, 2008). Their peculiar biological and eco-physiological properties (section 3.3.2) make *Phaeocystis* colonies particularly well adapted to take benefit from the excess nitrate in the low phosphate conditions characterizing the coastal waters of the BCZ (Lancelot *et al.*, 1998; 2002). This is evidenced by the positive relationship existing between *Phaeocystis* colonial cell abundance and nitrates (Fig. 3.8; Lancelot *et al.*, 1998; Breton *et al.*, 2006). The control of phytoplankton blooms by anthropogenic nutrient emissions is however not direct due to the complex interaction between hydro-meteorological and human-induced variability of the ecosystem (section 3.2.1; Breton *et al.*, 2006).

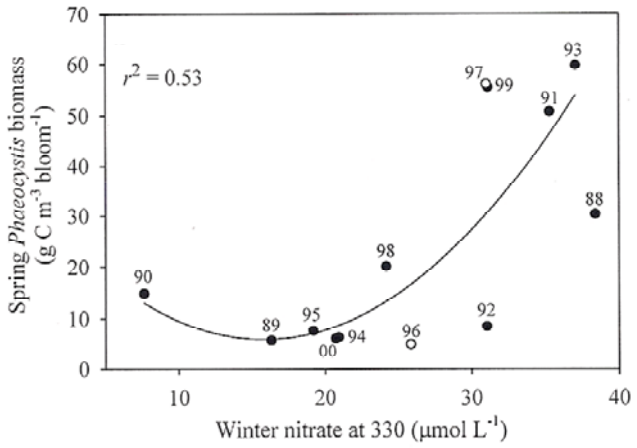

Figure 3.8. Relationship between spring *Phaeocystis* colony biomass and winter nitrate at station 330 between 1988 and 2000. Figures on the graph represent the years. From Breton *et al.* (2006). Copyright (2008) by the American Society of Limnology and Oceanography, Inc.

3.5. Conclusions and perspectives

The eutrophication event in BCZ occurs as high biomasses of the non-siliceous colonial haptophyte *Phaeocystis globosa*. Besides *Phaeocystis*, no other manifestation of eutrophication such as blooms of toxic algae have been recorded in BCZ. Recently however, blooms of the dinoflagellate *Noctiluca scintillans* have been linked to anthropogenic nutrient enrichment (Vasas *et al.*, 2007).
Phaeocystis occurs as massive spring blooms of ungrazed gelatinous colonies which are the diploid stage in a haplo-diploid life cycle where nano-sized haploid flagellates persist in water between two colonial events. *Phaeocystis* colonies occur within a recurrent successional pattern of diatom communities and are sustained by nitrate excess left over after the growth of silicate and/or phosphate-limited early spring diatoms in P-regenerated conditions.

Despite substantial progress achieved in understanding the mechanisms behind phytoplankton blooms dynamics in BCZ, some crucial questions still need to be addressed.

- The unique development of *Phaeocystis* colonies during springtime while diatoms persist along the vegetative season requires a better knowledge of factors driving the diatom-*Phaeocystis*–diatom succession as well as the eco-physiology of the different taxa.
- *P. globosa* life cycle must be substantiated by the direct observation of syngamy and meiosis and by identifying the factors inducing these sexual processes. Also, understanding the ecological significance of blooming as diploid cells but persisting as haploid stage throughout the year should be appraised through eco-physiological characterization of haploid and diploid stages.
- The extent of diatoms and *Phaeocystis* blooms is of major interest, particularly in the frame of international policies such as those of the OSPAR convention or the Water Framework Directive which recognize *Phaeocystis* as an indicator species for eutrophication. Remote sensing of ocean colour constitutes for this purpose, a significant and powerful tool for mapping phytoplankton blooms (*e.g.* Ruddick *et al.*, 2008). Research is in progress to provide more information than just the chlorophyll *a* concentration and optical remote sensing of phytoplankton functional groups is a key objective. Preliminary work (Astoreca, 2007) suggests that absorption by the chlorophyll c3, indicator of *Phaeocystis* may affect sufficiently reflectance spectra around 467nm to enable detection of at least strong *Phaeocystis* blooms, provided suitable wavelengths are available on satellite sensors.

3.6 References

Astoreca R. 2007. Study and application of the Inherent Optical Properties of coastal waters from the *Phaeocystis*-dominated Southern Bight of the North Sea. PhD Thesis, Université Libre de Bruxelles 137 pp.

Baumann M.E.M, Lancelot C., Brandini F.P., Sakshaug E. and D.M. John. 1994. The taxonomic identity of the cosmopolitan prymnesiophyte *Phaeocystis*: a morphological and ecophysiological approach. In: Ecology of *Phaeocystis*-dominated ecosystems. Lancelot C. and P. Wassmann (Eds). Journal of Marine Systems 5: 5-22

Billen G., Lancelot C. and M. Meybeck. 1991. N, P and Si retention along the Aquatic Continuum from Land to Ocean. In: Ocean Margin Processes in Global Change. Mantoura R.F.C., Martin J.-M. and R. Wollast (Eds). John Wiley & Sons, Ltd, P. 19-44

Borges A.V. and M. Frankignoulle. 2002. Distribution and air-water exchange of carbon dioxide in the Scheldt plume off the Belgian coast. Biogeochemistry 59: 41-67

Breton E., Brunet C., Sautour B. and J.-M. Brylinski. 2000. Annual variations of phytoplankton biomass in the Eastern English Channel: comparison by pigment signatures and microscopic counts. Journal of Plankton Research 22: 1423-1440

Breton E., Rousseau V., Parent J.-Y., Ozer J. and C. Lancelot. 2006. Hydroclimatic modulation of diatom/*Phaeocystis* blooms in the nutrient-enriched Belgian coastal waters (North Sea). Limnology and Oceanography 51(3): 1401-1409

Brion N., Jans S., Chou L. and V. Rousseau. 2008. Nutrient loads to the Belgian Coastal Zone. In: Current Status of Eutrophication in the Belgian Coastal Zone. Rousseau V., Lancelot C. and D. Cox (Eds). Presses Universitaires de Bruxelles, Bruxelles, pp.17-43

Brussaard C., Riegman R., Noordeloos A., Cadée G., Witte H., Kop A., Nieuwland G., van Duyl F. and R. Bak. 1995. Effects of grazing, sedimantation and phytoplankton cell lysis on the structure of a coastal pelagic food web. Marine Ecology Progress Series 123: 259-271

Brzezinski M.A. 1985. The Si:C:N ratio of marine diatoms: interspecific variability and the effect of some environmental variables. Journal of Phycology 21: 347-357

Cadée G.C. and J. Hegeman. 1991. Historical phytoplankton data of the Marsdiep. Hydrobiological Bulletin 24: 111-118

Daro N., Breton E., Antajan E., Gasparini S. and V. Rousseau. 2008. Do *Phaeocystis* colony blooms affect zooplankton in the Belgian coastal zone? In: Current Status of Eutrophication in the Belgian Coastal Zone. V. Rousseau, C. Lancelot and D. Cox (Eds). Presses Universitaires de Bruxelles, Bruxelles, pp. 61-72

Dutz J., Klein Breteler W.C.M. and G. Kramer. 2005. Inhibition of copepod feeding by exsudates and transparent exopolymer particles (TEP) derived from a *Phaeocystis globosa* dominated phytoplankton community. In: Harmful Algae. Veldhuis M.J.W. and P. Wassmann (Eds). 4: 915-940

Edvardsen B., Eikrem W., Green J.C., Andersen R.A., Moon-van der Staay S.Y. and L.K. Medlin. 2000. Phylogenetic reconstructions of the Haptophyta inferred from 18S ribosomal DNA sequences and available morphological data. Phycologia. 39 (1): 19-35

Escaravage V., Peperzak L., Prins T.C., Peeters J.C.H. and J.C.A. Joordens. 1995. The development of a *Phaeocystis* sp. bloom in a mesocosm experiment in relation to nutrients, irradiance and coexisting algae. Ophelia 42: 55-74

Hamm F.C. 2000. Architecture, ecology and biogeochemistry of *Phaeocystis* colonies. Journal of Sea Research 43: 307-315

Hansen FCR, Reckermann M, Klein Breteler WCM and Riegman R (1993) *Phaeocystis* blooming enhanced by copepod predation on protozoa: evidence from incubation experiments. Marine Ecology Progress Series 102: 51-57

Hurrell J. W. 1995. Decadal trends in the North Atlantic Oscillation: regional temperatures and precipitation. Science 269: 676-679

Jahnke J. and M. Baumann. 1987. Differenciation between *Phaeocystis pouchetii* (Har.) Lagerheim and *Phaeocystis globosa* Scherffel. Colony shapes and temperature tolerances. Hydrobiological Bulletin 21: 141-147

Kornmann P. 1955. Beobachtungen an *Phaeocystis*-Kulturen. Helgoländer Wiss. Meeresunt. 5: 218-233

Lancelot C. 1995. The mucilage phenomenon in the continental coastal waters of the North Sea. The Science of the Total Environment. 165: 83-102

Lancelot C. and V. Rousseau. 1994. Ecology of *Phaeocystis*: the key role of colony forms. In: The Haptophyte Algae. Green J.C. and B.S.C. Leadbeater (Eds). Clarenton Press, Oxford. Pp. 229-245

Lancelot C., Billen G., Sournia A., Weisse T., Colijn F., Veldhuis M.J.W., Davies A. and P. Wassmann. 1987. *Phaeocystis* blooms and nutrient enrichment in the continental coastal zones of the North Sea. Ambio 16 : 38-46

Lancelot C., Keller M., Rousseau V., Smith W.O.Jr and S. Mathot. 1998. Autoecology of the Marine Haptophyte *Phaeocystis* sp. In: NATO Advanced Workshop on the physiological ecology of Harmful Algal Blooms. NATO-ASI Series. Anderson D.A., Cembella A.M., Hallegraef G. (Eds). Springer-Verlag Berlin. Series G: Ecological Science 41: 209-224

Lancelot C., Rousseau V., Schoemann V. and S. Becquevort. 2002. On the ecological role of the different life forms of *Phaeocystis*. In: Proceedings of the workshop LIFEHAB: Life histories of microalgal species causing harmful blooms. Garcés E., Zingone A., Montresor M., Reguera B. and B. Dale (Eds). Calvia, Majorca, Spain, octobre 2001. Research in Enclosed Seas series 12: 71-75

Lancelot C., Rousseau V., Gypens N., Parent J.-Y., Bissar A., Lemaire J., Breton E., Daro M.-H., Lacroix G., Ruddick K., Ozer J., Spitz Y., Soetaert K., Chrétiennot-Dinet M.-J., Lantoine F. & F. Rodriguez. 2007. AMORE II : Advanced MOdelling and Rresearch on Eutrophication. Rapport final. Belgian Science Policy publication. D/2007/1191/5

Long J.D. and M.E. Hay. 2006. When intraspecific exceeds interspecific variance: Effects of phytoplankton morphology and growth phase on copepod feeding and fitness. Limnology and Oceanography 51: 988-996

Medlin L.K. and A. Zingone. 2007. A taxonomic review of the genus *Phaeocystis*. Biogeochemistry 83: 3-18

Meyer A., Tackx M. and N. Daro. 2000. Xanthophyll cycling in *Phaeocystis globosa* and Thalassiosira sp.: a possible mechanism for species succession. Journal of Sea Research 43: 373-384

Muylaert K, Gonzales R., Franck M., Lionard M., Van der Zee C., Cattrijsse A., Sabbe K., Chou L. and W. Vyverman. 2006. Spatial variation in phytoplankton dynamics in the Belgian coastal zone of the North Sea studied by microscopy, HPLC-CHEMTAX and underway fluorescence recordings. Journal of Sea Research 55: 253-265

Nejstgaard J.C., Tang K.W., Steinke M., Dutz J., Koski M., Antajan E. and J.D. Long. 2007. Zooplankton grazing on *Phaeocystis*: quantitative review and future challenges. Biogeochemistry. 83: 147-172

Noordkamp J.B., Gieskes W.W.C., Gottschal J.C., Forney L.J. and M. Van Rijssel. 2000. Acrylate in *Phaeocystis* colonies does not affect the surrounding bacteria. Journal of Sea Research 43: 287-296

Peperzak L. 1993. Daily irradiance governs growth rate and colony formation of *Phaeocystis* (Prymnesiophyceae). Journal of Plankton Research 15: 809-821

Peperzak L., Colijn F., Gieskes W.W.C. and J.C.H. Peeters. 1998. Development of the diatom-*Phaeocystis* spring bloom in the Dutch coastal zone of the North Sea: the silicon depletion versus the daily irradiance thresholdd hypothesis. Journal of Plankton Research 20 : 517-537

Riegman R., Noordeloos A. and G.C. Cadée, G.C. 1992. *Phaeocystis* blooms of the continental zones of the North Sea. Marine Biology 112: 479-484

Rousseau V. 2000. Dynamics of *Phaeocystis* and diatom blooms in the eutrophicated coastal waters of the Southern Bight of the North Sea. Ph.D. thesis. Université Libre de Bruxelles. 205 pp.

Rousseau V., Mathot S. and C. Lancelot. 1990. Calculating carbon biomass of *Phaeocystis* sp. from microscopic observations. Marine Biology 107: 305-314

Rousseau V., Vaulot D., Casotti R., Cariou V., Lenz J., Gunkel J. and M. Baumann. 1994. The life cycle of *Phaeocystis* (Prymnesiophyceae): evidence and hypotheses. In: Ecology of *Phaeocystis*-dominated ecosystems. Lancelot C. and P. Wassmann (Eds.) Journal of Marine Systems 5: 23-39

Rousseau V., Becquevort S., Parent J.-Y., Gasparini S., Daro M.-H., Tackx M. and C. Lancelot. 2000. Trophic efficiency of the planktonic food web in a coastal ecosystem dominated by *Phaeocystis* colonies. Journal of Sea Research 43: 357-372

Rousseau V., Leynaert A., Daoud N. and C. Lancelot. 2002. Diatom succession, silicification and silicic acid availability in the Belgian coastal waters (Southern North Sea). Marine Ecology Progress Series 236: 61-73

Rousseau V., Breton E., De Wachter B., Beji A., Deconinck M., Huijgh J., Bolsens T., Leroy D., Jans S. and C. Lancelot. 2004. Identification of Belgian maritime zones affected by eutrophication (IZEUT). Towards the establishment of ecological criteria for the implementation of the OSPAR Common Procedure to combat eutrophication. Belgian Science Policy, Brussels, Final report. 77 pp.

Rousseau V., Chrétiennot-Dinet M.-J., Jacobsen A., Verity P. and S. Whipple. 2007. The life cycle of *Phaeocystis*: state of knowledge and presumptive role in ecology. Biogeochemistry 83: 29-47

Ruddick K., Lacroix G., Lancelot C., Nechad B., Park Y., Peters S. and B. Van Mol. 2008. Optical remote sensing of the North Sea. In V. Barale and M. Gade [eds.], Remote sensing of the European Seas. Springer-Verlag, pp. 79-90

Sournia A. 1990. *Phaeocystis* (Prymnesiophyceae): How many species? Nova Hedwigia 47: 211-217

Smayda T.J. 1997. Bloom dynamics: physiology, behavior, trophic effects. Limnology and Oceanography 42: 1132-1136

Turner J.T., Ianora A., Esposito F., Carotenuto Y. and A. Miralto. 2002. Zooplankton feeding ecology : does a diet of *Phaeocystis* support good copepod grazing, survival, egg production and egg hatching success. Journal of Plankton Research 24(11): 1185-1195

van Boeckel W.H.M. and M.J.C. Veldhuis. 1990. Regulation of alkaline phosphatase synthesis in *Phaeocystis* sp. Marine Ecology Progress Series 61:281-289

Van der Zee C. and L. Chou. 2005. Seasonal cycling of phosphorus in the Southern North Bight of the North Sea. Biogeosciences 2: 27-42

Vaulot D., Birrien J.-L., Marie D., Casotti R., Veldhuis M.J., Kraay G.W. and M.-J. Chrétiennot-Dinet. 1994. Morphology, ploidy, pigment composition and genome size of cultured strains of *Phaeocystis* (Prymnesiophyceae). Journal of Phycology 30: 1022-1035

Veldhuis M.J.W., Brussaard C.P.D. and A.A.M. Noordeloos. 2005. Living in a *Phaeocystis* colony : a way to be successful algal species. In: Harmful Algae. Veldhuis M.J.W and P. Wassmann (Eds). 4: 841-858

Verity P.G., Villareal T.A. and T.J. Smayda. 1988 Ecological investigations of blooms of colonial *Phaeocystis pouchetii*. II. The role of life cycle phenomena in bloom termination. Journal of Plankton Research 749-766

van Boeckel W.H.M. 1991. Ability of *Phaeocystis* sp. to grow on organic phospahtes; direct measurement and prediction with the use of an inhibition constant. Journal of Plankton Research 13: 959-970

Vasas V., Lancelot C., Rousseau V. and F. Jordan. 2007. Eutrophication and overfishing in temperate nearshore pelagic food webs : a network perspective. Mar. Ecol. Progr. Ser. 336: 1-14

Weisse T., Tande K., Verity P., Hansen F. and W.W.C. Gieskes. 1994. The trophic significance of *Phaeocystis* blooms. In: Ecology of *Phaeocystis*-dominated ecosystems. Lancelot C. and P. Wassmann (Eds.). J. Mar.Syst. 5: 67-79

Zingone A., Chrétiennot-Dinet M.-J., Lange M. and L.K. Medlin. 1999. Morphological and genetic characterization of *Phaeocystis cordata* and *P. Jahnii* (Pymnesiophyceae), two new species from the Mediterranean Sea. J. Phycol. 35: 1322-1337

CHAPTER 4

Do *Phaeocystis* colony blooms affect zooplankton in the Belgian Coastal Zone?

Marie-Hermande Daro[1], Elsa Breton, Elvire Antajan, Stéphane Gasparini and Véronique Rousseau[2]

[1] Vrij Universiteit Brussel (VUB), Laboratorium voor Ekologie en Systematiek, Pleinlaan 2 B-1050 Brussels, Belgium
[2] Université Libre de Bruxelles (ULB), Ecologie des Systèmes Aquatiques (ESA), CP221, boulevard du Triomphe, B-1050 Brussels, Belgium

4.1 Introduction

The ability of herbivorous zooplankton to control phytoplankton blooms, and to efficiently transfer primary production towards higher trophic levels such as invertebrates, fish larvae and planktivorous fish, is considered as a sign of equilibrium in marine ecosystems. This is not the case in the Southern Bight of the North Sea where massive *Phaeocystis* colony spring blooms sustained by anthropogenic nitrates, are suggested to be the consequence of a high resistance to losses, in particular grazing (Lancelot *et al.*, 1994; 2002).

To which extent *Phaeocystis* colony blooms are negatively impacting zooplankton dynamic is investigated in this chapter, based on available information on zooplankton in the Belgian coastal zone (BCZ).

4.2 Seasonal distribution of zooplankton in the BCZ

Major zooplankton groups in the BCZ were defined based on their trophic position. They include microzooplankton, herbivorous copepods and gelatinous zooplankton such as *Noctiluca scintillans*. Figure 4.1b compares their seasonal occurrence with respect to phytoplankton, *i.e. Phaeocystis* colonies and diatoms (Fig. 4.1a). Small neritic copepods represent the dominant metazoan plankton from May to September. Moderate in early spring when diatoms prevail on *Phaeocystis* colonies, copepods become abundant after the *Phaeocystis* bloom showing two distinct peaks of biomass in spring-summer (Fig. 4.1b). The summer biomass minimum is also observed for diatoms which are dominated at that time by large species such as *Guinardia delicatula*, *G. striata*, and *Rhizosolenia shrubsolei.* Both diatom and copepod summer minima are concomitant with a massive development of *N. scintillans* which starts blooming

at the decline of *Phaeocystis* colonies (Fig. 4.1). Microzooplankton is particularly abundant from April to May (Fig. 4.1b). Beside these three zooplankton groups, reports exist on the occurrence of the tunicate *Oikopleura dioica* and meroplanktonic larvae (Cirripedia, Polychaetes, Bryozoa) but their biomass is not significant on a yearly basis (not shown). Predators such as cladocerans and Chaetognatha (*Sagitta elegans*) have also been observed in summer.

Based on the seasonal distribution of copepods, *N. scintillans* and microzooplankton with respect to *Phaeocystis*, a focus is given in the next sections on their respective feeding behaviour and trophic significance.

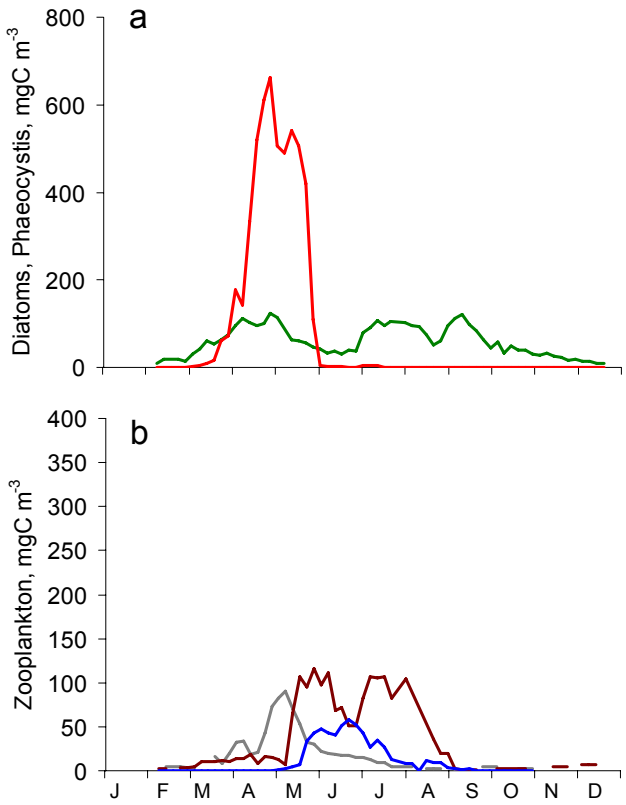

Figure 4.1. Seasonal distribution of phytoplankton (a): *Phaeocystis* colonies (red) and diatoms (green) and dominant zooplankton groups (b): microprotozooplankton (grey), copepods (brown) and *Noctiluca scintillans* (blue) at station 330 (N 51°26.0; E 2°48.5) in the central BCZ. All phyto- and zoo-plankton data available for the period 1988-2004 were 5-days averaged.

4.3 Copepods

Temora longicornis, Pseudocalanus elongatus, Centropages hamatus and Acartia clausii are the main species reported in the BCZ. *T. longicornis* is however much more dominant during spring, representing in average for the period 1988-2004 some 62% of the total copepod biomass. This small-sized copepod produces several generations during spring explaining the co-occurrence of different developmental stages (nauplii, copepodites I-V and adults), all of them susceptible to be affected by *Phaeocystis* colony blooms. The other copepod species, *i.e. Centropages*, *Pseudocalanus* and *Acartia,* are dominant later in the year (Daro, 1985; Antajan, unpublished data).

4.3.1 Diet and feeding activities of *T. longicornis*

Measurements of feeding activities of the major copepod species present during springtime in BCZ were investigated by combining several methods under shipboard and laboratory-controlled conditions. These methods, *i.e.* HPLC pigment analysis of gut content, $^{14}CO_3$ - prelabeling of phytoplankton given as a food source to copepods and the cell count method estimating clearance rates of different prey, are described in details in Gasparini *et al.* (2000) and Antajan (2004).

All together, in situ grazing experiments conclude that the late winter-early spring diatom community, dominated by small chain-forming *Thalassiosira* spp. and *Chaetoceros* spp. are efficiently grazed by copepods with mean daily ingestion rates of 1.6 µg C ind^{-1} d^{-1} (Gasparini *et al.*, 2000; Antajan, 2004). During *Phaeocystis* colony blooms, herbivorous feeding of copepod declines, being one order of magnitude lower (in average 0.26 µg C ind^{-1} d^{-1}) than during the late winter-early spring period due to the lack or insignificant grazing on *Phaeocystis* colonies (Daro, 1985; Hansen & van Boekel, 1991; Weisse *et al.*, 1994; Breton *et al.*, 1999). They also show that the large diatoms such as *Guinardia delicatula, G. striata and R. shrubsolei* prevailing during late spring and summer, were ingested at a much lower rates than during early spring (Gasparini *et al.*, 2000; Antajan, 2004). To sustain their food requirements during *Phaeocystis* blooms, copepods feed preferentially on microzooplankton, which can represent up to 50-96% of their diet at that time (Gasparini *et al.*, 2000). These studies conclude however, that daily ingestion rates on microzooplankton would not be sufficient to sustain copepod growth, amounting for only 7-21% of the adult copepod carbon weight during and after the *Phaeocystis* bloom (Gasparini *et al.*, 2000). As that time, phytodetritus can be another possible food source for copepods but this was not quantified.

The preferential grazing of *T. longicornis* on microzooplankton over large diatoms and *Phaeocystis* colonies was demonstrated by Antajan (2004) based on the Electivity index E* method (Vanderploeg & Scavia, 1979). As shown in Figure 4.2, *T. longicornis* positively selects dinoflagellates and ciliates of different sizes but responds negatively to *Phaeocystis*, nanoflagellates and large diatoms. The positive selection of microzooplankton by *T. longicornis* (Fig. 4.2) has been related to their size but also to their nutritional quality due to their

low carbon to nitrogen ratio compared to algae, making them a better source of proteins and amino acids (Stoecker & Capuzzo, 1990; Hitchcock, 1982).

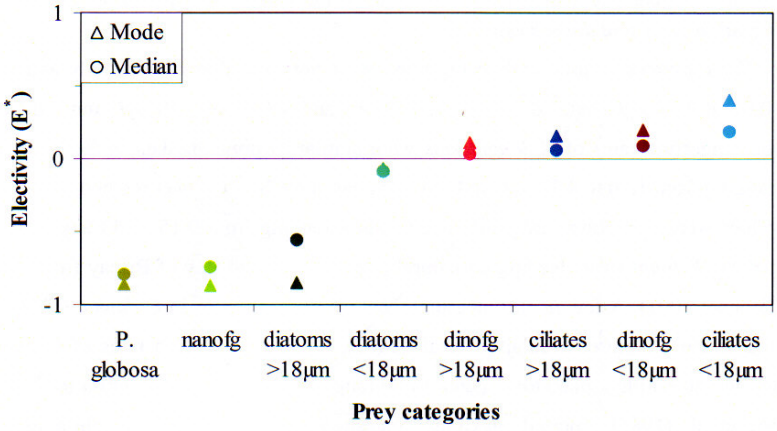

Figure 4.2. Mode and median of electivity index E* for the different prey items of *T. longicornis* calculated on basis of cell count incubations performed in the BCZ from 1999 to 2001. Redrawn from Antajan (2004).

The active predation of copepods on microzooplankton represents an important trophic pathway linking the microbial food web to the classical food chain (from diatoms to copepods). However this link could also be the basis of a trophic cascade where copepod grazing on microzooplankton could stimulate *Phaeocystis* colony blooms by releasing grazing pressure of *Phaeocystis* cells which are at the origin of colony formation (Fransz *et al.*, 1992).

The negative effect of *Phaeocystis* colonies on the feeding of the different developmental stages of *T. longicornis* was investigated, based on the measurement of day-night ingestion rates as a function of phytoplankton availability at three stages of the phytoplankton spring bloom, (in early spring when small colonial diatoms prevail, during the growing (small colonies) and stationary (large colonies) phases of *Phaeocystis* bloom; Fig. 4.3). Clearly, ingestion rates are 5 to 6 times higher during the early spring diatom bloom for all developmental stages. Feeding rates are significantly lower during the *Phaeocystis* bloom and no difference was observed for the small and large colonies.

The lack of grazing of *Phaeocystis* colonies by small copepods has been related to a prey-predator size mismatch (Weisse *et al.*, 1994), chemical deterrence by repulsive substances (Bautista *et al.*, 1992), feeding inhibition due to *Phaeocystis*-derived exopolymers (Dutz *et al.*, 2005) and/or growth stages of colonies (Long & Hay, 2006). The poor nutritional value of *Phaeocystis* colonies has also been incriminated (Claustre *et al.*, 1990; Tang *et al.*, 2001).

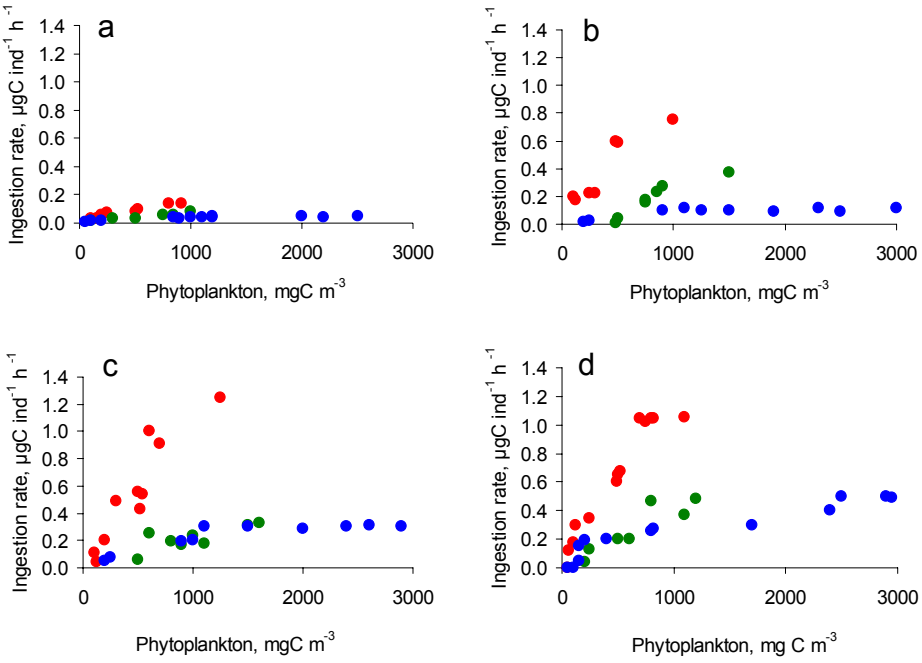

Figure 4.3. Day-night averaged ingestion rates of *T. longicornis* copepodites I & II (a); III & IV (b); V (c) and adults (d) at three different periods of the spring bloom, *i.e.* in March during the early spring diatoms (red); in mid April during the exponential (green) and in early May during the stationary (blue) growing phases of *Phaeocystis* colony bloom in the BCZ. Ingestion rates were calculated according to Daro & Baars (1986).

4.3.2 Effect of *Phaeocystis* colony bloom on *T. longicornis* reproduction

Grazing experiments suggest that adult copepods are in food shortage during *Phaeocystis* blooms (section 4.3.1), which could impact negatively egg production and therefore the next copepod generation (*e.g.* Peterson & Dam, 1996). Egg production and herbivorous feeding by freshly caught *T. longicornis* females were measured along a seasonal cycle in 2001 at 3 stations in the BCZ (Fig. 4.4; Antajan, 2004).

Clearly egg production at the time of *Phaeocystis* bloom (7-20 eggs female^{-1} d^{-1}; Fig. 4.4a) is far below the maximal rate of egg production reported for this copepod (40-65 eggs female^{-1} d^{-1}; Peterson & Dam, 1996). Such optimal values are however observed in end-March during the early-spring diatom bloom (30-60 eggs female^{-1} d^{-1}; Fig.4.4a). The contribution of herbivorous feeding to *T. longicornis* egg production (Fig. 4.4b) is very low in late spring, suggesting that ingestion of phytoplankton during *Phaeocystis* bloom is not sufficient to cover the needs for *T. longicornis* egg production (Antajan, 2004).

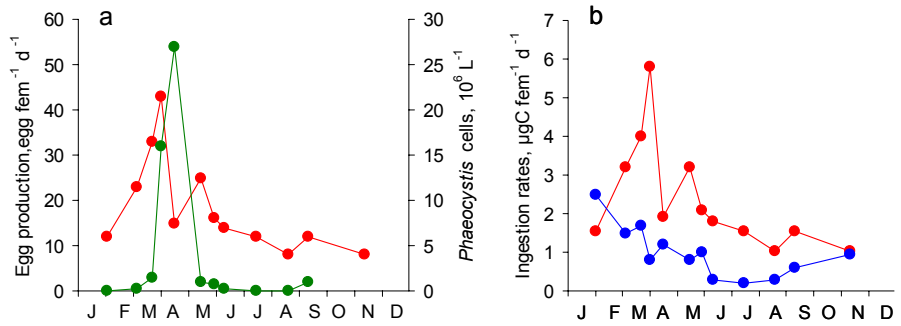

Figure 4.4. Seasonal evolution in 2001 of copepod eggs production (red) and *Phaeocystis* colonies (green) (a) and copepod ingestion rates estimated from egg production (red) and gut content (blue) (b). Redrawn from Antajan (2004).

The impact of *Phaeocystis* bloom development on *T. longicoris* reproduction was assessed by comparing the ingestion (Fig. 4.5a) and egg production (Fig. 4.5b) rates of three successive generations hatching respectively on 1st, 25 April and 25 May, i.e. at three distinct periods of the spring bloom. Daily ingestion rates were calculated considering the prevailing phytoplankton taxa (diatoms, *Phaeocystis*), size and concentrations and the copepod stages using the feeding functions represented on Figure 4.3. These results show that only the first generation of *T. longicornis* feeds properly, and produces eggs at a high rate. The second generation grazes properly up to the age of 15 days (dominance of young copepodites) when individual ingestion rates decrease up to the adult stage, lowering egg production rates. The third generation suffers much more from the very young stages with a strong impact on egg production which stops after 12 days. In the field, the production of dormant eggs by the first spring generations could well explain the summer occurrence of *T. longicornis*. The impact of *Phaeocystis* colony blooms on the other copepod species such as *Pseudocalanus* prevailing about one month later than *Temora* is less significant (Daro, 1985).

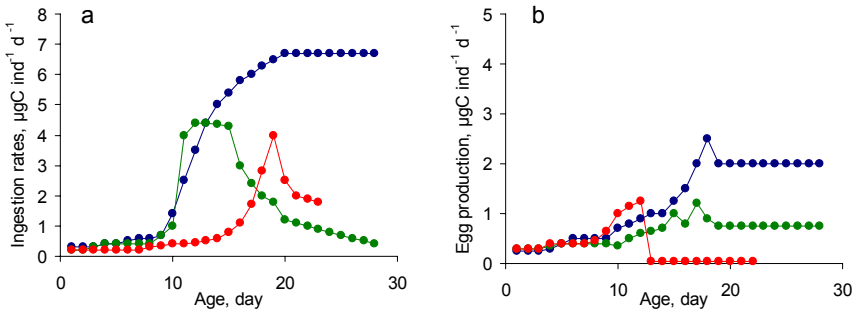

Figure 4.5. Daily ingestion (a) and egg production (b) rates of *T. longicornis* as a function of their age for 3 successive generations hatching on 1st April (blue), 25 April (green) and 25 May (red), at three stages of the phytoplankton spring bloom.

4.4 *Noctiluca scintillans*

The other main zooplankton playing a key trophic role in BCZ is the intriguing *N. scintillans*. This large-sized (in average 600 µm) heterotrophic red tide dinoflagellate is considered as ichtyotoxic due to the release of high concentrations of ammonium as catabolic by-product. Being largely un-preyed, *N. scintillans* is, like other gelatinous organisms, considered as dead end in food web. *N. scintillans* biomass culminates in June-July (Fig. 4.1b) but the maximum cell density reached varies significantly from year to year, being as high as 16 000 cells m^{-3}; Breton, unpublished data).
The diet of *N. scintillans as* determined on basis of vacuole content analysis, consists in diatoms, *Phaeocystis* aggregates, copepod eggs and moults, faecal pellets and various protists (dinoflagellates, ciliates and suctorians). The feeding strategy of *N. scintillans* is qualified as generalist based on the analysis of Costello (1990). This methodology compares the prey relative abundance (%A) and frequency of occurrence (%F) in the diet (Fig. 4.6). In this analysis, equivalence between %A and %F indicates a generalist feeding behaviour with the most important prey characterized by high %A and %F (Fig. 4.6). On the contrary, prey ingested at low occurrence but high abundance indicates a specialized feeding behaviour of the predator.

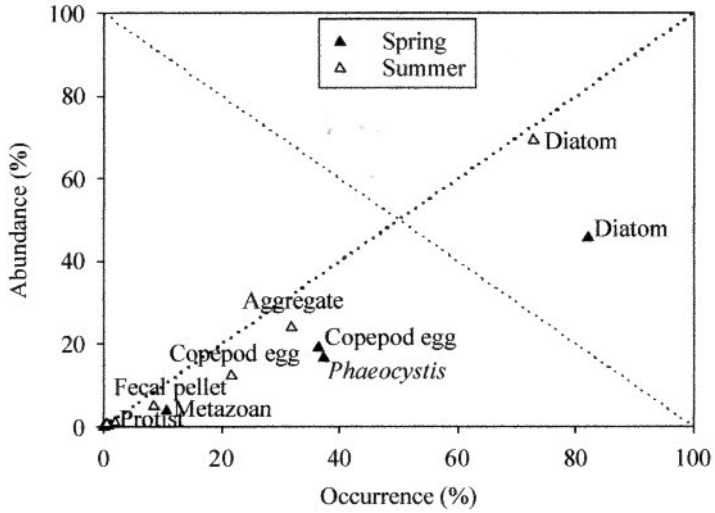

Figure 4.6. Feeding strategy of *N. scintillans* in the BCZ based on the Costello (1990) analysis which relates prey relative abundance (A in %) and its frequency of occurrence (F in %).

Both in spring and summer, large diatoms such as *Guinardia delicatula*, *G. striata* and *Rhizosolenia shrubsolei* are by far the most important food item found in *N. scintillans* vacuoles (Fig. 4.6). Copepod eggs and aggregates represent a significant part of the *N. scintillans* diet in spring and summer while

fecal pellets and protists are only minor components. Such a diet composed of a high variety of large items and few small-sized organisms was already observed in other areas (Enomoto, 1956; Prasad, 1958; Kimor, 1979). A predator - prey size ratio of 5:1 together with a linear functional feeding response to food concentration indicates that *N. scintillans* is characterized by a voracious feeding behaviour (Breton, unpublished data).
The preferential grazing of *N. scintillans* on large-sized prey is well illustrated on Figure 4.7 which indicates that the occurrence of prey in the *N. scintillans* diet corresponds to an unimodal function of the prey biovolume in both spring and summer. In spring the optimal volume corresponds to that of copepod eggs. By contrast, *Phaeocystis* healthy colonies or free-living cells are respectively at the lower and upper limits of the size range suggesting a trophic size mismatch (Fig. 4.7). During the bloom, size of un-preyed *Phaeocystis* colonies is indeed 5 times larger than those observed in *N. scintillans* food vacuoles. By contrast, the aggregates found in *N. scintillans* vacuoles at the end of the bloom have a smaller size and can represent suitable prey. These observations suggest that trophic interaction between *Phaeocystis* colonies and *N. scintillans* might be significant during the collapse of the bloom. In summer, the optimum biovolume is corresponding to that of the diatom *G. delicatula* (Fig. 4.7).

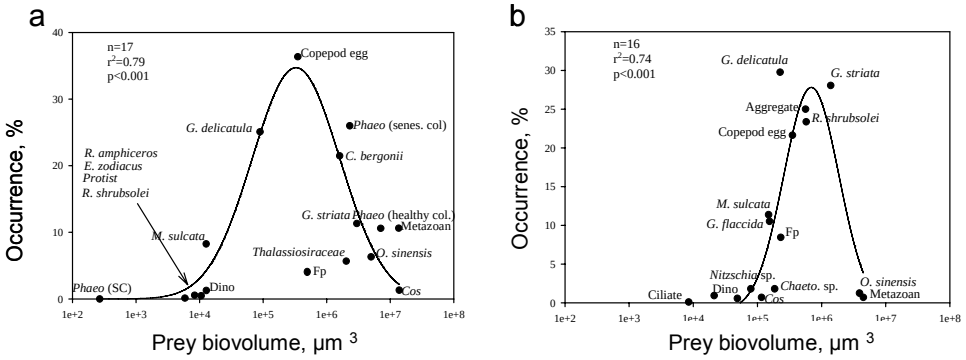

Figure 4.7. Gaussian relationship between the biovolume of prey and their occurrence (in %) in the diet of *N. scintillans* during spring (a) and summer (b).

N. scintillans ingestion rates, estimated from vacuole content during shipboard digestion experiments, are in average of 0.27 µg C cell^{-1} d^{-1} in spring and 0.14 µg C cell^{-1} d^{-1} in summer, corresponding to 118% and 59% of *N. scintillans* body carbon weight, respectively. From this, daily grazing pressure by the *N. scintillans* population can be calculated and expressed as the part (in %) of diatom, *Phaeocystis* and copepod eggs standing stocks. In spring, *N. scintillans* daily grazing pressure on *Phaeocystis* was estimated to 0.06, 2 and 60% per day for colonies, aggregates and small sized (< 300 µm) aggregates respectively. Daily grazing pressure on spring diatoms and copepod eggs amounts for 3% and 52% respectively. In summer, *N. scintillans* were shown to

graze some 15% and 31% of large diatoms and copepod eggs respectively. This indicates that *N. scintillans* has probably a minor role in controlling *Phaeocystis* colony blooms. On the contrary, our estimations suggest that *N. scintillans* has a strong impact on the large late spring and summer diatoms and copepod eggs.

4.5 Microzooplankton

Microzooplankton is a functional group which is not taxonomically homogeneous. This group is largely dominated by microprotozooplankton composed of heterotrophic protists such as dinoflagellates and ciliates but also includes young metazoan stages such as nauplii, copepodites I - II and pluteus larvae. Microzooplankton diet is composed of both nanophyto- (autotrophic flagellates) and nanoprotozoo- plankton (bacterivorous nanoflagellates). In the BCZ, microzooplankton is particularly abundant from the end of winter to April-May at the time of *Phaeocystis* blooms (Fig.4.1). At that time, it actively grazes on nanoplanktonic *Phaeocystis* free-living cells (Weisse & Scheffel-Möser, 1990) and heterotrophic nanoflagellates (Rousseau *et al.*, 2000). These latter feed on bacteria which degrade the dissolved organic matter supplied by *Phaeocystis* cell lysis and matrix dissolution (Rousseau *et al.*, 2000). Microzooplankton constitutes an alternative food item for copepods during *Phaeocystis* colony blooms, when copepod herbivorous feeding declines (section 4.3.1). Because it feeds on nanoplankton but is grazed by mesozooplankton, microzooplankton occupies a key trophic position in the BCZ ecosystem transferring part of the un-preyed *Phaeocystis* production (free-living cells and dissolved organic matter available to bacteria) to higher trophic levels (mesozooplankton).

4.6 Trophic efficiency of the *Phaeocystis*-dominated planktonic food-web in the BCZ

As shown in previous sections, phytoplankton groups that succeed along the spring bloom in the BCZ are feeding different zooplankton groups with different trophic efficiency, *i.e.* the ratio between zooplankton grazing and phytoplankton production). Early spring diatoms feed copepods, late spring-summer large diatoms are ingested by *N. scintillans* and *Phaeocystis* colonies resist grazing by both zooplankton groups. During *Phaeocystis* decline however, ungrazed colonies are releasing in the ambient dissolved organic matter available to bacteria and colony cells which are grazed by microzooplankton.

The carbon budget and trophic efficiency of the *Phaeocystis*-related food web was calculated, based on field measurements (Rousseau *et al.*, 2000) and model simulation (Lancelot *et al.*, 2005) of carbon biomass and activities associated to the different plankton groups. Both conclude that *Phaeocystis* colonies represent 70-75% of the spring phytoplankton biomass production. The produced biomass escapes grazing by copepods but feeds the microbial

network formed of microzooplankton and bacteria throughout the release of *Phaeocystis* cells and organic matter. The trophic efficiency of this pathway is estimated to 1.5%. One third of the diatom production fuels directly the mesozooplankton corresponding to a trophic efficiency of 34%. However, this figure is lowered to 5.6% if the total available phytoplankton production is considered.

Altogether these estimations conclude that most of the *Phaeocystis*-derived production is remineralised in the water column.

4.7 Conclusions

Anthropogenic loads of nutrients to the BCZ have stimulated the phytoplankton production without enhancing the overall yield of biological resources. In this area the unbalanced nutrient sources, over-enriched in nitrates with respect to phosphate and silicic acid have stimulate the development of *Phaeocystis* colonies resistant to grazing. As a consequence, the trophic interactions in the eutrophied BCZ show a prevalence of the remineralisation processes over the transfer of matter and energy towards higher trophic levels. This contrasts with the less eutrophied Northern and Central North Sea, where the phytoplankton development is submitted to a top-down control by copepods (Daro, 1980). Using qualitative structural network analysis of a generic food web, Vasas *et al.* (2007) demonstrate that HAB-forming species (as *Phaeocystis* colonies) and *N. scintillans* blooms are resulting from anthropogenic nutrient enrichment. These undesirable species reduce the abundance of the principal bottom-up controllers with far-reaching effects throughout the food-web. Stimulating the microbial network but inhibiting the higher trophic levels seems to be intrinsic properties of temperate pelagic ecosytems strongly affected by human activities. This effect is exacerbated by overfishing (Vasas *et al.*, 2007).

4.8 References

Antajan E. 2004. Responses of calanoid copepods to changes in *phytoplankton* dominance in the diatom-*Phaeocystis globosa* dominated Begium waters. PhD thesis, University of Brussels

Bautista B., Harris R.P., Tranter P.R.G. and D. Harbour. 1992. In situ copepod feeding and grazing rates during a spring bloom dominated by *Phaeocystis sp*. in the English Channel. Journal of Plankton Research 14: 691-703

Breton E., Sautour B. and J.-M. Brylinski. 1999. No feeding on *Phaeocystis sp*. as solitary cells (post bloom period) by the copepod *Temora longicornis* in the coastal waters of the English Channel. Hydrobiologia 414: 13-23

Claustre H., Poulet S.A., Williams R., Marty J.-C., Coombs S., ben Mlih F., Harpette A.M. and V. Martin-Jezequel. 1990. A biochemical investigation of a *Phaeocystis* sp. bloom in the Irish Sea. Journal of the Marine Association of United Kingdom 70: 197-207

Costello M.J. 1990. Predator feeding strategy and prey importance: a new graphical analysis. Journal Fisheries Biol 36: 261-263

Daro M.-H. 1980. Field study of the diel feeding of a population of *Calanus finmarchicus* at the end of a phytoplankton bloom. “Meteor” Forsch.-Ergebnisse 22(A): 123-132

Daro M.-H. 1985. Field study of the diel, selective and efficiency feeding of the marine copepod in the Southern Bight of the North Sea. In: Van Grieken R and R. Wollast (Eds). Progress in Belgian Oceanographic research. University of Antwerp, p. 250-263

Daro M.-H. and M.A. Baars. 1986. Calculations of zooplankton grazing rates according a closed, steady-state, three-compartment model applied to different 14C methods. Hydrobiological Bulletin 19: 159-170

Dutz J., Klein Breteler W.C.M. and G. Kramer 2005 Inhibition of copepod feeding by exsudates and transparent exopolymer particles (TEP) derived from a *Phaeocystis globosa* dominated phytoplankton community. In: Veldhuis MJW and Wassmann P (Eds). Harmful Algae. 4: 915-940

Enomoto Y. 1956. On the occurrence and food of *Noctiluca scintillans* in the waters adjacent to the West Coast of Kyushu, with special reference to the possibility of damage caused to fish eggs by that plankton. Bull. Japonese Society Science Fisheries 22:82-88

Fransz H.G., Gonzales S.R., Cadée G.C. and F.C. Hansen. 1992. Long-term changes of *Temora* longicornis (Copepoda Calanoida) abundance in a Dutch tidal inlet (Marsdiep) in relation to eutrophication. Netherlands Journal of Sea Research 30: 23-32

Gasparini S., Daro M.-H., Antajan E., Tackx M., Rousseau V., Parent J.-Y. and C. Lancelot. 2000. Mesozooplankton grazing during the *Phaeocystis globosa* bloom in the Southern Bight of the North Sea. Netherlands Journal Sea Research 43: 345-356

Hansen F.C. and W.H.M. Van Boekel. 1991. Grazing pressure of the calanoid copepod *Temora longicornis* on a *Phaeocystis* dominated spring bloom in a Dutch tidal inlet. Marine Ecology Progress Series 78: 123-129

Hitchcock G.L. 1982. A comparative study of the size-dependant organic composition of marine diatoms and dinoflagellates. Journal Plankton Research 4: 363-377

Kimor B. 1979. Predation by *Noctiluca miliaris* Souriray on *Acartia tonsa* Dana Eggs in the Inshore Waters of Southern California. Limnology & Oceanography 24: 568-572

Lancelot C., Wassmann P. and H. Barth 1994. Ecology of *Phaeocystis*-dominated ecosystems. Journal of Marine Systems 5: 1-4

Lancelot C., Rousseau V., Schoemann V. and S. Becquevort S. 2002. On the ecological role of the different life forms of *Phaeocystis*. In: Garcés E, Zingone A, Montresor M., Reguera B and Dale B (Eds). Proceedings of the workshop LIFEHAB: Life histories of microalgal species causing harmful blooms. Calvia, Majorca, Spain, octobre 2001. Research in Enclosed Seas series 12: 71-75

Lancelot C., Spitz Y., Gypens N., Ruddick K., Becquevort S., Rousseau V., Lacroix G. and G. Billen. 2005. Modelling diatom and *Phaeocystis* blooms and nutrient cycles in the Southern Bight of the North Sea: the MIRO model. Marine Ecology Progress Series 289: 63-78

Long J.D. and M.E. Hay. 2006. When intraspecific exceeds interspecific variance: Effects of phytoplankton morphology and growth phase on copepod feeding and fitness. Limnology and Oceanography 51: 988-996

Peterson W.T. and H.G. Dam. 1996. Pigment ingestion and egg production rates of the calanoid copepod *Temora* longicornis: implications for gut pigment loss and omnivorous feeding. Journal of Plankton Research 18: 855-861

Prasad R.R.. 1958. Swarming of *Noctiluca* in the Palk Bay and its effect on the Chaesai fishery, with a note on the possible use of *Noctiluca* as an indicator species. Proceedings Indian Academic Sciences 38:82-88

Rousseau V., Becquevort S., Parent J.-Y., Gasparini S., Daro M.-H., Tackx M. and C. Lancelot. 2000. Trophic efficiency of the planktonic food web in a coastal ecosystem dominated by *Phaeocystis* colonies. Journal of Sea Research 43: 357-372

Stoecker D.K. and J.M. Capuzzo. 1990. Predation on protozoa: its importance to zooplankton. Journal of Plankton Research 12: 891-908

Tang K.W., Jakobsen H.H. and A.W. Visser. 2001. *Phaeocystis globosa* (Prymnesiphyceae) and the planktonic food web: feeding, growth and trophic relationships among grazers. Limnology and Oceanography 46(8): 1860-1870

Vanderploeg H. and D. Scavia. 1979a. Calculation and use of selectivity coefficients of feeding: zooplankton grazing. Ecological Modeling 7: 135-149

Vasas V., Lancelot C., Rousseau V. and F. Jordán. 2007. Eutrophication and overfishing in temperate nearshore pelagic food webs: a network perspective. Marine Ecology Progress Series 336:1-14

Weisse T. and U. Scheffel-Möser. 1990. Growth and grazing loss rates in single-celled *Phaeocystis* sp. (Prymnesiophyceae). Marine Biology 106: 153-158

Weisse T., Tande K., Verity P., Hansen F. and W. Gieskes. 1994. The trophic significance of *Phaeocystis* blooms. In: Lancelot C and P. Wassmann (Eds). Ecology of *Phaeocystis*-dominated ecosystems. Journal of Marine Systems 5: 67-79

CHAPTER 5

Benthic responses to sedimentation of phytoplankton on the Belgian Continental Shelf

Jan Vanaverbeke[1], Maria Franco[1], Dick van Oevelen[2], Leon Moodley[2], Pieter Provoost[2], Maaike Steyaert[1], Karline Soetaert[2] and Magda Vincx[1]

[1] Ghent University, Marine Biology Section, Krijgslaan 281/S8, B-9000 Gent, Belgium
[2] NIOO-CEME, Korringaweg 7, PO Box 140, 4400 AC Yerseke, The Netherlands

5.1 Introduction

The Belgian Continental Shelf (BCS), located in the nutrient enriched Southern Bight of the North Sea, is characterised by a high levels of primary production and algal biomasses (Lancelot *et al.*, 1987; Rousseau, 2000). Phytoplankton dynamics displays strong seasonal patterns with diatom blooms initiating the succession in February-March and the main spring bloom composed of diatoms and *Phaeocystis* in April-May (Rousseau *et al.*, 2002; 2008). At that time, *Phaeocystis* colonies can contribute up to 99% of the autotrophic biomass in the pelagic realm (Hamm & Rousseau, 2003). Phytoplankton summer blooms are mainly composed of diatoms which last as late as end October (Rousseau *et al.*, 2008). Although the bulk of phytoplankton production is mostly remineralized in the water column after the bloom (Rousseau *et al.*, 2000), still 24% is deposited on the sediment of the BCS, 65% of it being under the form of *Phaeocystis* colonies (Lancelot *et al.*, 2005).

Sedimentation of phytoplankton and derived matter, the phytodetritus, represents a major source of organic matter (OM) for the benthic system where it fuels benthic life (Graf, 1992). In return, benthic regeneration of nutrients is an important process for sustaining high rates of primary production in coastal areas (Nixon, 1980). The benthic response to phytoplankton sedimentation is however not unique. The receiving sediment type is a key factor determining the fate of freshly deposited OM. In fine-grained depositional areas, accumulation and sharp vertical profiles of labile OM can emerge after the phytodetritus sedimentation in spring (Steyaert *et al.*, 1999) and remineralisation can be delayed until late summer (Boon & Duineveld, 1998). On the contrary, rapid degradation of OM often takes place in coarser, permeable sediments (Ehrenhauss *et al.*, 2004; Janssen *et al.*, 2005; Bühring *et al.*, 2006). In these areas, tide induced lateral advective currents above the sediments prevent a mass sedimentation of phytodetritus (Huettel & Rush, 2000; Precht & Huettel, 2004). In addition, pore water is refreshed with tidal movement, keeping the

sediment oxygenated (Ziebis *et al.*, 1996; Janssen *et al.*, 2005) and removing the toxic by-products generated by remineralisation processes (Huettel *et al.*, 1998). All these factors accelerate the aerobic degradation of OM and the recycling of nutrients (Huettel & Rush, 2000; Janssen *et al.*, 2005; Bühring *et al.*, 2006) preventing the establishment of strong biogeochemical vertical profiles in these sediments.

Although the biogeochemical patterns in depositional and permeable sediments are well described and understood, little is known about the response of benthic organisms in sediments. The sediment distribution in the BCS shows contrasted areas with both fine-grained depositional areas and coarser, permeable sediments where this issue can be addressed. Two stations with contrasted sediments, Stn 115bis and Stn 330 (Figure 5.1), were therefore investigated in order to better understand how benthic organisms, from bacteria to macrobenthos, are responding to phytoplankton sedimentation.

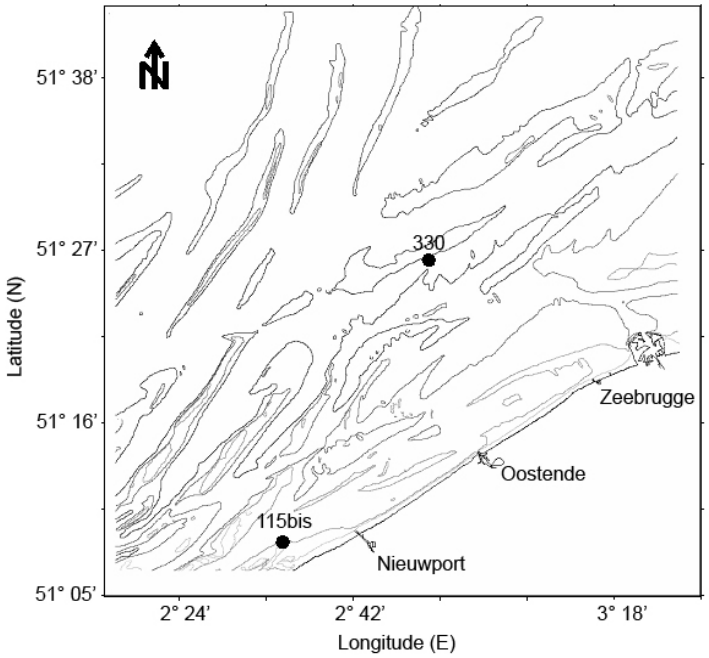

Figure 5.1. Location of the sampling Stn 115bis and Stn 330 of the BCS.

Stn 115bis is located close to the coast (51°09.2 N - 02°37.2 E; 13 m depth) and is characterized by fine sandy sediments according to the classification scale of Buchanan (1984) with a median grain size of 185 µm and a small fraction of mud (4%>63 µm; Steyaert, 2003). The sediment of Stn 330 (51°26.0 N - 02°48.5 E; 20 m depth), situated further off shore, is classified as medium sand (median grain size between 321 µm and 361 µm; Vanaverbeke *et al.*,

2004a) and has no mud. Both stations were intensively studied before, during and after the phytoplankton blooms in 1999 and 2003 in order to:

- describe the changes in the biogeochemical patterns;
- quantify the remineralisation processes;
- describe the response of the benthic organisms, *i.e.* bacteria, meiobenthos and macrobenthos, and;
- assess the relative importance of pelagic diatoms and *Phaeocystis* as food source for the benthos.

In this chapter, we compare the patterns and processes occurring in the two sediment types, focusing on the response of bacteria and nematodes. Nematodes are indeed the dominant taxon in the meiofauna, *i.e.* all metazoan animals passing a 1 mm but retained on a 38 µm sieve. Due their exclusively benthic life style, short generation times, high diversity and density, they are an ideal tool to reflect changes in the benthic environment (Kennedy & Jacoby, 1999).

5.2 Seasonal dynamics of phytodetritus sedimentation and mineralisation

5.2.1 Seasonal patterns of phytodetritus benthic distribution

Figure 5.2 compares the seasonal dynamics of phytoplankton, expressed as bulk Chlorophyll a (Chl *a*) in the surface and bottom waters at both Stn 115bis and Stn 330. The seasonal trend, with a well marked phytoplankton spring bloom and further moderate summer and fall outbursts, is similar to that found in other years (Steyaert, 2003; Vanaverbeke *et al.*, 2004 a,b; Franco *et al.*, 2007). As a general trend the similar Chl *a* concentrations measured in the surface and bottom water of both stations reflect the permanent well-mixed water column on the BCS. The higher Chl *a* maxima reached at the inshore Stn 115bis probably reflect the higher nutrient availability near the coast (Brion *et al.*, 2008; Rousseau *et al.*, 2008).

Sedimentation of phytodetritus can be estimated based on the integration of the Chl *a* concentration vertical profiles in the sediment column (Fig. 5.3). Sedimentation mainly occurs in April after the peak of the phytoplankton bloom (Fig. 5.2). Interestingly enough much higher sedimentary Chl *a* concentrations and a steeper vertical profile are observed in the fine sandy sediments of Stn 115bis (Fig. 5.3a). In contrast, the vertical Chl *a* profile in the medium sands at Stn 330 never displays such clear vertical gradient during the sampling period (Fig. 5.3b).

The oxygenation status in the sediments of the two stations is also different. The coarser sediments at Stn 330 remain completely oxic over the whole sediment column whereas at Stn 115bis anoxic sediments are observed just after the deposit of phytodetritus, and propagate from 0.4 cm sediment depth onwards. The lower Chl *a* concentrations, the full oxygenation and the absence

of steep vertical profiles reflect all together the permeable nature of the sediment at Stn 330, contrasting with the characteristics of a depositional sediment such as that of Stn 115bis.

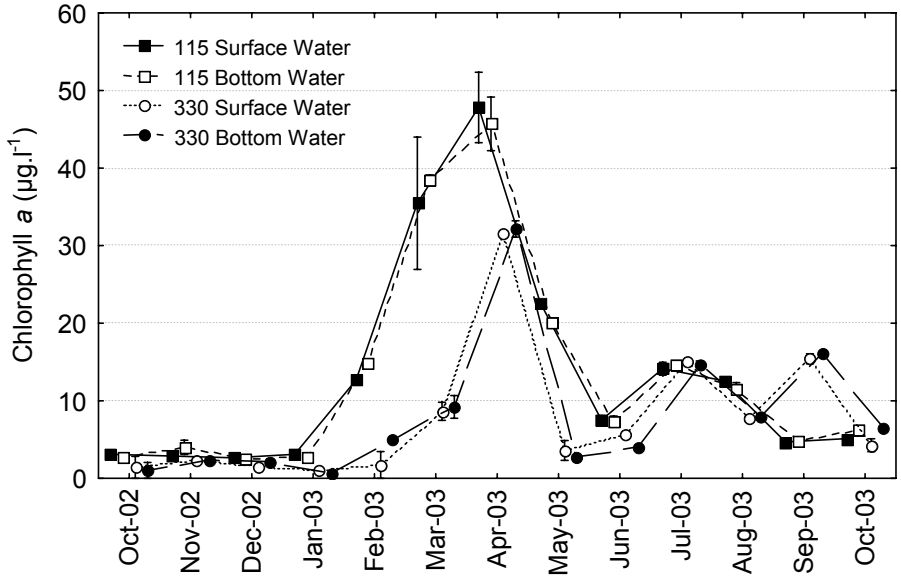

Figure 5.2. Chlorophyll *a* concentration (µg L-1) in the surface and bottom water at Stn 115bis and Stn 330 over the period October 2002-October 2003. Vertical bars represent the Standard Error. From Franco *et al.* (2007).

5.2.2 Seasonal patterns in mineralisation processes

The global mineralisation of the OM deposited to the sediment by the benthic community (bacteria, meiobenthos, macrobenthos) is generally estimated from the measurement of Sediment Oxygen Consumption (SOC) rates either *in situ* or under dark and temperature-controlled laboratory conditions (Moodley *et al.*, 1998). For this purpose, perspex cores with an internal diameter of 9.5 cm were sampled at both stations and transported to the laboratory, closed with a detachable lid containing an YSI 5739 oxygen electrode and a Teflon coated magnetic stirrer. The oxygen concentration in the water was then continuously monitored and SOC was calculated from the linear decrease of oxygen concentration over time (Moodley *et al.*, 1998).

a.

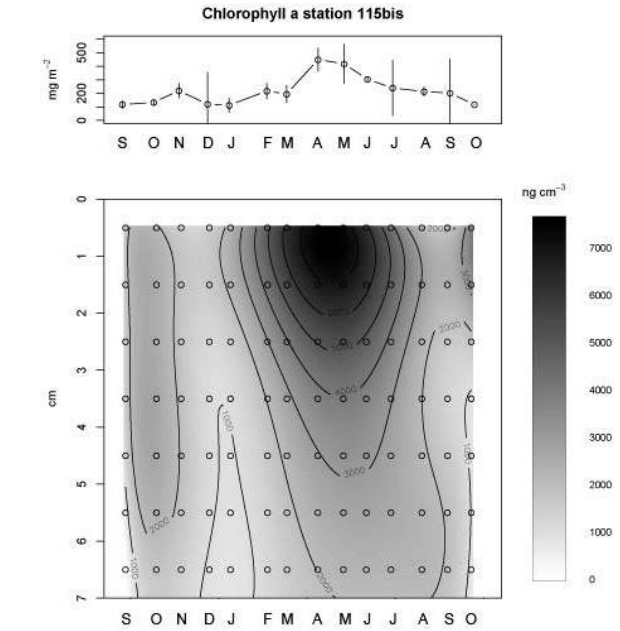

b.

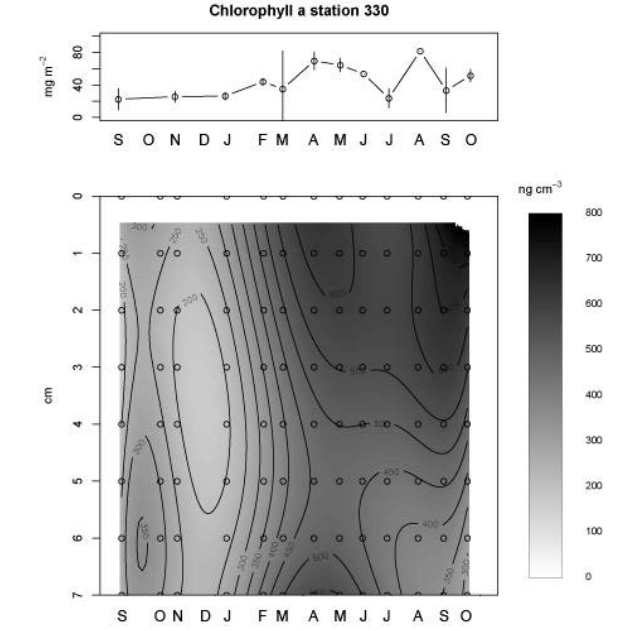

Figure 5.3. Vertical profiles of Chl *a* concentrations in the sediments (lower panels) and integrated Chl *a* concentrations in the sediment column (upper panels) of Stn 115bis (a) and Stn 330 (b) over the period October 2002 – October 2003.

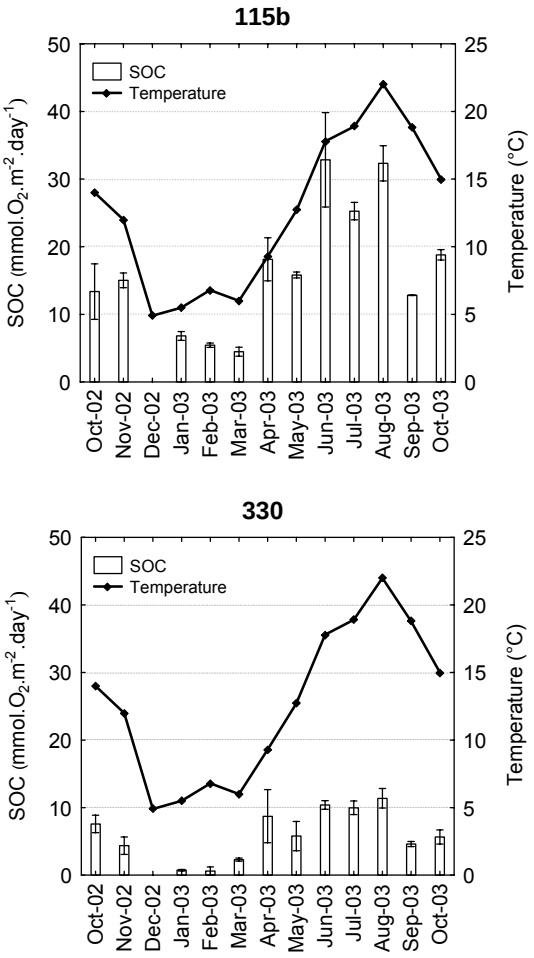

Figure 5.4. Sediment Oxygen Consumption (mmol O_2 m^{-2} d^{-1}) and water temperature (°C) at Stn 115bis and Stn 330 over the period October 2002-October 2003. The vertical bars represent the standard error.

As a general trend, SOC values calculated at Stn 115 bis were much higher than at Stn 330 at all sampling dates. This is due to the higher amount of phytodetritus deposited at the sediment surface of the fine sands of Stn 115bis than at Stn 330 (Fig. 5.3). At this latter station, surface primary production is lower and the higher bottom water currents above the seafloor prevent the deposition of the sedimenting phytodetritus (Franco *et al.*, 2007). In addition, SOC values measured at Stn 330 could well be underestimated due to the absence, in our laboratory experiments, of advective currents through these permeable sediments which prevents the continuous oxygenation of the sediment and removal of remineralisation byproducts. The absence of

porewater flow through the sediment can result in a SOC underestimation by a factor of 1.4, or even 2-3 when diatoms are added to experimental mesocosms (Ehrenhauss & Huettel, 2004). Even when taking this factor into account, SOC values measured for Stn 330 are lower than those recorded for St 115bis, but the difference is less obvious.

In both stations, SOC values were lowest in winter and increased after the phytodetritus sedimentation following the spring bloom. This suggests that in both sediment types, SOC is dependent on the quality and quantity of the available OM. In addition, the actual maximum SOC values calculated for the fine sediments of Stn 115bis are reached only 2 months (in June) after the main sedimentation event in April. This coincides with a drastic increase in water temperature (Fig. 5.4), suggesting that in fine sediments SOC is dependent on temperature as well (Provoost *et al.*, in preparation). This was not so clear at Stn 330, where values close to the maximum values were observed immediately after the arrival of phytodetritus to the seafloor, indicating that in permeable sediments, SOC rates are mainly dependent on the availability of degradable OM.

5.3 Benthic response to phytoplankton sedimentation

5.3.1 Bacterial communities

Marine benthic bacterial communities are known to react fast to OM deposition in terms of biomass production, cell division and activity which result in an increase in biomass, density and productivity (Graf *et al.*, 1982; Meyer-Reil, 1983; Goedkoop & Johnson, 1996; Boon *et al.*, 1998). This response is mainly influenced by the co-variation of OM supply and temperature (Graf *et al.*, 1982; Boon *et al.*, 1998; Van Duyl & Kop, 1994). Even though the bacterial response to sedimentation events in terms of biomass, density and productivity is well documented, little is known about possible changes in bacterial community composition and/or diversity. Changes in bacterial community composition were here investigated before, during and after a phytoplankton bloom at both stations and at two sediment depths, *i.e.* surface (0-1 cm) and sub-surface (4-5 cm). Denaturating Gradient Gel Electrophoresis (DGGE; Muyzer, 1999) was used after extraction of the bacterial DNA from the sediment following Dembo Diolla (2003) and Franco *et al.* (2007). Bacterial community composition was statistically analysed using a non-metric Multi Dimensional Scaling (MDS) which allows to group samples based on their similarity level. In the 2D ordination plot, samples characterized by similar bacterial communities are close to each other and reversely, are far away from one another when having very different communities. Figure 5.5 shows examples of DGGE gels and their corresponding statistical analysis. The MDS of bands shows that bacterial communities vary between stations, sediment depths and seasons (Franco *et al.*, 2007).

The bacterial community composition at both stations is significantly influenced by the Chl *a* concentration in the sediment, reflecting the importance of quantity and quality of OM (Franco *et al.*, 2007).

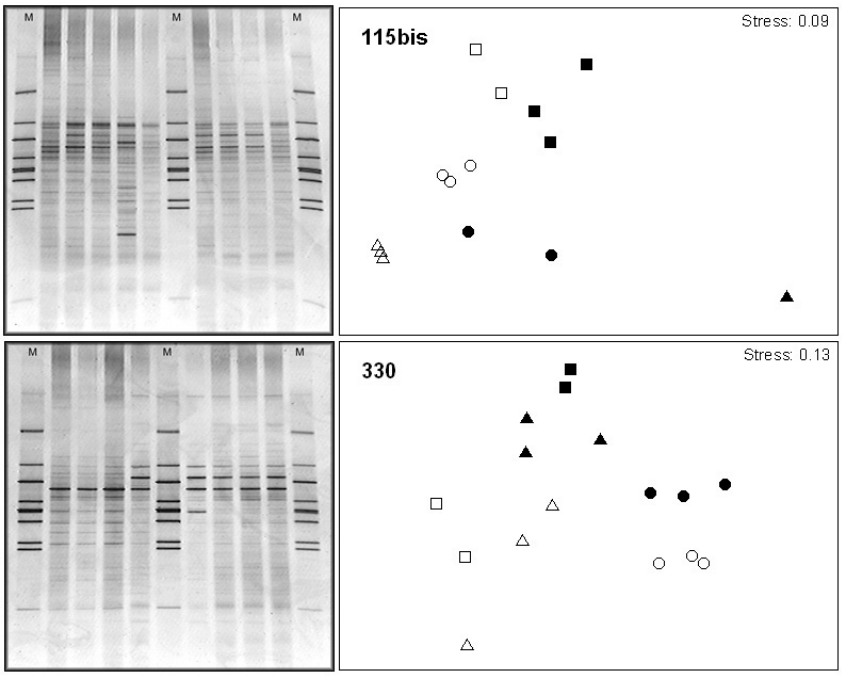

Figure 5.5. Example of DDGE gels and corresponding MDS analysis of bacterial community composition at Stn 115bis and Stn 330. Squares: February; triangles: April, circles: October. Open symbols: 0-1 com; solid symbols: 4-5 cm. Each band on the gels represents one Operational Taxonomical Unit. Redrawn from Franco *et al.* (2007).

Oxygen depletion resulting from OM mineralization might also contribute to the observed changes in bacterial communities (Janse *et al.*, 2000). Diversity was higher at the fine sediment station, probably due to the higher food availability and the co-existence of aerobic and anaerobic bacteria at that station. Bacterial community composition also varies with phytoplankton bloom stage, *i.e.* pre-bloom, bloom and post-bloom situation, suggesting an effect of phytoplankton sedimentation. The response of bacteria in terms of community composition is sediment-dependent and is influenced by local characteristics such as anoxia following OM sedimentation at Stn 115bis *vs* oxic sediment at Stn 330. Bacterial community composition and diversity is therefore regulated by food availability and quantity in combination with hydrodynamic stress and oxygenation.

5.3.2 Nematode communities

Nematode communities from both sites react differently to the OM sedimentation from the water column. The fastest response was observed at Stn 330 where nematode densities increase shortly after the sedimentation of the bloom, start decreasing already two months after the bloom and increase again during the moderate summer blooms (Fig. 5.7b; Franco *et al.*, 2007). The pattern of nematode density variation is similar to that observed in 1999 at Stn 330 where it was concomitant to an increase in nematode diversity

(Vanaverbeke *et al.*, 2004b). This seasonal distribution was attributed to an opportunistic response of an aberrant morphotype, the so-called stout nematodes (Fig. 5.6; Vanaverbeke *et al.*, 2004a) which are characterised by a length/width ratio <15 (Soetaert *et al.*, 2002).

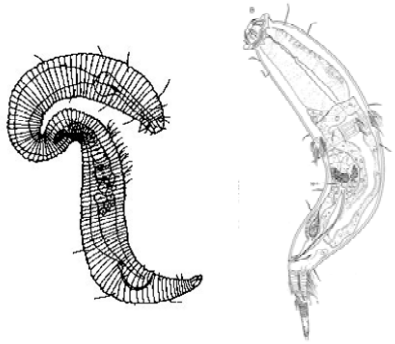

Epsilonema *Richtersia*

Figure 5.6. Illustrations of *Epsilonema* sp. and *Richtersia* sp., two examples of stout nematodes.

Stout nematodes increase their densities at a much faster rate (6.5% d^{-1}) than that of the total community (1.5% d^{-1}) after the phytoplankton bloom deposition (Vanaverbeke *et al.*, 2004a). When OM is remineralised, which is a fast process due to the permeability of the sediment, the density decreases at a much faster rate as well (3% d^{-1}) compared to the total community (0.7% d^{-1}).This opportunistic behaviour can be explained by their small length (Vanaverbeke *et al.*, 2004a) which enables them to reach adulthood faster than the longer slender nematodes. As a consequence, they reproduce faster, triggering a fast increase in densities. Stout nematodes are however more sensitive to food shortage and starvation when OM is mineralised, dying earlier since smaller animals have a shorter life span (Kooijman, 1986). The increase in diversity was explained by the availability of a more wider variety of food particles (Vanaverbeke *et al.*, 2004b).

A different picture emerges at Stn 115bis where nematode densities increase gradually after the sedimentation event and reach maximum values in October (Fig. 5.7a; Steyaert, 2003; Franco, 2007). Contrary to Stn 330, no increase in diversity was observed (Steyaert, 2003). Increase in nematode densities is a consequence of successive reproduction periods of the dominant nematode species at well-defined sediment depths (Steyaert, 2003). The timing of nematode density increase at a given sediment depth coincides with the burial of phytodetritus, indicating that nematode species need a specific food quality to increase their densities. In addition to seasonal fluctuations, nematode densities also vary between stations (Fig. 5.7). Densities at Stn 115bis are always much higher in comparison with densities observed at St 330, which is a consequence of the higher availability of OM at Stn 115bis (Fig. 5.3).

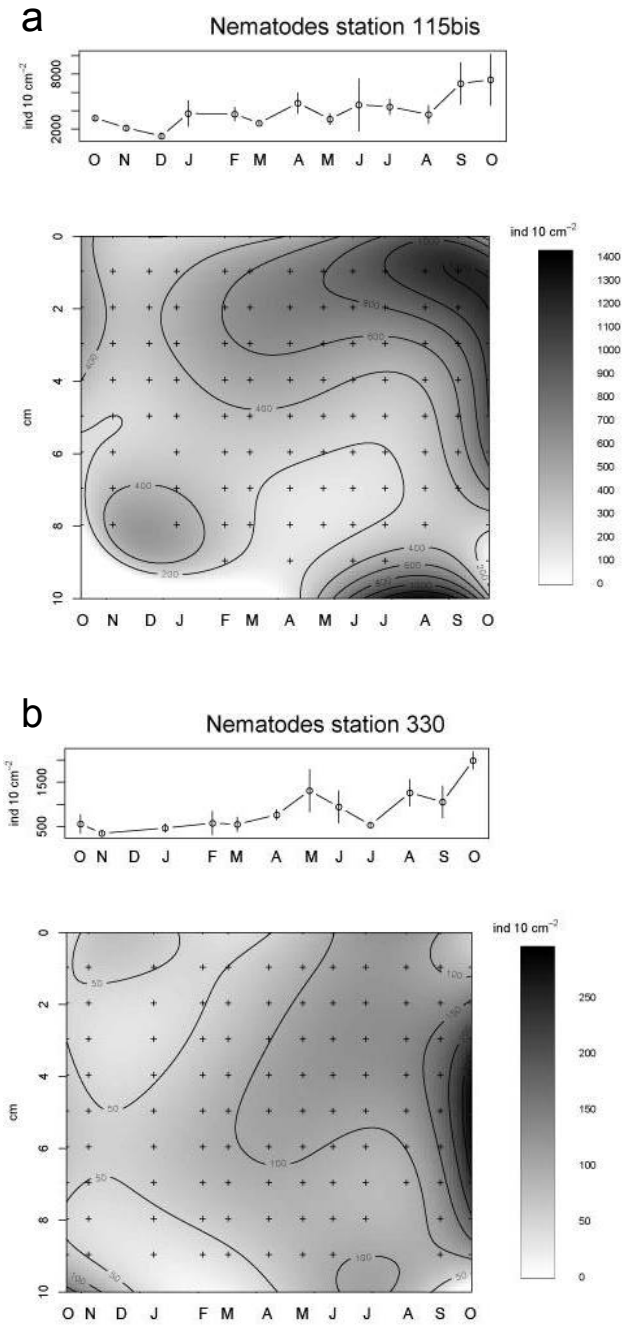

Figure 5.7. Vertical distribution of nematode total densities (lower panels) and average density in the sediment column (upper panels) at Stn 115bis (a) and Stn 330 (b) during the period October 2002 - October 2003. From Franco *et al.* (2007).

5.4 Phytodetritus as a food source for benthic organisms

5.4.1 Natural conditions

Stable isotopes ^{13}C and ^{15}N can be used to trace the food ingested by animals and hence to determine their trophic position. The ^{13}C of consumers is indeed a weighted average of the ^{13}C of their food sources whilst the ^{15}N signal increases of ± 3 ‰ at each trophic level (Post, 2002). During the seasonal cycle 2002-2003, ^{13}C and ^{15}N of particulate organic matter (POM) of the water column and the sediment and of meiobenthos were measured at three different periods, *i.e.* before (February), during (April) and after (October) the phytoplankton bloom. Meiobenthic organisms were picked from 2 depth layers, 0-1 cm and 4-5 cm (Franco, 2007). When possible, nematodes were identified at the genus level and the difference between stout and slender nematodes was made.

Measurements of $\delta^{13}C$ at Stn 115bis (Fig. 5.8) and at Stn 330 (Fig. 5.9) show, for both stations, different $\delta^{13}C$ values in the meiobenthic organisms and in the sediment POM, indicating that OM as a whole cannot be considered as an appropriate food source. Results show also little temporal fluctuation of the meiobenthos isotopic signature in the upper cm suggesting a constant food source throughout the year. These two observations suggest that the organisms living in the sediment surface depend on a constant but limited supply of fresh algal material originating from the water column (Franco *et al.*, 2008). The absence of vertical differences in the $\delta^{13}C$ values in the organisms from Stn 330 is due to the permeability of the sediment, suggesting that, at this station, the benthic food web is solely depending on fresh phytoplankton. At St 115bis, vertical differences in the $\delta^{13}C$ values in the nematodes except the genus *Richtersia* and *Sabatieria*, refered here as “other nematode”, reveal the use of different sources, with the deeper-dwelling nematodes being part of a food web based on older more fractionated and decomposed OM. These observations reflect the gradual burial and mineralisation process of fresh phytodetritus in finer sediments of Stn 115bis. The extremely low values of $\delta^{13}C$ measured in the benthic copepods in October suggest the existence, at Stn 115bis, of a chemoautotrophic food source based on sulphur-oxidising bacteria (Felbeck & Distel, 1999).

Except for copepods at Stn 115 bis in October 2003, $\delta^{15}N$ values show no significant differences between the meiobenthic taxa and within the nematodes (Franco *et al.*, 2008). This suggests that only limited predator-prey relationships exist within the meiobenthic community in our subtidal stations. Predatory nematodes were not dominant at the two sites (Steyaert 2003, Vanaverbeke *et al.*, 2004b) so that their higher $\delta^{15}N$ value could well be diluted in the “bulk nematode” value.

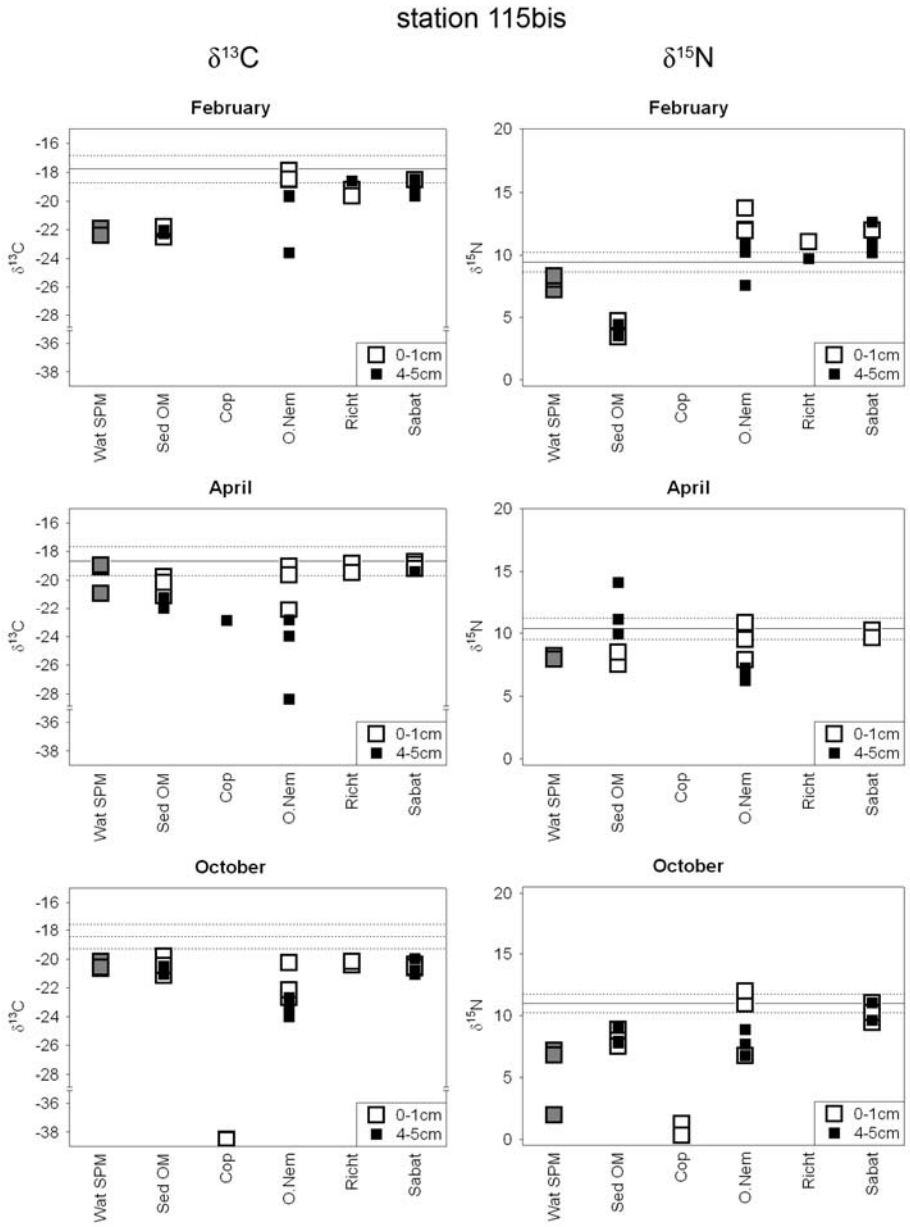

Figure 5.8. $\delta^{13}C$ (left panel) and $\delta^{15}N$ (right panel) signatures of water column (1 m above seafloor) suspended particulate matter (SPM), sediment OM and meiobenthic taxa at Stn 115bis. Horizontal line: mean (solid) and ± Standard Error (dotted) of $\delta^{13}C$ and $\delta^{15}N$ in benthic organisms in Stn 330. Organisms reported as Cop: copepods; O. Nem: other nematodes; Richt: *Richtersia*; Sabat: *Sabatieria.*

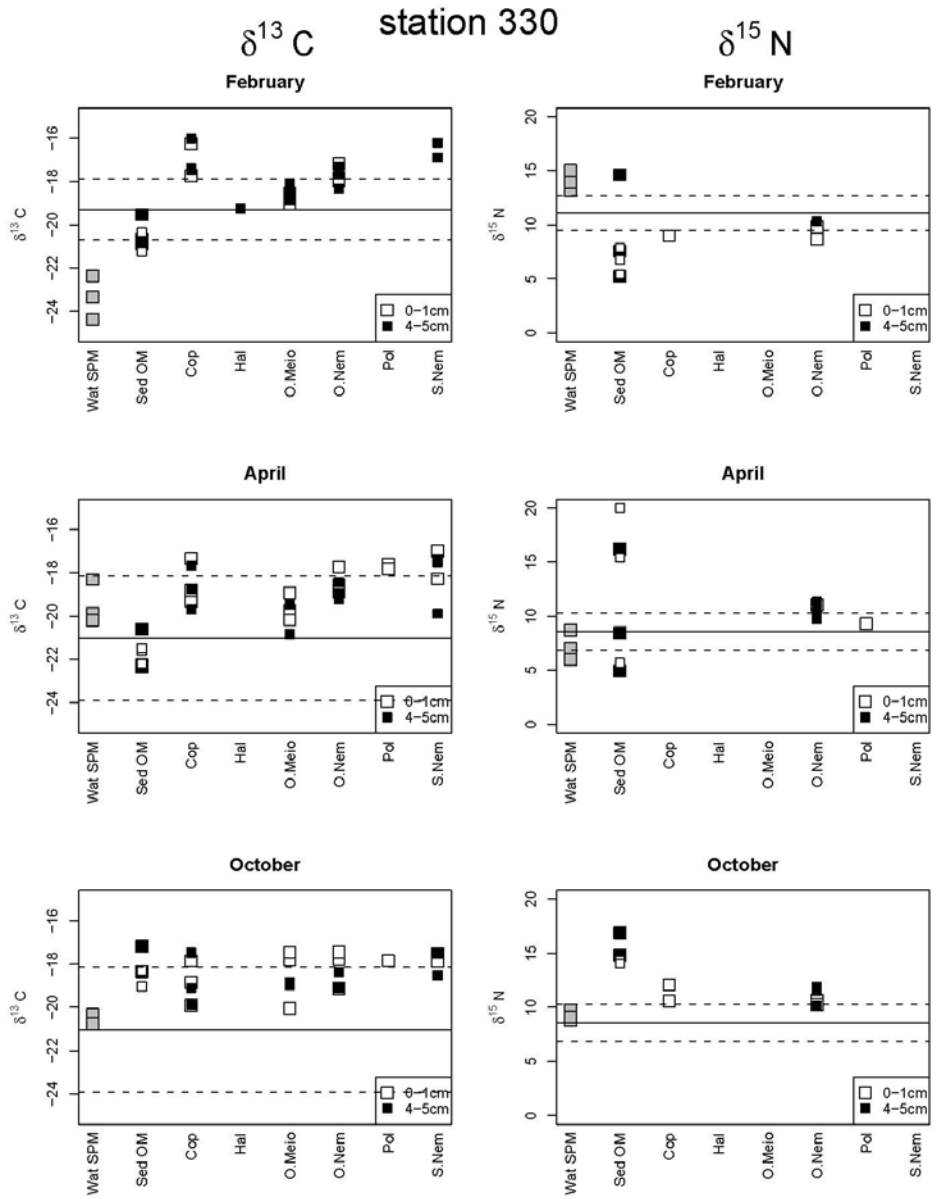

Figure 5.9. $\delta^{13}C$ (left panel) and $\delta^{15}N$ (right panel) signatures of water column (1 m above seafloor) suspended particulate matter (SPM), sediment OM and meiobenthic taxa at Stn 330. Horizontal line: mean (solid) and mean ± Standard Error (dotted) of $\delta^{13}C$ and $\delta^{15}N$ in benthic organisms at Stn 115bis. Organisms reported as Cop: copepods; Hal: Halacaroidea; O. Meio: other meiobenthos; O. Nem.: other nematodes; Pol: Polychaetes; St. Nem.: stout nematodes.

5.4.2 Planktonic diatoms and *Phaeocystis* as food source for the benthos

Although *Phaeocystis* is significantly contributing to the phytoplankton communities during spring (Rousseau *et al.*, 2000; 2008), the sedimentation of *Phaeocystis*-derived matter and its possible contribution as food resource for benthic organisms on the BCS is still unknown. So far, grazing on settled *Phaeocystis* colonies by benthic gastropods has been reported in tidal flats (Cadée, 1996), but no information on the trophic fate of *Phaeocystis* in the subtidal benthic ecosystem is available.

In order to resolve this question natural sediments sampled at Stn 115bis were incubated in presence of ^{13}C pre-labelled cultures of the diatom *Skeletonema costatum* (1000 mg C m^{-2}, 193 mg ^{13}C m^{-2}) and *Phaeocystis* (128 mg C m^{-2}, 50 mg ^{13}C m^{-2}) under laboratory-controlled conditions (see details in Franco *et al.*, in press). After two weeks, meiobenthic organisms from four sediment depths, 0-1, 1-3, 3-5 and 5-8 cm, were collected for isotope analysis (Fig. 5.10). Clearly the uptake of labelled phytoplankton was the highest in the upper cm-layer and was realized by the nematodes, the dominant taxon in the samples. *Phaeocystis* C uptake is one order of magnitude lower than *S. costatum* C uptake. On average over the whole core, some 0.20 ± 0.05% and 0.14 ± 0.02% of carbon added as *S. costatum* and *Phaeocystis,* respectively, were retrieved in the nematodes suggesting that both phytoplankton species enter the meiobenthic food web in low but comparable quantities.

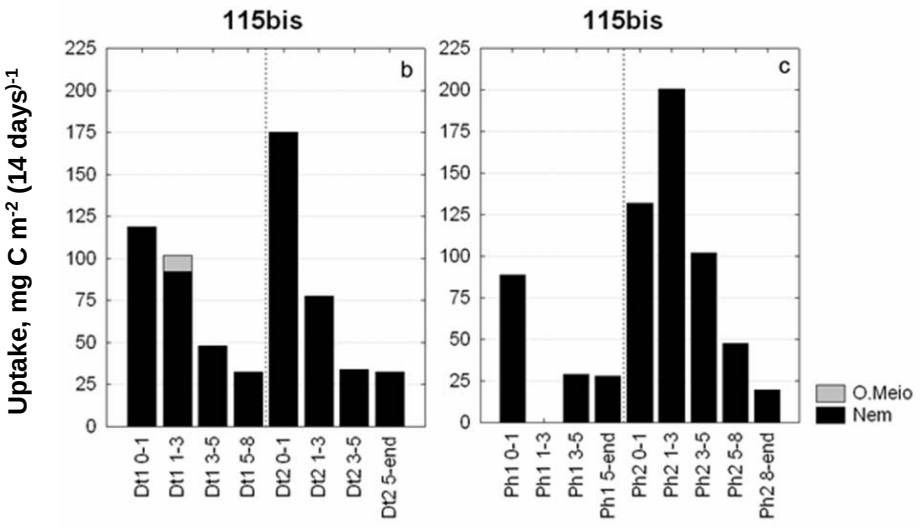

Figure 5.10. Total uptake (mgC m^{-2}) after 14 days of incubation of ^{13}C labelled diatoms *S. costatum* (left panel - Dt) and *Phaeocystis* (right panel - Ph) by nematodes (Nem) and other meiobenthos taxa (O. Meio) from Stn 115bis at 4 different sediment depths, 0-1, 1-3, 3-5 and 5-8 cm. Two replicates were performed for each treatment and depth. Note different Y-axis scaling (Redrawn from Franco, 2007).

When integrated over the sediment column and averaged over the incubation period, daily C uptake rates were estimated to 0.144 ± 0.033 and 0.014 ± 0.002 mgC m^{-2} d^{-1} in the *S. costatum* and *Phaeocystis* treatment respectively. This is largely unsufficient to sustain nematode C requirements as estimated from their respiration rates. These C uptake rates represent indeed only 0.66% (*S. costatum*) and 0.06% (*Phaeocystis*) of the C respired by nematodes (Franco *et al.*, in press). These experiments show that, although both *S. costatum* and *Phaeocystis* derived-carbon is consumed by nematodes, these organisms have to rely on other food sources to sustain their energy needs (Franco *et al.*, in press).

Although not important for nematodes, the role of both pelagic diatoms and *Phaeocystis* for the functioning of the benthic food web seems to important. Preliminary results reveal indeed that after 1 week, about 25% of C added as *S. costatum* and 10% of C added as *Phaeocystis* was respired in the benthic ecosystem in experimental microcosms (Moodley *et al.*, unpubl.).

5.5 Conclusions and perspectives

Our results show clearly that processes occurring in the sediment of the BCS are highly depending on the sedimentation of phytoplankton-derived material from the water column. However, the remineralisation is depending on the sediment type, which has a clear influence on the benthic response. When remineralisation is fast, as in permeable sediments, nematode densities increase fast after a sedimentation event. Although phytodetritus-derived carbon seems not to be the main food source for subtidal nematodes, animals inhabiting the surface of the sediments feed on freshly produced diatoms year-round.

In finer sediments, remineralisation is slower and more influenced by the water temperature, quality and quantity of the organic material. In these sediments, the organic loading is much higher and triggers anoxia during prolonged periods of the year. Nematode response in these sediments depends on the burial and degradation of organic matter and shows a time delay with respect to the peak sedimentation event. This coincides with the fact that different food sources were found at different depths at the fine sandy station. Both diatoms and *Phaeocystis* derived carbon is ingested by the benthic organisms, although diatoms are more important in the diet of the nematodes compared to *Phaeocystis*.

Future work should ideally focus on the role of the larger benthic animals, the macrofauna, in the mineralisation processes of the phytodetritus. Indeed, especially in the finer sediments, mineralisation processes and the response of the meiofauna to these processes is time-lagged with respect to the peak sedimentation event, and differs between sediment horizons. Macrobenthic activities such as bioturbation and bio-irrigation, greatly affect both the vertical distribution of organic matter and oxygen in the sediment. By altering the biogeochemical environment, these organisms have great influence on (1)

mineralisation rates of organic matter and (2) the availability of appropriate food sources for the meiobenthos.

5.6 References

Boon A.R. and G.C.A. Duineveld. 1998. Chlorophyll *a* as a marker for bioturbation and carbon flux in southern and central North Sea sediments. Marine Ecology Progress Series 162: 33-43

Boon A.R., Duineveld G.C.A., Berghuis E.M. and J.A. van der Weele. 1998. Relationships between benthic activity and the annual phytopigment cycle in near-bottom water and sediments in the Southern North Sea. Estuairne Coastal Shelf Science 46: 1-13

Brion N., Jans S., Chou L. and V. Rousseau. 2008. Nutrient loads to the Belgian Coastal Zone**.** In: Current Status of Eutrophication in the Belgian Coastal Zone. Rousseau V., Lancelot C. and D. Cox (Eds). Presses Universitaires de Bruxelles, Bruxelles, pp. 17-43

Buchanan J.B. 1984. Sediment analysis. In: Methods for the study of marine benthos. Holme N.A. and A.D. McIntyre (Eds). Blackwell Scientific Publications, Oxford and Edingburgh. 41-65

Bühring S.I., Ehrenhauss S., Kamp A., Moodley L. and U. Witte. 2006. Enhanced benthic activity in sandy sublittoral sediments: Evidence from C-13 tracer experiments. Marine Biology Research 2: 120-129

Cadée G.C. 1996. Accumulation and sedimentation of *Phaeocystis globosa* in the Dutch Wadden Sea. Journal of Sea Research 36: 321-327

Daro N., Breton E., Antajan E., Gasparini S. and V. Rousseau. 2008. Do *Phaeocystis* colony blooms affect zooplankton in the Belgian coastal zone? In: Current Status of Eutrophication in the Belgian Coastal Zone. V. Rousseau, C. Lancelot and D. Cox (Eds). Presses Universitaires de Bruxelles, Bruxelles, pp. 61-72

Demba Diallo M. 2003. Molecular study of the microbial community in pasture soil under *Acacia tortilis*_subsp. *Raddiana* and *Balanites aegyptica* in North Senegal. PhD thesis, Ghent University, Gent.

Ehrenhauss S. and M. Huettel. 2004. Advective transport and decomposition of chain-forming planktonic diatoms in permeable sediments. Journal of Sea Research 52: 179-197

Ehrenhauss S., Witte U., Buhring S.L. and M. Huettel. 2004. Effect of advective pore water transport on distribution and degradation of diatoms in permeable North Sea sediments. Marine Ecology Progress Series 271: 99-111

Felbeck H. And D.L. Distel. 1999. Prokaryotic Symbionts of Marine Invertebrates. In: The Prokaryotes: An Evolving Electronic Resource for the Microbiological Community. Dworkin M. *et al.* (Eds). 2nd edition, release 3.0, Springer-Verlag, New York

Franco M.A., De Mesel I., Demba Diallo M., van der Gucht K., Van Gansbeke D., Van Rijswijk P., Costa M.J., Vincx M. and J. Vanaverbeke. 2007. Impact of phytoplankton bloom deposition on benthic bacterial communities at two contrasting sediments in the Southern North Sea. Aquatic Microbial Ecology 48: 241-254.

Franco M.A., Soetaert K., Van Oevelen D., Van Gansbeke D., Costa M.J., Vincx M. and J. Vanaverbeke. 2008. Density, vertical distribution and trophic responses of metazoan meiobenthos to phytoplankton deposition in contrasting sediment types. Marine Ecology Progress Series 358:51-62

Franco M.A., Soetaert K., Costa M.J., Vincx M. and J. Vanaverbeke (in press). Uptake of phytodetritus by meiobenthos using ^{13}C labelled diatoms and *Phaeocystis* in two contrasting sediments from the North Sea. Journal of Experimental Biology and Ecology

Goedkoop W. and R.K. Johnson. 1996. Pelagic-benthic coupling: Profundal benthic community response to spring diatom deposition in mesotrophic Lake Erken. Limnology and Oceanography 41: 636-647

Graf G. 1992. Benthic-Pelagic Coupling - A Benthic View. Oceanogr Marine Biology 30: 149-190

Graf G., Bengtsson W., Diesner U., Schulz R. and H. Theede. 1982. Benthic response to sedimentation of a spring phytoplankton bloom - process and budget. Marine Biology 67: 201-208

Hamm C.E. and V. Rousseau. 2003. Composition, assimilation and degradation of *Phaeocystis globosa*-derived fatty acids in the North Sea. Journal of Sea Research 50: 271-283

Huettel M., Ziebis W., Forster S. And G.W. Luther. 1998. Advective transport affecting metal and nutrient distributions and interfacial fluxes in permeable sediments. Geochimica et Cosmochimica Acta 62: 613-631

Huettel M. and A. Rusch. 2000. Transport and degradation of phytoplankton in permeable sediment. Limnology and Oceanography 45: 534-549

Janse I., Zwart G., Van der Maarel M.J.E.C. and J.C. Gottschal. 2000. Composition of the bacteria community degrading *Phaeocystis* mucoplysaccharides in enrichment cultures. Aquatic Microbial Ecology 22: 119-133

Janssen F., Huettel M. And U. Witte. 2005. Pore-water advection and solute fluxes in permeable marine sediments (II): Benthic respiration at three sandy sites with different permeabilities (German Bight, North Sea). Limnology and Oceanography 50: 779-792

Kennedy A.D. and C.A. Jacoby. 1999. Biological indicators of marine environmental health: Meiofauna: a neglected benthic component. Environmental Monitoring and Assesment 54: 47-68

Kooijman S. 1986. Energy budgets can explain body size relations. Journal of Theoretical Biology 121: 269-282

Lancelot C., Billen G., Sournia A., Weisse T., Colijn F., Veldhuis M., Davies A. And P. Wassmann. 1987. *Phaeocystis* blooms and nutrient enrichment in the continental coastal zone of the North Sea. Ambio 16: 38-46

Lancelot C., Spitz Y., Gypens N., Ruddick K., Becquevort S., Rousseau V., Lacroix G. and G. Billen. 2005. Modelling diatom and *Phaeocystis* blooms and nutrient cycles in the Southern Bight of the North Sea: the MIRO model. Marine Ecology Progress Series 289: 63-78

Meyer-Reil L.A. 1983. Benthic response to sedimentation events during autumn to spring at a shallow-water Station in the western Kiel Bight 2. Analysis of benthic bacterial-populations. Marine Biology 77: 247-256

Moodley L., Heip C.H.R. and J.J. Middelburg. 1998. Benthic activity in sediments of the northwestern Adriatic Sea: sediment oxygen consumption, macro- and meiofauna dynamics. Journal of Sea Research 40: 263-280

Muyzer G. 1999. DGGE/TGGE a method for identifying genes from natural ecosystems. Current Opinion in Microbiology 2: 317-322

Nixon S.W. 1980. Between coastal marshes and coastal waters: A review of twenty years of speculation and research on the role of salt marshes in estuarine productivity and water chemistry. In: Estuarine and Wetland Processes. Hamilton P. and K.B. MacDonald (Eds). Plenum Press, New York. Pp 437–525

Precht E. and H. Huettel. 2004. Rapid wave-driven advective pore water exchange in a permeable coastal sediment. Journal of Sea Research 51: 93-107

Rousseau V. 2000. Dynamics of *Phaeocystis* and diatom blooms in the eutrophicated coastal waters of the Southern Bight of the North Sea. Ph.D. thesis. Université Libre de Bruxelles. 205 pp.

Rousseau V., Becquevort S., Parent J.-Y., Gasparini S., Daro M.-H., Tackx M. and C. Lancelot. 2000. Trophic efficiency of the planktonic food web in a coastal ecosystem dominated by *Phaeocystis* colonies. Journal of Sea Research 43: 357-372

Rousseau V., Leynaert A., Daoud N. and C. Lancelot. 2002. Diatom succession, silicification and silicic acid availability in Belgian coastal waters (Southern North Sea). Marine Ecology Progress Series 236: 61-73

Rousseau V., Park Y., Ruddick K., Vyverman W., Jans S. and C. Lancelot. 2008. Phytoplankton blooms in response to nutrient enrichment. In: Current Status of Eutrophication in the Belgian Coastal Zone. Rousseau V., Lancelot C. and D. Cox (Eds). Presses Universitaires de Bruxelles, Bruxelles, pp. 45-59

Soetaert K., Muthumbi A. and C.H.R. Heip. 2002. Size and shape of ocean margins nematodes: morphological diversity and depth-related patterns. Marine Ecology Progress Series 242:179–193

Steyaert M. 2003. Spatial and temporal scales of nematode communities in the North Sea and Westerschelde. PhD thesis, Ghent Univeristy, 114 pp.

Steyaert M., Garner N., Van Gansbeke D. and M. Vincx. 1999. Nematode communities from the North Sea: environmental controls on species diversity and vertical distribution within the sediment. Journal of the Marine Biological Association of United Kingdom 79:253-264

Vanaverbeke J., Soetaert K. And M. Vincx. 2004a. Changes in morphometric characteristics of nematode communities during a spring phytoplankton bloom deposition. Marine Ecology Progress Series 273: 139-146

Vanaverbeke J., Steyaert M., Soetaert K., Rousseau V., Van Gansbeke D., Parent J.-Y., and M. Vincx. 2004b. Changes in structural and functional diversity of nematode communities during a spring phytoplankton bloom in the southern North Sea. Journal of Sea Research 52: 281-292

Van Duyl F.C., Kop A.J. 1994. Bacterial production in North-Sea sediments - Clues to seasonal and spatial variations. Marine Biology 120: 323-337

Ziebis W., Huettel M. And S. Forster. 1996. Impact of biogenic sediment topography on oxygen fluxes in permeable seabeds. Marine Ecology Progress Series 140: 227-237

CHAPTER 6

Ecological modeling as a scientific tool for assessing eutrophication and mitigation strategies for Belgian coastal waters

Christiane Lancelot[1], Geneviève Lacroix[2], Nathalie Gypens[1] and Kevin Ruddick[2]

[1] Université Libre de Bruxelles (ULB), Ecologie des Systèmes Aquatiques (ESA), CP221. boulevard du Triomphe, B-1050 Brussels, Belgium
[2] Management Unit of the North Sea Mathematical Models (MUMM), Royal Belgian Institute for Natural Sciences (RBINS), Gulledelle 100, B-1200 Brussels, Belgium

6.1 Unresolved 'eutrophication' issues in Belgian coastal waters (BCZ) that can be addressed by ecological models

The role of model simulation in understanding system complexity and in decision-making is nowadays recognized. Models offer the ability to test conceptual understanding of how components of a given system are linked, and to simulate complex biogeochemical interactions in a quantifiable and repeatable manner. Modeling, however, is useful only if new insights subsequently lead to validation or rejection of hypotheses upon more detailed examination. Thus information extracted from model simulations is strongly linked to the chosen structure (trophic resolution) of the model and to the parameterization of the interactions between the components. When properly validated, models can be useful in both hindcast and forecast modes and used for testing environmental policy alternatives and their impact. Models are indeed the only tools which can be used to investigate future developments by simulating scenarios with different constraints.

Anthropogenic eutrophication in the BCZ results from the input of transboundary (SW- Atlantic waters enriched by the Seine, Somme, Authie and Canche, and Rhine) and local (IJzer, Leie and Scheldt) sources (Fig. 6.1) of land-based nutrients (N, P, Si). The relative importance of these different sources in the BCZ has transnational implications for eutrophication management but is not accurately known. The impact of each source will depend on the evolution of human activity on the watershed and on large scale climatic phenomena such as the North Atlantic Oscillation (NAO; Hurrell 1995; Ruddick & Lacroix, 2008), which determines the weather conditions over North-western Europe. The eutrophication problem in the BCZ is most visible as massive undesirable algal

blooms in spring. These blooms are composed mainly of ungrazable colony forms of the Haptophycea *Phaeocystis* that supplement diatoms (Rousseau *et al.*, 2008) and spread over the whole area along a SW-NE gradient (Lancelot *et al.*, 1987), impacting the ecosystem function and services (Lancelot, 1995, Rousseau *et al.*, 2004). In spite of more than 20 years' survey of phytoplankton blooms in BCZ and adjacent waters, the spatio-temporal coverage and magnitude of *Phaeocystis* colony blooms is not clearly known. Also unclear still today is the link between *Phaeocystis* colonies and nutrient loads of anthropogenic origin. Nowadays, these blooms are recurrent and occur after an early-spring diatom bloom controlled by dissolved silicate availability (Rousseau *et al.* 2002; Rousseau *et al.*, 2008). *Phaeocystis* colonies grow on nitrogen and phosphorus and form with diatoms the bulk of phytoplankton biomass during the growing season but their magnitude varies from year-to-year (Lancelot *et al.* 1998). Attempts have been made to relate long-term fluctuations of *Phaeocystis* blooms in the Southern Bight of the North Sea to changes either in climate (Owens *et al.* 1989; Gieskes *et al.*, 2007) or in anthropogenic nitrogen and phosphorus river loads (Cadée & Hegeman, 1991), but the outcome is unclear. These hypotheses were recently reconciled by Breton *et al.* (2006) who showed that in coastal waters like the BCZ large-scale variability correlated with the NAO interacts with the local influence of river nutrient loads.

Therefore, due to the complexity and temporal variability of controls on marine planktonic food webs, the link between nutrient change and the coastal ecosystem function cannot be understood by simple correlation between events. Mechanistic models which are based on chemical and biological principles and describe ecosystem carbon and nutrient cycles as a function of environmental constraints are ideal tools to handle this complexity. Constructing a mathematical tool for understanding and advising on mitigation strategies for combating eutrophication problems in the *Phaeocystis*-dominated BCZ and its adjacent waters is the long term purpose of AMORE (Advanced Modeling and Research on Eutrophication; http://www.ulb.ac.be/assoc/esa/AMORE), a multidisciplinary consortium of scientists focusing their research activity on coastal eutrophication since 1997. To achieve such a long term objective AMORE has developed an integrated research methodology that combines field observations, process-level studies and models development in an iterative way. In this approach model development has a key position as integrator and test of new knowledge. The main mathematical tool is the three-dimensional (3D)-MIRO&CO model (Lacroix *et al.*, 2007a) that combines the 3D hydrodynamical model COHSNS (Lacroix *et al.*, 2004) determining the physical transport of water and of ecosystem components, and the ecological model MIRO describing interactions between the ecosystem components as previously tested in a multibox frame (OD-MIRO; Lancelot *et al.*, 2005). In this chapter 0D-MIRO and 3D-MIRO&CO models are used to address scientific unresolved issues such as:

- The geographical extent of *Phaeocystis* colony blooms in the Channel and Southern Bight of the North Sea with a focus on the Belgian waters;

- The relative contribution of Channel/Atlantic inflow and local sources to the nutrient status of the BCZ;
- The relationship between *Phaeocystis* colony blooms in the BCZ and nutrient enrichment

As well as managerial concerns such as:

- The geographical limits of problem and non-problem maritime areas in terms of eutrophication as defined by the Oslo and Paris Commission for the Prevention of Marine Pollution (OSPAR, 2005);
- The level of nutrient reduction needed to decrease *Phaeocystis* blooms in the BCZ to ecologically acceptable biomass and the achievement to be expected in 2015 after implementation of the European Union's Water Framework Directive (2000) in the Great North Basin.

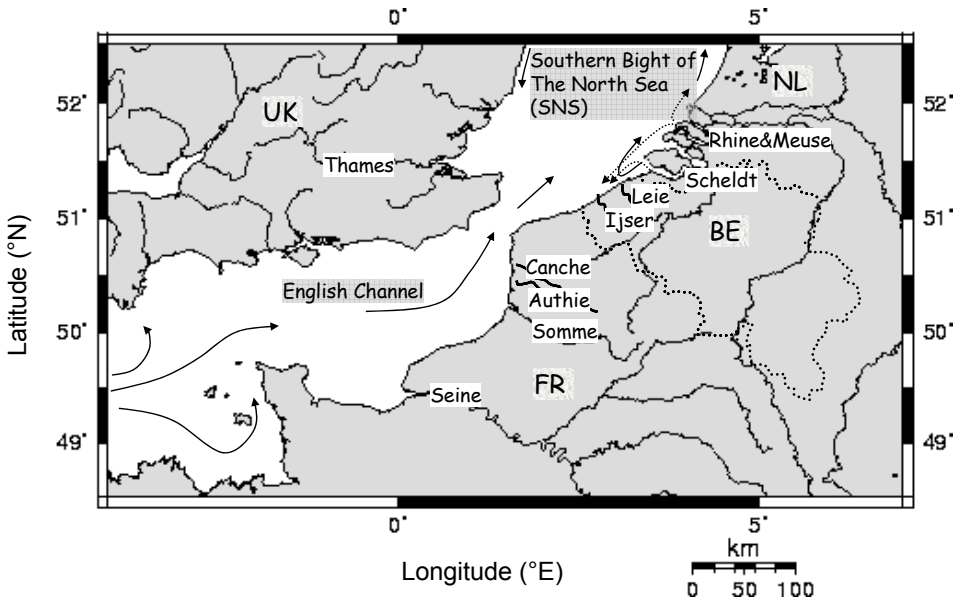

Figure 6.1. Map showing the modeled domain with river inputs and the mean general circulation

6.2 Model tools

Figure 6.2 shows the methodological approach chosen to construct the ecological model MIRO as well as the different implementation frames (0D-MIRO and 3D-MIRO&CO) used for tests and applications. The trophic resolution of MIRO was chosen based on the current mechanistic understanding of the eutrophication problem in the BCZ. MIRO describes C, N, P and Si cycling through aggregated components of the planktonic and benthic realms of *Phaeocystis*-dominated ecosystems (see justification of chosen state variables in Lancelot *et al.*, 2005). Its structure includes thirty-eight state variables assembled in four modules describing the dynamics of phytoplankton (three groups: diatoms, nanoflagellates and *Phaeocystis* colonies), zooplankton (two groups: copepods and microzooplankton), dissolved and particulate organic matter (each with two classes of biodegradability) degradation and nutrients [NO_3, NH_4, PO_4 and $Si(OH)_4$] regeneration by bacteria in the water column and the sediment. Equations and parameters were formulated based on current knowledge of the kinetics and factors controlling the main auto- and heterotrophic processes involved in the functioning of the coastal marine ecosystem. These are fully documented in Lancelot *et al.* (2005) and www.int-res.com/journals/suppl/appendix_lancelot.pdf. MIRO was first calibrated in a multi-box frame (0D-MIRO) delineated on the basis of the hydrological regime and river inputs. In order to take into account the cumulated nutrient enrichment of Atlantic waters by the Seine and Scheldt rivers, two successive boxes, assumed to be homogeneous, were chosen from the Seine Bight (French Coastal Zone, FCZ) to the BCZ (Fig. 6.2). Each box has its own morphological characteristics and river inputs (Table 1 in Lancelot *et al.*, 2005) and is treated as an open system, receiving waters from the upward adjacent box and exporting water to the downward box. In the current applications, river nutrient inputs are either extracted from national data bases (Lancelot *et al.*, 2005; Gypens *et al.*, 2007; Lacroix *et al.*, 2007a, b) or provided by RIVERSTRAHLER simulations (Lancelot *et al.*, 2007).

The RIVERSTRAHLER model establishes the link between the biogeochemical functioning of large river systems and the constraints set by the meteorological conditions, the morphology of the drainage network and the human activity on the watershed (Billen *et al.*, 1994, 1999; Garnier *et al.*, 1995). It is therefore an excellent tool to assess historical trends of eutrophication in BCZ.

The 3D version of MIRO, 3D-MIRO&CO, resulting from the implementation of MIRO in the 3D hydrodynamical COHSNS model (Lacroix *et al.*, 2004), simulates the transport and dynamics of inorganic and organic nutrients, phytoplankton, bacterioplankton and zooplankton biomass in the Western Channel and Southern Bight of the North Sea. For this purpose the 3D-MIRO&CO model has been set up for the region between 4° W (48.5°N) and 52.5°N (4.5°E) with the bathymetry shown in Figure 6.2, using a 109 by 97 horizontal grid with resolution 5’ longitude (approx. 5.6 km) by 2.5’ latitude (approx. 4.6 km) and with 5 vertical sigma coordinate layers. All details of its implementation and the description of forcing, boundary and initial conditions can be found in Lacroix *et al.* (2007a).

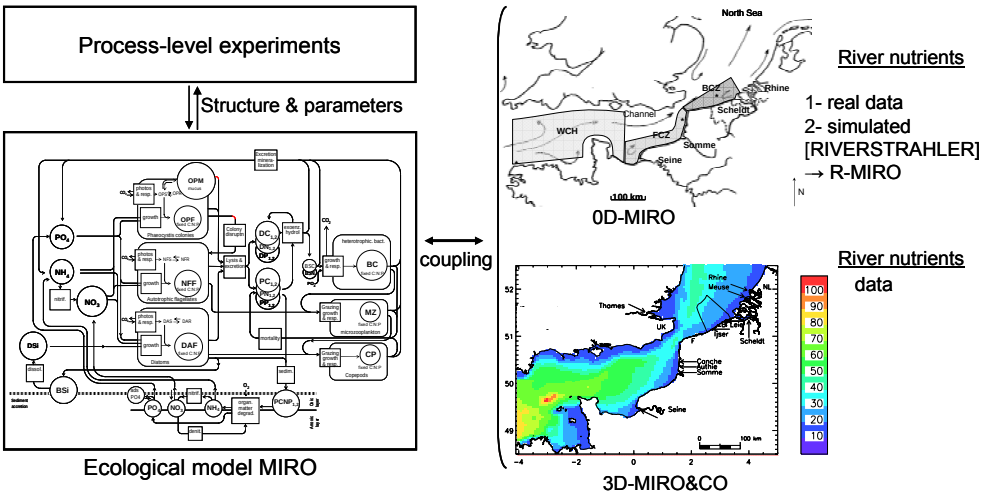

Figure 6.2. Schematic representation of the ecological model MIRO and its implementation frame (0D-MIRO and 3D-MIRO&CO) and river forcing.

6.3 Improved understanding of bloom dynamics and nutrient sources

6.3.1 Present-day geographical extent of *Phaeocystis* colony blooms

Figure 6.3 shows 3D-MIRO&CO simulations of biomass distribution of diatoms and *Phaeocystis* colonies in respectively early- (Fig. 6.3a) and end- (Fig. 6.3b) April 2004, *i.e.* at the time of their own blooming. In agreement with observations the simulated diatoms are blooming earlier in spring compared to *Phaeocystis* colonies. Both phytoplankton taxa show the highest biomass in the vicinity of the river mouths and correspond with areas of elevated nutrient stocks illustrated by the simulated distribution of nutrients in end-January (Fig. 6.3c), *i.e.* when remineralization is achieved and biological uptake is the lowest due to temperature and light limitation. In the eastern part of the 3D-MIRO&CO domain *Phaeocystis* colonies are simulated in the whole area extending from the Seine Bay up to the Northern limit of the 3D-MIRO&CO domain. According to 3D-MIRO&CO simulations the whole BCZ area is invaded by *Phaeocystis* colonies but the highest concentrations are to be found inshore especially in the vicinity of the Scheldt mouth (Fig. 6.3b). Nevertheless, the highest *Phaeocystis* concentrations in the geographical domain are simulated in the Dutch coastal waters due to SW-NE cumulated fluxes of nutrients to which are added land-based nutrients discharged by the river Rhine. In general the simulated *Phaeocystis* colony presence (Fig. 6.3b) agrees with what is known from sporadic monitoring sampling except for the Seine Bay where colonies have never been recorded. This discrepancy is intriguing and suggests that there is some aspect of ecosystem functioning that is not well understood and therefore not represented by the model equations. The reason for this is under investigation.

The analysis of 3D-MIRO&CO simulations over 12 years (1993-2004) indicates significant interannual variations in the timing, the magnitude and the geographical extent of *Phaeocystis* blooms. This is visible on Figure 6.4 which compares 3D-MIRO&CO simulations of *Phaeocystis* colonies in the investigated domain as obtained on 3rd May in 1995, 1998, 2002 and 2004. Such interannual difference in the spreading of *Phaeocystis* colonies is due to different meteorological conditions that determine the onset of the bloom and the timing of the maximum bloom development (Fig. 6.5). However, as shown on Figure 6.5 that maps the *Phaeocystis* colony distribution at the time of their maximum spreading in 1995, 1998, 2002 and 2004, there are also significant difference between years in magnitude and geographical extent. These are explained both by the varying meteorological conditions and nutrient river loads which together will determine the spreading of nutrients in the coastal area.

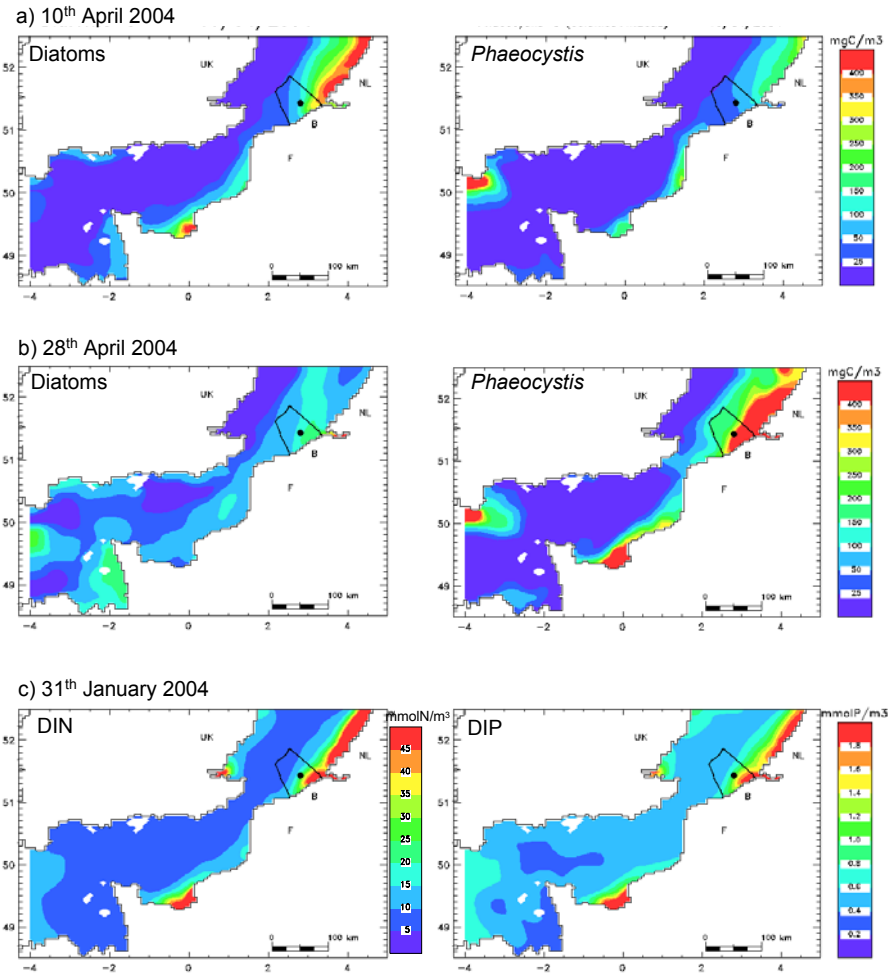

Figure 6.3. 3D-MIRO&CO simulations of diatom and *Phaeocystis* blooms in early (a) and end- (b) April 2004 and of nutrient concentrations in January 2004 (c).

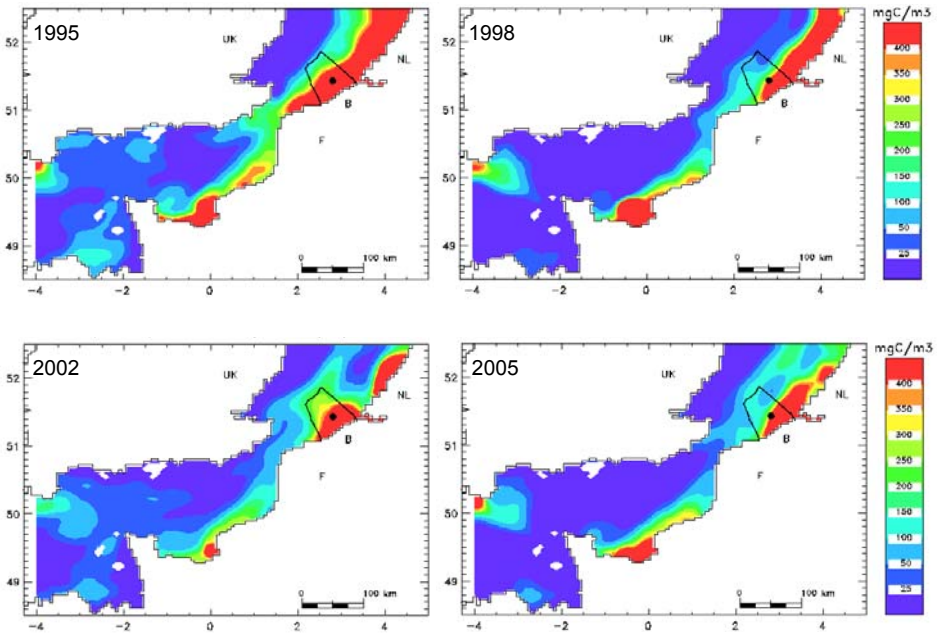

Figure 6.4. 3D-MIRO&CO simulations of *Phaeocystis* blooms on 3rd May in 1995, 1998, 2002 and 2004.

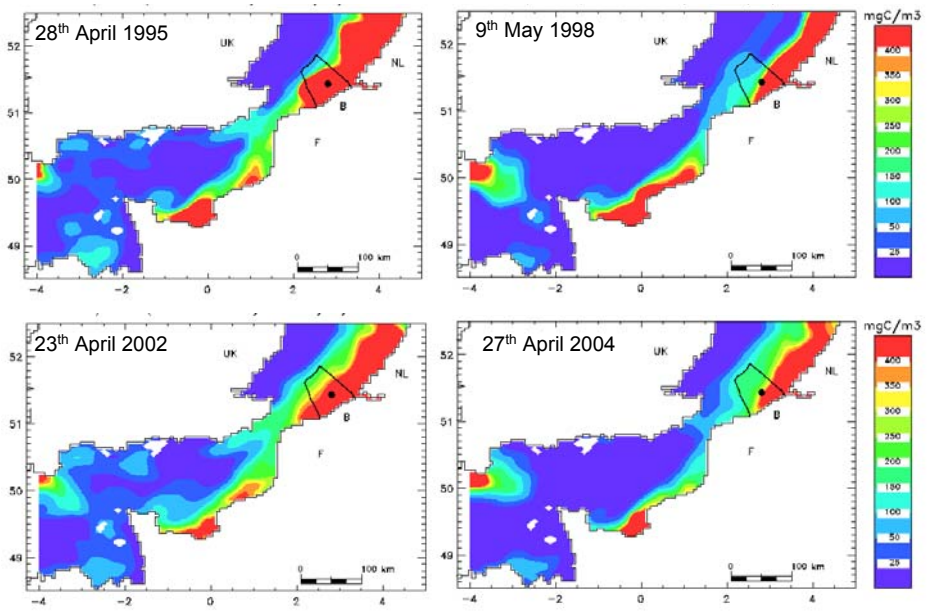

Figure 6.5. Maximum spreading of 3D-MIRO&CO *Phaeocystis* blooms in 1995, 1998, 2002 and 2004.

6.3.2 Contribution of different rivers (Seine, Scheldt and Rhine/Meuse) to the BCZ nutrient pool

The origin of inorganic nutrients (Dissolved inorganic nitrogen DIN and inorganic phosphate DIP) available for phytoplankton growth in the BCZ is indirectly investigated by running 3D-MIRO&CO sensitivity scenarios with decreasing nutrient inputs from inflowing Channel waters, Scheldt/Leie/IJzer and Rhine/Meuse by respectively 1% (Lacroix *et al.*, 2007b). Such a small decrease is chosen in order to ensure a quasi linear ecosystem response, effectively tracing the fate of nutrients from different sources in the current situation. The effect of this reduction is estimated by comparing the obtained average 1993-2003 field concentrations with those obtained with the non-perturbed simulation. Figure 6.6 illustrates which river contributes the most to the surface nutrient relative difference. Clearly, the nutrient reduction from the Seine has the strongest impact on surface DIN and DIP in the whole 3D-MIRO&CO domain, except the Belgian and Netherlands coastal zones (Fig. 6.6). Interestingly, the Scheldt has a larger effect than the Seine in the BCZ where eutrophication is most severe. The region of highest influence by the Rhine/Meuse (NE area of the model domain) extends more southward (until the Scheldt mouth) for DIN than that for DIP (Fig. 6.6). The fate of nutrients is thus somewhat different from the fate of freshwater (Lacroix *et al.*, 2004), where the Rhine/Meuse discharge was found to be more important in the BCZ. This difference can be attributed to the longer time scale for dispersion of freshwater, which is effectively conserved over decadal time scales whereas nutrients are transported as a conserved, dissolved constituents only for a few months (winter).

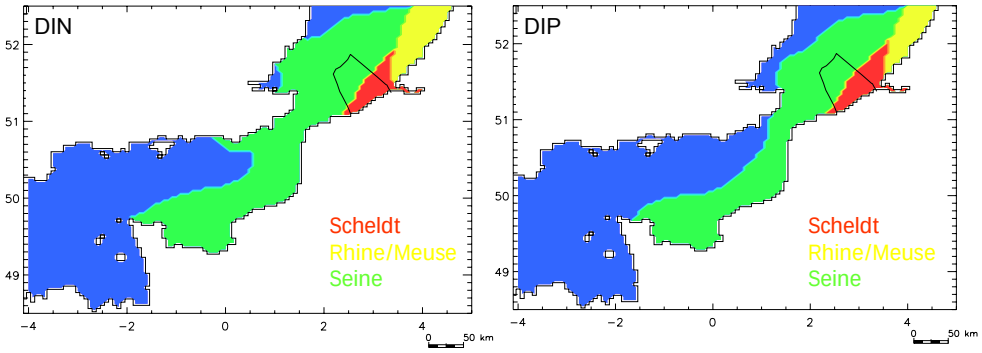

Figure 6.6. 1993-3003 highest river contribution (Seine, Scheldt, Rhine-Meuse) to the surface nutrients in the 3D-MIRO&CO domain.

6.3.3 Relationship between *Phaeocystis* colonies and nutrient enrichment in the BCZ: R-MIRO simulations over the past 50 years

Recent statistical analysis of fourteen-years (1988-2001) of intensive phytoplankton monitoring in the central BCZ (Breton *et al.*, 2006) in relationship with basin scale and local constraints indicates that the current interannual variability of *Phaeocystis* colony blooms is determined by river-based nitrate pulses modulated by NAO which affects the local hydrology, *i.e.* the relative contribution of Scheldt and Atlantic waters to the BCZ water budget. The variability of the hydrodynamics makes it difficult to establish links between *Phaeocystis* colonies and direct and indirect anthropogenic sources of nutrients when based on time series at fixed grid stations (Breton *et al.*, 2006). An additional difficulty is the lack of long-term time series of river nutrient inputs.

Long-term model simulations over periods of sustained human pressure provide a useful tool to analyze the link between blooms and nutrient enrichment. In this section, the link between *Phaeocystis* colony blooms in the BCZ and direct (Scheldt) and transboundary (Atlantic waters flowing into the BCZ) inputs of land-based nutrients is explored by performing 0D-MIRO simulations. The model is forced with nutrient fluxes simulated by the RIVERSTRAHLER model applied to the Seine and the Scheldt watersheds (Billen *et al.*, 2001; 2005) over the past 50 years, a period of intensive changes in land use and human activity. For this application targeting nutrients, an average meteorological year (global solar radiation, temperature, rainfall) is considered for the 1950-2000 period while changes in land use and changes in annual urban and industrial wastewater discharges are documented by 10 year periods and by 5 year periods respectively. Details on the coupling between RIVERSTRAHLER and MIRO (R-MIRO) are to be found in Lancelot *et al.* (2007). Simulations are analyzed in terms of historical evolution of nutrient sources to BCZ and nutrient enrichment and phytoplankton maxima in BCZ.

Nutrient inputs to BCZ over 50 years

Figure 6.7 compares the R-MIRO simulated 1950-2000 evolution of nutrient inputs to the BCZ distinguishing between the Seine-enriched Atlantic (S-Atl) inflow and the local Scheldt delivery. A contrasted historical evolution is clearly visible for the three nutrients considered (DSi, DIN and DIP). Between 1950 and 2000, Scheldt and S-Atl are contributing almost equally as DSi sources to the BCZ and both decrease slowly over the period up to 1995 after which a small increase is simulated (Fig. 6.7a). These variations result from the level of DSi consumption simulated by RIVERSTRAHLER in the rivers in response to the increased (or decreased) inputs of N and P from the watershed. On the other hand, DIP simulations show for both sources significant and similar trends: a sustained increase between 1950 and 1985 (factor 3; Fig. 6.7b) explained by the population increase and economical development, followed after 1985 by a progressive decrease until values typical of around 1965 are reached in 2000 (Fig. 6.7b). This decrease reflects the efficiency of P reduction measures implemented in the late eighties (mainly the abolition of polyphosphates in washing powders; Billen *et al.*, 2001; 2005). When comparing the two nutrient sources, it is clear that DIP is brought mostly by the S-Atl (74-94%). As for DIP,

R-MIRO simulates a factor 3 enrichment of DIN fluxes to the BCZ over the 1950-1985 period (Fig. 6.7c). A difference here with respect to DIP is the contribution of the different sources and the simulated evolution of DIN inputs which remain high until 2000 (Fig. 6.7c). Interestingly the contribution of the Scheldt to the DIN pool in the BCZ increases over the simulated period (1950-1970: 25%; 1975-2000: 40%) probably related to the importance of cattle wastes on the Scheldt watershed. Altogether, the historical R-MIRO reconstruction of nutrient inputs to the BCZ indicates that increased human activities on the watershed were modifying not only the quantity but also the quality of nutrient fluxes delivered to the coastal sea, being already Si-depleted in 1950 and in excess N with respect to P (N:P>25) after 1990.

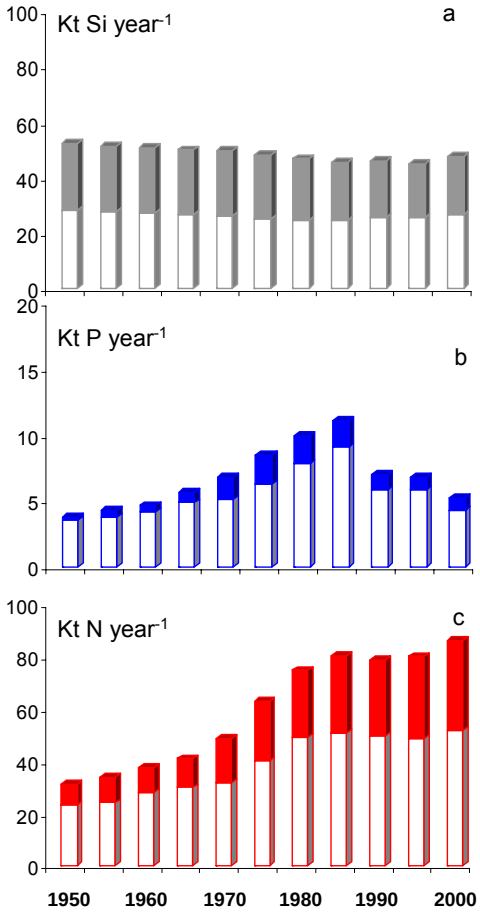

Figure 6.7. R-MIRO simulations of DSi (a), DIP (b) and DIN (c) inputs to the BCZ over the 1950-2000 period discriminating between the S-Atl inflow (open block) and the local Scheldt delivery (filled block).

50 year evolution of nutrient enrichment in BCZ

The quantitative and qualitative changes in DSi, DIN and DIP delivery to the BCZ (for which simulation results are shown in Figure 6.7) affect the nutrient status of the coastal area. This is best seen from the R-MIRO simulated winter stock (Fig. 6.8a) and molar ratios of DSi, DIP and DIN when the later are compared to phytoplankton needs (Fig. 6.8b). The DSi stock maintains a value of 15.7 mmole m^{-3}, *i.e.* close to the reference given for Atlantic waters (Radach *et al.*, 1995), up to 1980 after which it gradually decreases to 13.4 mmole m^{-3} in 2000. The simulated evolution of winter DIN and DIP concentrations parallels that shown for their inputs (Fig. 6.7 & 6.8). For both DIN and DIP, Figure 6.8 shows an exponential increase after 1960 reaching in 1985 a maximum value (DIP: 2.75 mmole m^{-3}; DIN: 47.8 mmole m^{-3}; Fig. 6.8a). The simulated trends of DIN and DIP winter concentrations diverge after 1985 with DIN increasing slowly up to 48.5 mmole m^{-3} in 2000 and DIP decreasing gradually up to 50% of the maximum 1985 value in 2000 (Fig. 6.8a). These contrasted trends have an impact on the qualitative nutrient status of the BCZ which, when compared to the nutrient requirement of coastal diatoms (molar N:Si:P=16:16:1), suggests a Si limitation between 1960 and 1985 but P limitation after this period (Fig. 6.8b). DIN is always in excess, especially after 1990 when N:P simulated values are above 25 (Fig. 6.8b).

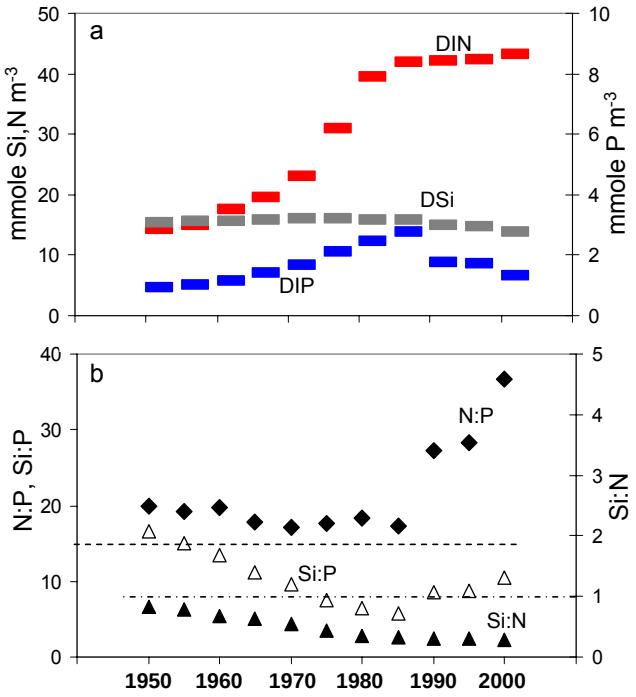

Figure 6.8. R-MIRO simulations of BCZ winter nutrient concentrations (a) and their elemental ratio (b) over the 1950-2000 period.

50 year evolution of phytoplankton blooms in BCZ

Phytoplankton blooms are usually defined as maximum concentration reached and/or as bloom-integrated biomass. Here we choose maximum biomass reached in spring as an indicator of an ecological imbalance between phytoplankton and zooplankton development. The analysis of R-MIRO simulations of phytoplankton bloom dynamics in the BCZ over the 1950-2000 period (not shown) indicates that nutrient enrichment has no effect on the timing of the spring diatom-*Phaeocystis* colonies-summer diatoms succession but does have an effect on their relative abundance. The long term evolution of R-MIRO spring maxima of bulk phytoplankton (Chl *a*; Fig. 6.9a), spring and summer diatom and *Phaeocystis* colony biomass (Fig. 6.9b) are then analyzed in comparison with concomitant changes in nutrient enrichment (Fig. 6.8). Clearly, phytoplankton biomass increases in response to DIN and DIP enrichment (r^2=0.99) up to 1985 when a Chl *a* maxima three times higher than in 1950 is simulated (Fig. 6.9a). After 1985, model results show significant decreases (30% over 15 years) of total biomass which can be related to DIP decrease (Fig. 6.8a, Fig. 6.9a).

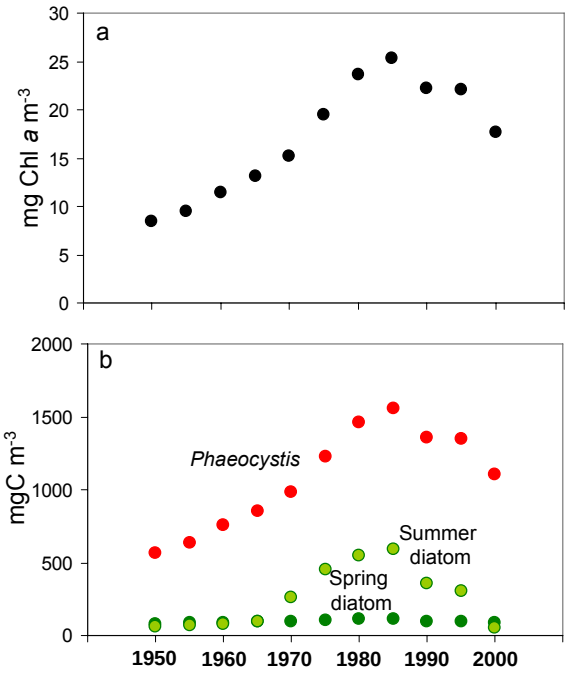

Figure 6.9. R-MIRO simulations in BCZ of maximum spring phytoplankton expressed in Chl *a* (a) and diatoms (spring and summer) and *Phaeocystis* colony biomass (b) over the 1950-2000 period.

Curiously the maximum biomass reached by spring diatoms seems little modified by increased nutrient enrichment which affects both *Phaeocystis* colonies and summer diatoms (Fig. 6.9b). After 1960, the maximum biomasses of summer diatoms and *Phaeocystis* colonies increase in parallel and both reach their maxima (~one order of magnitude higher than in 1950; Fig. 6.9b) in 1985 when DIN and DIP enrichment is maximum (Fig. 6.8a). Then, summer diatom and *Phaeocystis* colony maxima decrease in parallel apparently correlated with the simulated DIP decrease. In 2000 summer diatoms don't bloom and are maintained at biomass less than in 1950. In comparison, the decrease of *Phaeocystis* colonies is of little significance, *i.e.* 30% between 1985 and 2000 (Fig. 6.9b). Altogether this suggests that a well-balanced DIN and DIP enrichment is beneficial to *Phaeocystis* colonies and summer diatoms while spring diatoms remain unaffected; the imbalanced decreases of DIP and DIN in favor of elevated N:P ratios (>25) limit the growth of summer diatoms more than *Phaeocystis* colonies that are maintained at high biomass.

6.4 Support for eutrophication assessment and mitigation in the BCZ

6.4.1 Disturbance indicators due to eutrophication

Any assessment or mitigation of eutrophication requires the definition of reference indicators or thresholds to undesirable perturbation. There exists no unambiguous and universal indicator of disturbance due to marine eutrophication because of the high diversity of coastal ecosystems and their sensitivity to a sustained nutrient pressure. Simple bulk indicators such as winter stock of nutrients and maximum Chl *a* can be defined regionally in comparison with reference conditions. The latter are difficult to set both because unperturbated marine ecosystems are mostly inexistent and monitoring data are generally limited to the past 50 years, *i.e.* often too short to properly define reference conditions. In the scope of the OSPAR Strategy to combat eutrophication (2005), Belgium has provided 'best educated guesses' for bulk indicators of eutrophication problems in the BCZ. These thresholds are defined on basis of the winter concentrations of DIN (15 mmole m^{-3}), DIP (0.8 mmole m^{-3}) and molar DIN:DIP (24) and maximum Chl *a* (15 mg m^{-3}). *Phaeocystis* is cited as an indicator species but there is no clear consensus on the definition of a critical value in the OSPAR document. Most suggestions are based on the presence during 30 consecutive days of a number of cells (10^6 or 10^7 cells L^{-1}) which, from an ecological point of view, is of little significance as only colony forms are undesirable. Recently Lancelot *et al.* (in press) suggest a more ecologically- based criterion considering that most undesirable effects reported to *Phaeocystis* are due to its ability to form colonies which grow in size during their development and rapidly exceed the filtering capability of zooplankton (Lancelot *et al.*, 1994). On this basis, a *Phaeocystis* colony reference value of 150 mg C m^{-3} can be proposed for the BCZ, estimated from field observations of maximum biomass reached by zooplankton grazable *Phaeocystis* colonies (maximum diameter of 400 µm; Weisse *et al.*, 1994).

6.4.2 The geographical limits of BCZ waters affected by eutrophication

The geographical limits of problem (PA) and potential- (PPA) and non-problem (NPA) maritime areas in terms of eutrophication can be determined based on 3D-MIRO&CO simulations in winter and in spring and making use of OSPAR criteria for winter DIN, DIP, DIN:DIP and maximum Chl *a*. Figure 6.10 shows for each of above criteria the geographical frontier between eutrophied and non-eutrophied waters suggested by 3D-MIRO&CO simulations for the 1993-2000 period. Clearly the simulated area affected by eutrophication differs between criteria being more extended when using the winter nutrient criterion than the Chl *a* one (Fig. 6.10). Combining this allows to propose for the first time geographical limits to PA, PPA and NPA for not only the BCZ but also the 3D-MIRO&CO domain in general (Fig. 6.11). Clearly, following the OSPAR criteria, the eutrophication problem in the 3D-MIRO&CO domain is limited to nearshore waters in the vicinity of river mouths (Seine, Scheldt, Rhine/Meuse and Thames). PPA extends the affected area offshore showing a band parallel to the coast and pointing 70% of the BCZ area as PA and PPA with respect to eutrophication (Fig. 6.11a; Fig. 6.12). Interestingly enough the use of the *Phaeocystis* colony threshold of 150 mgC m^{-3} suggests that non-grazable *Phaeocystis* colonies are invading the whole BCZ in spring (Fig. 6.11b).

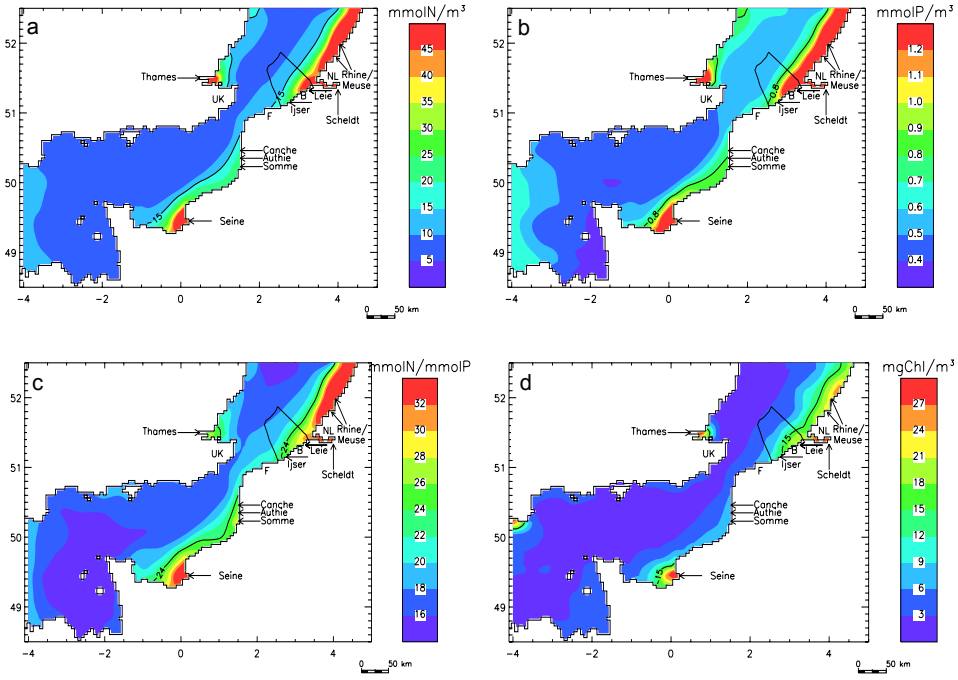

Figure 6.10. Eutrophication assessment based on 3D-MIRO&CO simulations of DIN (a), DIP (b), DIN:DIP (c) and Chl *a* (d) and making use of OSPAR criteria. (black line parallel to the coast)

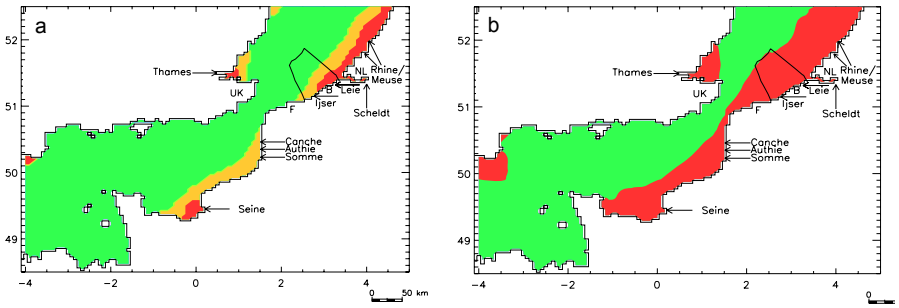

Figure 6.11. Eutrophication status of the 3D-MIRO&CO domain and the BCZ based on the combination of maps shown on Figure 6.10 with red: PA, orange: PPA, green: NPA (a) and geographical distribution of grazable (green) and non-grazable (red) *Phaeocystis* colonies in spring (b).

6.4.3 Mitigation

Which nutrient reduction needs to be targeted?

The first way to approach eutrophication mitigation with ecological models consists in the identification of the optimal nutrient reduction [which nutrient(s) to reduce and by how much?] needed for decreasing substantially eutrophication. Sensitivity tests can be made on river inputs, comparing results obtained for winter nutrients and Chl *a* maxima with OSPAR targets. The nutrient reduction needed to limit the geographical extension of undesirable eutrophication in BCZ can therefore be estimated through 3D-MIRO&CO model scenarios with changing river nutrient inputs.

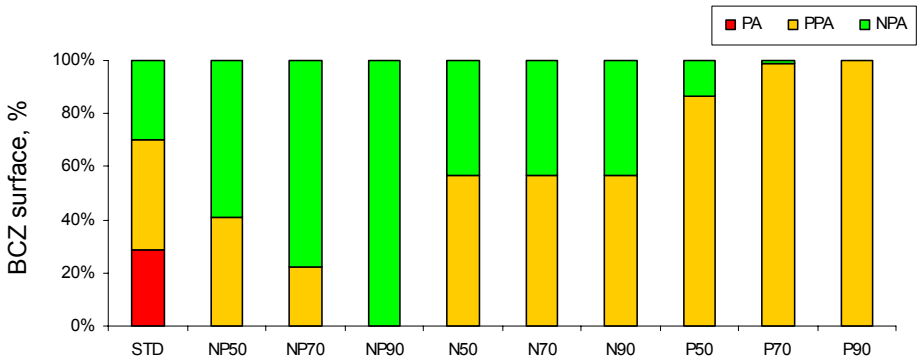

Figure 6.12. Changing BCZ areas (in % of the total BCZ surface) affected (PA), potentially affected (PPA) and non-affected (NPA) by eutrophication after nutrient reduction (50, 70, 90% of N; 50, 70, 90% of P and 50, 70, 90% of NP).

Figure 6.12 shows for each nutrient reduction tested (50, 70 and 90% N, P and N+P) the predicted decrease in the BCZ area affected or potentially affected by eutrophication. Clearly all the 50% nutrient reduction scenarios eliminate PA in the BCZ while a full recovery of the latter is obtained when both N and P are decreased by 90% (Fig. 6.12). As a general trend the best mitigation of eutrophication in BCZ is obtained when both N and P are decreased. The reduction of the only P predicts PPA for almost the whole BCZ surface (Fig. 6.12) explained by the elevated N:P (>24) resulting of P reduction while high N is maintained. The N reduction scenarios predict a similar distribution of NPA and PPA areas in BCZ whatever the N reduction level is, because the limit between PPA and NPA is here determined by DIP distribution and is not affected by N reduction scenarios

What is feasible?

Best nutrient reduction measures suggested by model sensitivity analysis are not necessarily feasible either technically or due to socio-economical constraints. As most nutrient reduction measures are implemented on the watershed and concern waste water treatment, industrial emissions and agricultural practices, the R-MIRO model is an appropriate tool for assessing the efficiency of ongoing or planned nutrient reduction measures. Figure 6.13 shows R-MIRO simulations of nutrient inputs to the BCZ, winter nutrient enrichment and maximum phytoplankton biomass reached in the BCZ obtained for 2015 after careful implementation of measures on waste water treatment and agricultural practices decided by Belgium and France in the scope of the Water Framework Directive of the European Union. These simulations are compared with the current situation illustrated by year 2000 simulations as well as a pristine scenario considering that the whole North Sea watershed is covered by forests. Analysis of results shows the efficiency of planned measures for reducing P and N, the latter however to a less extent. Interestingly DIP inputs simulated in 2015 are close to values obtained for the pristine reference. This is not found for DIN inputs which remain largely above pristine fluxes (Fig. 6.13). The reduction of nutrient inputs to the BCZ reached in 2015 is reflected in the nutrient status of the BCZ (Fig. 6.13). In 2015 DIP enrichment is expected to have been counteracted yielding a concentration in the BCZ of 0.9 mmole P m^{-3} i.e close to the OSPAR target of 0.8 mmole P m^{-3} and the pristine reference of 0.7 mmole P m^{-3}. The N reduction achieved in 2015 is largely insufficient with a winter DIN concentration of 43.6 mmole N m^{-3}, *i.e.* above the OSPAR target of 15 mmole N m^{-3} and 5 times higher than the pristine value (9.8 mmole N m^{-3}). This unbalanced nutrient reduction has dramatic consequences for the N:P ratio which reaches values as high as 46 (not shown) *i.e.* well above the OSPAR threshold of 24. The nutrient reduction reached in 2015 has positive feedbacks on the maxima reached by phytoplankton (Chl *a*), diatom and *Phaeocystis* colony biomass (Fig. 6.13). It is interesting to observe that, while the bulk phytoplankton target of 15 mg Chl *a* m^{-3} recommended by OSPAR is well achieved in 2015, the simulated decrease of *Phaeocystis* colony biomass is very disappointing and well above the ecologically-based criterion of 150 mg C m^{-3} (Fig. 6.13). The DIP reduction mostly affects summer diatoms which reach an annual maximum lower than under pristine conditions (Fig. 6.13). These simulations indicate that a bulk indicator of ecosystem change such as

maximum Chl *a* is not sufficient for appraising the ecosystem health of the BCZ. A *Phaeocystis* indicator and/or an unbalanced N:P winter ratio appear necessary.

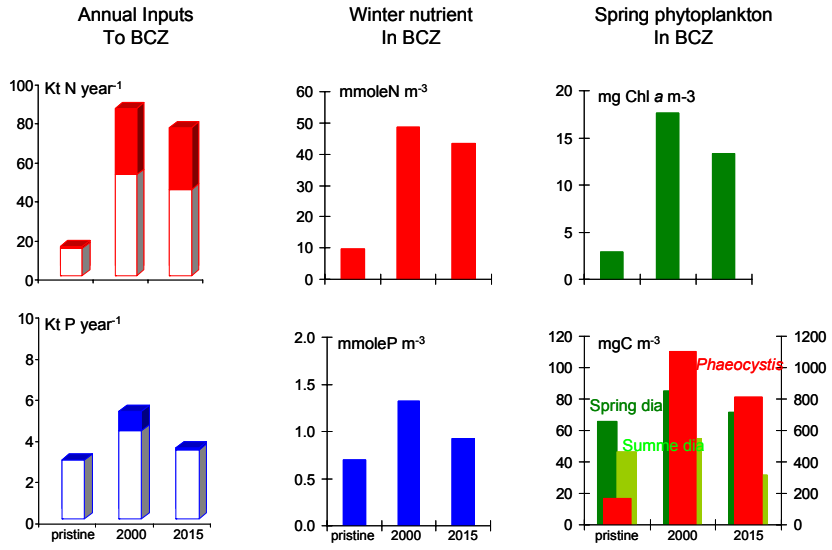

Figure 6.13. R-MIRO simulations of annual N and P inputs to BCZ (left panel; filled block: Scheldt; open block: Atlantic waters+Seine); winter N and P enrichment in BCZ (middle panel) and maximum phytoplankton biomass reached in spring (right panel) obtained for the pristine reference, the current situation (2000) and the 2015 projection.

6.5 Concluding remarks and perspectives

The sustained modeling effort in Belgium has provided mathematical models (0D-MIRO and 3D-MIRO&CO) that can be used for assessing eutrophication problems and addressing issues that cannot be resolved based on field studies. Being based on the current scientific knowledge, these models have their own limitations and need to be continuously developed. As pointed here the obtained simulation of *Phaeocystis* colonies in the Baie de Seine, an area where colonies have never been reported, will not be understood before a full resolving of the *Phaeocystis* life cycle and especially the identification of factors triggering the formation of colonies. In this way 0D-MIRO and 3D-MIRO&CO are complementary to field studies and cannot be substituted to them.

The validation of ecological models is recognized as critical for their reliable use in policy support (Radach & Moll, 2006), yet validation data is extremely sparse compared to the space, time and parameter coverage of these models. For most parameters, including nutrients and phytoplankton species, data is available only from a limited number of seaborne cruises and/or a single weekly

monitoring location (*e.g.* Rousseau, 2000). For secondary trophic levels such as zooplankton, biomass data are even sparser. Good spatial and reasonable temporal coverage is provided by optical remote sensing but the parameter measured, Chl *a* concentration, is not a model state variable and gives no indication of the species composition of the phytoplankton community. Moreover, there are concerns about satellite chlorophyll data quality in coastal waters with high non-algae particle concentration or coloured dissolved organic matter absorption (Ruddick *et al.*, 2008). In the future, data for model validation should become more extensive. In this respect automated flow cytometer instruments could provide unparalleled temporal resolution of phytoplankton species composition. Satellite remote sensing data quality and quantity will improve considerably giving a reliable and almost complete description of surface Chl *a* concentrations. Combination of these two technologies and/or the possible improvement of remote sensing algorithms and hyperspectral sensors to discriminate between different phytoplankton species would greatly enhance the potential for model validation.

When coupled to the RIVERSTRAHLER model, a model calculating nutrient delivery to the sea as a function of change in land use and economical activity, these models can provide to decision makers a way of testing and evaluating the results of planned measures for nutrient reduction.

6.6 References

Billen G., Garnier J. and P. Hanset. 1994. Modelling phytoplankton development in whole drainage networks: The RIVERSTRAHLER model applied to the Seine river system. Hydrobiologia 289: 119-137

Billen G., Garnier J., Deligne C. and C. Billen. 1999. Estimates of early industrial inputs of nutrients to river systems : implication for coastal eutrophication. The Science of the Total Environment 243/244: 43-52

Billen G., Garnier J., Ficht A. and C. Cun. 2001. Modeling the response of water quality in the Seine river estuary to human activity in its watershed over the last 50 years. Estuaries 24(6B): 977-993

Billen G., Garnier J. and V. Rousseau. 2005. Nutrient fluxes and water quality in the drainage network of the Scheldt basin over the last 50 years. Hydrobiologia 540: 47-67

Breton E., Rousseau V., Parent J.Y., Ozer J. and C. Lancelot. 2006. Hydroclimatic modulation of diatom/*Phaeocystis* blooms in the nutrient-enriched Belgian coastal waters (North Sea). Limnology and Oceanography 51(3): 1-14

Cadée G.C. and J. Hegeman J. 1991. Historical phytoplankton data of the Marsdiep. Hydrobiological Bulletin 24: 111-118

European Union's Water Framework Directive. 2000. Official Journal of the European Communities 2000/60/CE

Garnier J., Billen G. and M. Coste. 1995. Seasonal succession of diatoms and chlorophyecae in the drainage network of the River Seine : Observations and modelling. Limnology and Oceanography 40: 750-765

Gieskes W.W.C., Leterme S.C., Peletier H., Edwards M. and P.C. Reid. 2007. *Phaeocystis* colony distribution in the North Atlantic since 1948 and interpretation of long-term changes in the *Phaeocystis* hotspot in the North Sea. Biogeochemistry 83: 49-60

Gypens N., Lacroix G. and C. Lancelot. 2007. Causes of variability of the diatoms and *Phaeocystis* blooms in the Belgian coastal waters between 1989 and 2003: a model study. Journal of Sea Research 57(1): 19-35

Hurrell J. W. 1995. Decadal trends in the North Atlantic Oscillation: regional temperatures and precipitation. Science 269: 676-679

Lacroix G., Ruddick K., Ozer J. and C. Lancelot. 2004. Modelling the impact of the Scheldt and Rhine/Meuse plumes on the salinity distribution in Belgian waters (southern North Sea). Journal of Sea Research 52(3): 149-163

Lacroix G., Ruddick K., Park Y., Gypens N. and C. Lancelot. 2007a. Validation of the 3D biogeochemical model MIRO&CO with field nutrient and phytoplankton data and MERIS-derived surface chlorophyll a images. Journal of Marine Systems 64(1-4): 66-88. doi: 10.1016/j.jmarsys.2006.01.010

Lacroix G., Ruddick K., Gypens N. and C. Lancelot. 2007b. Modelling the relative impact of rivers (Scheldt/Rhine/Seine) and Channel water on the nutrient and diatoms/*Phaeocystis* distributions in Belgian waters (Southern North Sea). Continental Shelf Research 27: 1422-1446. Doi: 10.1016/j.csr.2007.01.013

Lancelot C., Billen G., Sournia A., Weisse T., Colijn F., Veldhuis M., Davies A. and P. Wassman. 1987. *Phaeocystis* blooms and nutrient enrichment in the continental coastal zones of the North Sea. Ambio 16 : 38-46

Lancelot C., Wassmann, P. and H. Barth. 1994. Ecology of *Phaeocystis*-dominated ecosystems. Journal of Marine Systems 5(1): 1-4

Lancelot C. 1995. The mucilage phenomenon in the continental coastal waters of the North Sea. In: The Science of the Total Environment, Elsevier 165: 83-112

Lancelot C., Keller M., Rousseau V., Smith W.O.Jr and S. Mathot. 1998. Autoecology of the Marine Haptophyte *Phaeocystis* sp. In: NATO Advanced Workshop on the physiological ecology of Harmful Algal Blooms. NATO-ASI Series. Anderson D.A., Cembella A.M., Hallegraef G. (Eds). Springer-Verlag Berlin Series G : Ecological Science 41: 209-224

Lancelot C., Spitz Y., Gypens N., Ruddick K., Becquevort S., Rousseau V., Lacroix G. and G. Billen. 2005. Modelling diatom and *Phaeocystis* blooms and nutrient cycles in the Southern Bight of the North Sea: the MIRO model. Marine Ecology Progress Series 289: 63-78

Lancelot C., Gypens N., Billen G., Garnier J. and Roubeix V. 2007. Testing an integrated river-ocean mathematical tool for linking marine eutrophication to land use: The *Phaeocystis*-dominated Belgian coastal zone (Southern North Sea) over the past 50 years. Journal of Marine Systems 64(14): 216-228

OSPAR. 2005. Common Procedure for the Identification of the Eutrophication Status of the OSPAR maritime area, OSPAR agreement 2005-3.

Owens N.J.P, Cook D., Colebrook M., Hunt H. and P.C. Reid. 1989. Long term trends in the occurrence of *Phaeocystis* sp. in the North-East Atlantic. Journal of the Marine Biological Association of United Kingdom 69: 813-821

Radach G, Pätsch J, Gekeler J and K. Herbig. 1995. Annual cycles of nutrients and chlorophyll in the North Sea. Ozeanographie berichte 20, Zentrum für Meeres- und Klimaforschung

Radach G. And A. Moll. 2006. Review of three-dimensional ecological modelling related to the North Sea shelf system. Part 2: Model validation and data needs. Oceanogr. Mar. Biol. Ann. Rev. 44: 1-60

Rousseau V., Leynaert A., Daoud N. and C. Lancelot. 2002. Diatom succession, silicification and silicic acid availability in Belgian coastal waters (Southern North Sea). Marine Ecology Progress Series 236: 61-73

Rousseau V., Breton E., De Wachter B., Beji A., Deconinck M., Huijgh J., Bolsens T., Leroy D., Jans S. and C. Lancelot. 2004. Identification of Belgian maritime zones affected by eutrophication (IZEUT). Towards the establishment of ecological criteria

for the implementation of the OSPAR Common Procedure to combat eutrophication. Belgian Science Policy, Brussels, Final report 77 pp

Rousseau V., Park Y., Ruddick K., Vyverman W., Jans S. and C. Lancelot. 2008. Phytoplankton blooms in response to nutrient enrichment. In: Current Status of Eutrophication in the Belgian Coastal Zone. Rousseau V., Lancelot C. and D. Cox (Eds). Presses Universitaires de Bruxelles, Bruxelles, pp. 45-59

Ruddick K. and G. Lacroix. 2008. Hydrodynamics and meteorology of the Belgian Coastal Zone. In: Current Status of Eutrophication in the Belgian Coastal Zone. Rousseau V., Lancelot C. and D. Cox (Eds). Presses Universitaires de Bruxelles, Bruxelles, pp. 1-15

Ruddick K., Lacroix G., Lancelot C., Nechad B., Park Y., Peters S., and B. van. Mol. 2008. Optical remote sensing of the North Sea. In: Remote sensing of the European Seas. Barale V. and Gade M. (Eds). Springer-Verlag, pp. 79-90

Weisse T., Tande K., Verity P., Hansen F. and W.W.C. Gieskes. 1994. The trophic significance of *Phaeocystis* blooms. In: Ecology of *Phaeocystis*-dominated ecosystems. Lancelot C., Wassmann, P. and H. Barth (Eds). Journal of Marine Systems 5: 67-79

CHAPTER 7

Carbon dynamics in the eutrophied Belgian Coastal Zone

Nathalie Gypens[1] and Alberto Vieira Borges[2]

[1] Université Libre de Bruxelles (ULB), Ecologie des Systèmes Aquatiques (ESA), CP221, boulevard du Triomphe, B-1050 Brussels, Belgium
[2] Université de Liège, MARE, Unité d'Océanographie Chimique, Institut de Physique B5, B-4000 Sart Tilman, Belgium

7.1 Carbon cycle in coastal waters

Net autotrophic ecosystems, where gross primary production (GPP) exceeds community respiration (CR), decrease carbon dioxide (CO_2) in the surrounding waters, while net heterotrophic systems, where GPP<CR, enrich the water in CO_2. Net ecosystem production (NEP = GPP-CR) is then one of the main drivers of the exchange of CO_2 between aquatic systems and the atmosphere. Nevertheless, in coastal environments, the link between the exchange of CO_2 with the atmosphere and the ecosystem metabolic status is not always direct (Gattuso *et al.*, 1998; Borges, 2005; Borges *et al.*, 2006). Besides NEP, the net CO_2 flux between the water column and the atmosphere is modulated by other factors such as other biogeochemical processes (*e.g.* $CaCO_3$ precipitation/dissolution), temperature and hydrodynamics (horizontal advection, down and up-welling of waters with different CO_2 concentration, residence time, decoupling between organic carbon production and degradation within the water column).

Eutrophication manifests as a general increase of phytoplankton production and sometimes changes in planktonic composition in coastal zones (Billen *et al.*, 1991; Cloern, 2001). The effect of eutrophication on NEP and air-water CO_2 fluxes has been investigated with the one-box global Shallow-water Ocean Carbonate Model (SOCM; Andersson & Mackenzie, 2004). This model simulates a decrease of the CO_2 emission from the coastal ocean to the atmosphere since pre-industrial times and a neutral flux at present time (Andersson & Mackenzie, 2004; Mackenzie *et al.*, 2004; 2005). This evolution is explained by the combination of atmospheric CO_2 rising and NEP enhancement by the increased discharge of anthropogenic nutrients. Poorly investigated at the regional and local scale, the carbon dynamics in eutrophied coastal ecosystems is discussed in this chapter based on a synthesis of carbon

measurements and model simulations obtained in the Scheldt river plume, the Belgian Coastal Zone (BCZ) and adjacent marine waters.

7.2 Present-day carbon cycle in the Scheldt river plume

Figure 7.1 shows the time series of the partial pressure of CO_2 (pCO_2), air-water CO_2 fluxes (FCO_2) and NEP obtained in front of the Zeebrugge harbour between 2001 and 2004. As suggested by Borges and Frankignoulle (1999; 2002), this station is influenced by Scheldt waters and the observed carbon dynamics is representative of the Scheldt river plume. As shown on Figure 7.1a, surface waters are under-saturated in CO_2 with respect to atmospheric equilibrium during spring and over-saturated during the rest of the year with the maximum over-saturation observed in late-summer. The NEP seasonal evolution shows a transient but pronounced autotrophic period occurring every spring but with a different timing (early April in 2001 and 2002, mid April in 2003 and 2004) and amplitude (maximal values ranging from 134 mmol m^{-2} d^{-1} in 2004 to 269 mmol m^{-2} d^{-1} in 2003; Fig. 7.1c). This autotrophic period can be ascribed to the diatom-*Phaeocystis* spring bloom (*e.g.* Rousseau *et al.*, 2002; 2008). It is followed by a marked heterotrophic period corresponding to zooplankton grazing (Daro *et al.*, 2008) and bacterial degradation of the organic matter produced during spring (Rousseau *et al.*, 2002). In summer, a net autotrophic event was recorded in 2001 and 2003, and a balanced metabolic status in 2002 and 2004 (Fig. 7.1c). This variability might be explained by the year-to-year fluctuation in time and amplitude of summer phytoplankton growth (Breton *et al.* 2006; Rousseau *et al.*, 2008). Late summer is clearly characterized by net heterotrophy that decreases during fall, and a nearly balanced metabolic status is observed in winter.

At the annual scale the nearshore waters behave as a net heterotrophic system in 2001, 2002 and 2004, but autotrophic in 2003 (Table 7.1). Net heterotrophy of the Scheldt estuarine plume has been previously shown by Borges and Frankignoulle (2002) based on a simple organic carbon input/output budget. This latter suggests that CO_2 emission to the atmosphere observed in the nearshore waters is only partly due to the input of CO_2 from the Scheldt. Therefore the net heterotrophy estimated for the nearshore waters must be subsidized by external inputs of organic carbon that can originate from either coastal tributaries and/or from the Scheldt.

The potential degradation of the organic matter discharged into the BCZ by the Scheldt, estimated to 0.8-2 (Wollast, 1976) and 0.7-1.8 mol C m^{-2} yr^{-1} (Wollast, 1983), would correspond to a carbon flux of the same order of magnitude than the NEP values computed here (Table 7.1). These figures are however higher than those provided by Borges and Frankignoulle (2002) and based on the Soetaert and Herman (1995)'s estimations of organic matter discharged by the Scheldt, *i.e.* between 0.3 and 0.6 mol C m^{-2} yr^{-1} depending on the surface area of the Scheldt plume.

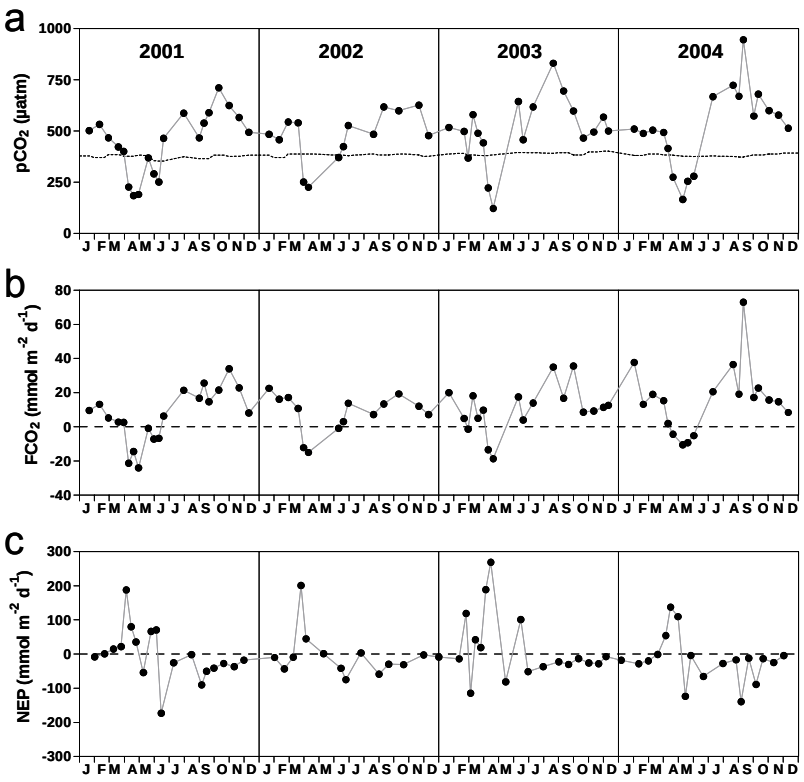

Figure 7.1 Time series of pCO_2 (a), FCO_2 (b) and NEP (c) in the Scheldt plume at a fixed station off the Zeebrugge harbour. NEP is estimated from a mass balance of dissolved inorganic carbon (Borges *et al.*, 2008).

Table 7.1. Scheldt winter freshwater discharge (Q) computed as the average of January and December of the previous year, and annual averages of pCO_2, air-sea gradient of pCO_2 (ΔpCO_2), FCO_2 and NEP at a fixed station off the Zeebrugge harbour.

	Q $m^3\ s^{-1}$	*pCO_2* *µatm*	*ΔpCO_2* *µatm*	*FCO_2* *mol $m^{-2}\ yr^{-1}$*	*NEP* *mol $m^{-2}\ yr^{-1}$*
2001	*348*	*481*	*107*	*3.6*	*-4.2*
2002	*302*	*480*	*97*	*3.2*	*-3.8*
2003	*393*	*527*	*136*	*4.6*	*2.4*
2004	*210*	*533*	*153*	*6.6*	*-5.7*

The pronounced spring (Fig.7.1c) and annual (Table 7.1) NEP computed in 2003 could be due to the stronger Scheldt discharge in winter (393 $m^3 s^{-1}$; Table 7.1) The latter increases the delivery of nutrients from diffuse source but not of organic matter from point source stimulating therefore the GPP without modifying heterotrophy sustained by allochthonous organic carbon. Supporting this, Gypens *et al.* (2004) showed in a model study comparing two contrasted years that annual GPP in the BCZ could increase by about 27% for an increase of wintertime fresh water discharge from about 100 to 350 $m^3 s^{-1}$. Interestingly, despite their net autotrophic status in 2003, the nearshore coastal waters were estimated to act as net source of CO_2 for the atmosphere (Table 7.1). This confirms that a fraction of this CO_2 emission is sustained by CO_2 inputs from the Scheldt (Borges & Frankignoulle, 2002; Schiettecatte *et al.*, 2006) that would also be expected to increase with freshwater discharge.
The stronger annual heterotrophy computed for 2004 than for 2001 and 2002 could be due to a transient accumulation of part of the excess organic matter produced in 2003. Hence, we hypothesize that part of the non-steady accumulation of organic matter from 2003 to 2004 occurred in the sediments. Sedimentation of organic matter is important in the BCZ in agreement with the fact that nearshore sediments in the BCZ are exceptionally rich in organic carbon compared to the rest of the North Sea (Wollast 1976; de Haas *et al.* 2002; Vanaverbeke *et al.*, 2008).

7.3 Present-day annual budget of NEP and FCO_2 along the Scheldt river-Southern Bight of the North Sea continuum

Based on the present results obtained in nearshore waters influenced by the Scheldt, those of Gazeau *et al.* (2005) for the Scheldt estuary, and those of Schiettecatte *et al.* (2007) for the Southern Bight of the North Sea (SBNS), we established an annual budget of NEP and FCO_2 along a continuum from the Scheldt estuary to the SBNS (Fig. 7.2).

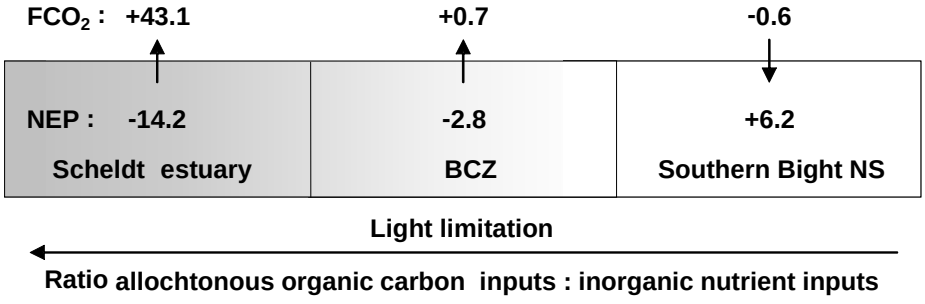

Figure 7.2. Annual budgets of NEP and FCO_2 along a continuum from the Scheldt estuary to the SBNS (fluxes in mol $m^{-2} d^{-1}$), adapted from Schiettecatte (2006).

The figures obtained are in agreement with the conceptual model of Borges *et al.* (2006) whereby estuaries are strong sources of CO_2 sustained by a net heterotrophic metabolism, while temperate continental shelves act as sinks of CO_2 sustained by efficient carbon export. Also, estuaries are effective reactors for organic matter mineralisation, hence strong sources of CO_2 and inorganic nutrients to the adjacent coastal ocean that acts as a sink for atmospheric CO_2 (at temperate latitudes). Finally, this also confirms the role of physical settings in determining the auto or heterotrophic status and direction of air-sea CO_2 fluxes in river plumes, whereby well mixed systems do not export efficiently organic matter and act as sources of CO_2, while stratified river plumes export organic matter across the pycnocline and act as sinks of CO_2 (Borges, 2005).

7.4 Past evolution of carbon dynamics in the BCZ in relation to eutrophication and increased atmospheric CO_2

7.4.1 Effect of eutrophication on NEP and air-sea CO_2 fluxes

The impact of changing human activities on the watershed and increased atmospheric CO_2 over the past 50 years on the role as sink or source for atmospheric CO_2 of the BCZ was investigated using a coupled river-coastal model. The R-MIRO-CO_2 model results from the off-line coupling between two biogeochemical models, the RIVERSTRAHLER river model (*e.g.* Billen *et al.*, 1994) and the marine MIRO model (Lancelot *et al.*, 2005) including a description of the carbonate system (MIRO-CO_2; Gypens *et al.*, 2004). Details on the coupling between RIVERSTRAHLER and MIRO are provided in Lancelot *et al.* (2007). For this application, the R-MIRO-CO_2 model was implemented in a multi-box frame from the Eastern Channel to the Belgian coastal zone (Fig. 6.2). Model simulations were performed using daily wind speed and sea surface temperature and monthly atmospheric CO_2. Nutrient river inputs were provided by the RIVERSTRAHLER model applied to the Seine and Scheldt river systems. RIVERSTRAHLER implementation and description of meteorological forcing and nutrient point and diffuse sources at the scale of the Seine and Scheldt river systems over the past 50 years are reported in respectively Billen *et al.* (2001) and Billen *et al.* (2005). For both basins, the following forcing functions to the model were documented for the period 1950-2000: year-to-year variation of rainfall by 10 days period; land use modifications by 10 year period; changes in annual urban and industrial wastewater discharges by 5 year period. Model results are here shown in terms of historical evolution of nutrient and carbon loads as well as annual air-sea CO_2 fluxes and NEP simulated in the BCZ.

Figure 7.3 shows the evolution of total nitrogen (Ntot), phosphorus (Ptot), dissolved silicate (DSi) and organic carbon annual loads simulated by the RIVERSTRAHLER model for the Seine and the Scheldt rivers between 1951 and 1998. The annual carbon and nutrient fluxes delivered by both rivers show similar trend but the magnitude of the nutrient loads delivered by the Seine is higher than by the Scheldt (about 5, 10 and 3 times respectively, for Ntot, Ptot and DSi). This results from the higher water discharge of the Seine while

nutrient concentrations are similar in both rivers (not shown). However, the organic carbon inputs from the Scheldt are up to three times higher than the Seine loads during the eighties (Fig. 7.3.d).

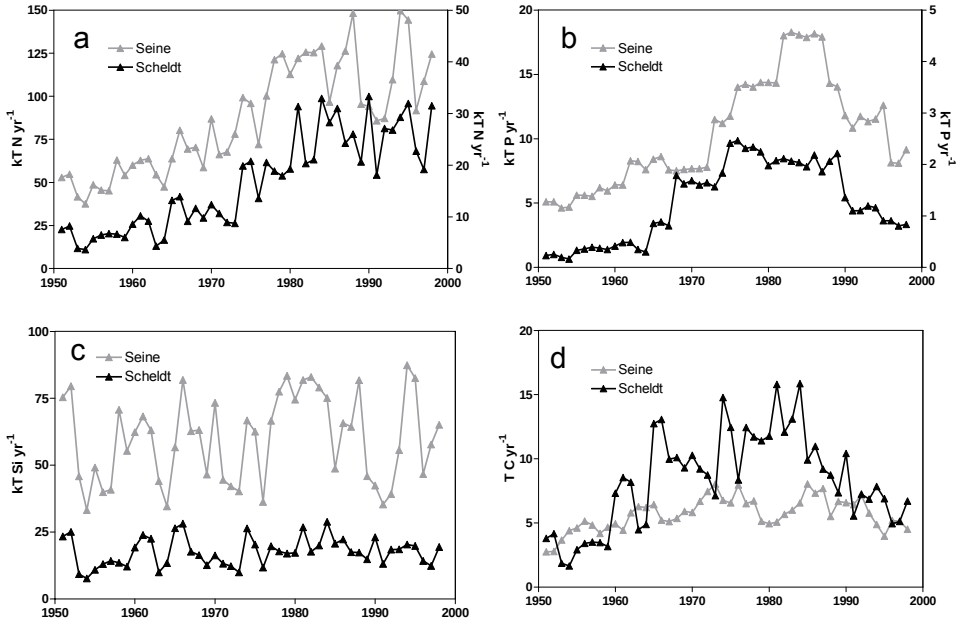

Figure 7.3. Evolution between 1951 and 1998 of Ntot (a), Ptot (b), DSi (c) and organic carbon (d) annual loads from the Seine and the Scheldt. Seine: left scale; Scheldt: right scale.

Although some part of the nutrient and organic carbon loads inter-annual variability can be attributed to the river discharge (not shown), the long-term trend simulated over the past 48 years results from the changing nutrient and carbon emissions to surface water in response to modification of human activities on the watershed. From 1950 to 1965, Ntot, Ptot and DSi loads stay relatively constant both for the Seine and the Scheldt rivers (Fig. 7.3). As a result of the combined effect of increasing leaching of agricultural soils and rising emissions from domestic and industrial activities (Billen *et al.*, 2001; 2005), the annual Ntot fluxes delivered by the Seine show, after 1965, a clear increase up to values greater than 100 kt N yr^{-1} during the 1990's (Fig. 7.3.a). A similar increase is simulated for the Scheldt with annual Ntot loads reaching 30 kt N yr^{-1} in 1990. In parallel, annual Ptot loads from the Seine and the Scheldt increase by a factor 5 between 1965 and 1985 (Fig. 7.3.b). After 1985, P loads progressively decrease until 1998 when values corresponding to those simulated in 1960's are obtained. This decrease results from the removal of PO_4 in washing powders as well as the improved treatment of urban effluents (Billen *et al.*, 2001; 2005). The simulated inter-annual variability of dissolved silicate

(DSi) loads (Fig. 7.3.c) is mainly driven by river discharges (not shown) while the river DSi concentration stays relatively constant. Organic carbon loads, as Ntot and Ptot loads, show, after 1960, a marked increase in response to human development in the watershed before decreasing in the mid-eighties due to the implementation of waste water treatment plants (Fig. 7.3.d).

R-MIRO-CO_2 simulations obtained for the BCZ (Fig. 7.4) show marked historical changes in both NEP and air-sea CO_2 fluxes. Annual NEP shows important inter-annual fluctuations, with annual simulated values ranging between -1.24 and + 0.44 mol C m^{-2} yr^{-1} in respectively 1966 and 1992 (Fig. 7.4). From 1950 to 1967, the BCZ is shown as net heterotrophic with NEP values between -0.68 and -1.24 mol C m^{-2} yr^{-1}. From 1967 to 1982, the BCZ ecosystem is still heterotrophic but the NEP strongly decreases to value near zero (-0.2 mol C m^{-2} yr^{-1}). Over the next ten years (1983-1993), the BCZ is shifted from net heterotrophy to net autotrophy and NEP values of +0.3 mol C m^{-2} yr^{-1} are simulated in 1989 and 1992. After 1993, the system returns to heterotrophy up to the end of the simulated period and NEP values are close to those simulated before 1967 except in 1996 (Fig. 7.4).

The simulated annual air-sea CO_2 fluxes also show important inter-annual fluctuations between 1951 and 1998 (Fig. 7.4). Air-sea CO_2 flux simulated by the model is positive when the flux is directed from the sea to the atmosphere meaning that the BCZ acts as a source for atmospheric CO_2. From 1951 to 1970, the BCZ is clearly releasing CO_2 towards the atmosphere when estimated on an annual basis. The magnitude of this source ranges between 0.03 and 0.5 mol C m^{-2} yr^{-1} without any clear trend. The simulated trend of annual air-sea CO_2 flux decrease to values close to zero between 1970 and 1974 after which it reverses to negative values (Fig. 7.4). From 1975 to 1993, the BCZ is a net sink for atmospheric CO_2 with a maximal value of -0.4 mol C m^{-2} yr^{-1} in 1985. After 1985, the magnitude of the sink gradually decreases and, between 1994 and 1998, the BCZ becomes again a net source of CO_2 excepted in 1996.

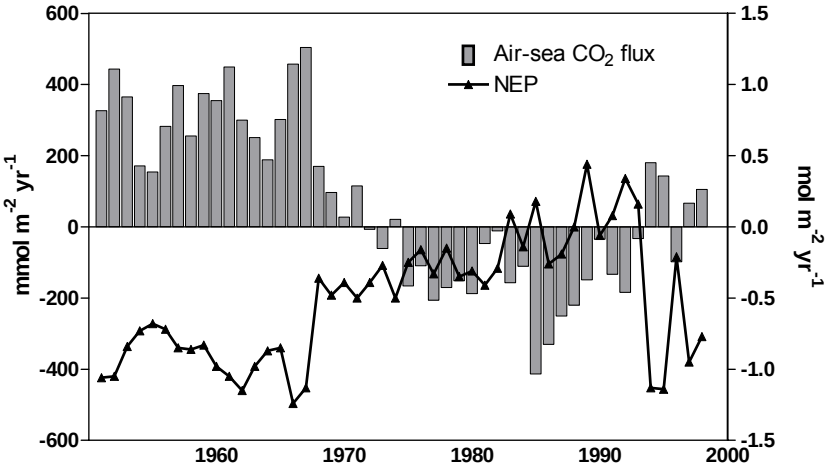

Figure 7.4. Evolution between 1951 and 1998 of annual air-sea CO_2 fluxes (left scale) and NEP (right scale) in the BCZ.

7.4.2 Factors affecting air-sea CO_2 fluxes variability in the eutrophied BCZ

Seawater temperature, wind speed, atmospheric CO_2 and carbon and nutrient loads directly or/and indirectly are constraining air-sea CO_2 fluxes. While wind speed and atmospheric CO_2 only directly affect carbonate chemistry, carbon, nutrients and temperature also indirectly modulate the magnitude of this flux by controlling autotrophic and heterotrophic activities in the water column. The importance of the variability of these forcings for the simulated air-sea CO_2 flux in the BCZ is estimated by comparison to their importance in 1951. The contribution of each forcing to the annual air-sea CO_2 flux variability is investigated based on the comparison between model results obtained using real forcing for the 1951-1998 period and those obtained by running R-MIRO-CO_2 with the 1951 values of either temperature, wind speed, atmospheric CO_2 or carbon and/or nutrient loads for each year of the considered period.

The comparison of annual air-sea CO_2 fluxes simulated using real and 1951 values of temperature, wind speed and atmospheric pCO_2 suggests that the inter-annual variability of these forcings has no significant influence on the magnitude and the direction of the simulated air-sea CO_2 flux for the 1951-1998 period (not shown). Similarly, temperature variability has no major influence on long-term trend of NEP (not shown).

Most of the variability of air-sea CO_2 fluxes computed with the R-MIRO-CO_2 model between 1951 and 1998 is due to river loads (Fig. 7.5). When compared to the reference simulation, the use of 1951 nutrient and carbon loads for both the Seine and the Scheldt leads to an important modification of the magnitude and the direction of the annual air-sea CO_2 flux. When using 1951 river loads (carbon and nutrients) for each year of the simulated period, BCZ is annually net heterotrophic (not shown) and acts as a source for CO_2 during the whole period. Comparison of annual air-sea CO_2 fluxes obtained when using real and 1951 river loads shows that river loads increase the autotrophy and the sink capacity of the BCZ from 1951 to 1998. The magnitude of this sink stays relatively constant between 1951 and 1967, after what it progressively increases up to 1992 when river loads are maximal. Increase of the sink due to river loads can be related to both N and P load increases. After 1992, the decrease of P loads, in spite of sustained elevated N ones, limits primary production (Lancelot *et al.*, 2007) in the BCZ and the associated air-sea CO_2 sink. This imbalance in N and P delivery explains the simulated CO_2 source from 1993 to 1998.

As a general pattern, the simulated magnitude of air-sea CO_2 fluxes in the BCZ is significantly related to the variations of the nutrient and carbon loads from the Seine and the Scheldt. When comparing the respective effect of Seine and Scheldt loads variability on the air-sea CO_2 flux, the model results evidence a similar impact of both rivers during the 1950's after which the Seine is suggested to have a larger influence on the simulated annual air-sea CO_2 flux in the BCZ.

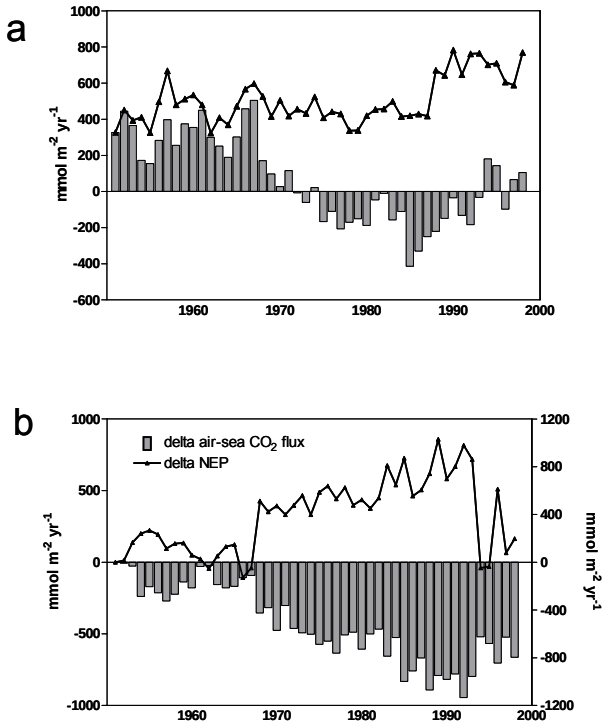

Figure 7.5. Relative contribution of carbon and nutrient river loads to air-sea CO_2 fluxes computed from 1951 to 1998. Comparison of air-sea CO_2 fluxes computed using real forcing (grey bar) and 1951 (triangle) value for Seine and Scheldt river loads (a) and the delta air-sea CO_2 flux (grey bar) and delta annual NEP (triangle) computed as the difference between model results obtained using real and 1951 carbon and nutrient loads (b).

7.5 Conclusions

Using an observation-based approach and a modeling tool, we show that air-water CO_2 fluxes and NEP are subject to strong inter-annual variability in the BCZ mainly driven by riverine inputs of nutrients. We also show that NEP is one of the main drivers of air-water CO_2 fluxes in the BCZ but there is not a perfect match between direction of the CO_2 fluxes and the ecosystem autotrophic or heterotrophic status. Nevertheless, both approaches are converging and suggest that, for present day conditions, the BCZ is net heterotrophic and acts as a source of CO_2 to the atmosphere.

The reconstruction of NEP and air-water CO_2 fluxes over the last 50 years suggests that the BCZ shifted from a CO_2 source during the 1960's and 1970's to a sink during the 1980's and 1990's, explained by increased eutrophication. Due to imbalanced nitrogen to phosphorus loads, the BCZ shifted back to a CO_2 source in the late 1990's. While eutrophication during the 1970's and 1980's leads to quantitative and qualitative phytoplankton changes with undesirable

effects (Lancelot, 1995; Lancelot *et al.*, 2007), our model results suggest that it was accompanied by a strong carbon sink.

This points an important but so far neglected coupling between nutrient regulation and mitigation of the emission of greenhouse gases that must be evaluated jointly in management policies. We also show that the link between nutrient delivery to the coastal zone and atmospheric carbon pumping is complex. Sustained long-term monitoring along inshore-offshore gradients is then required to further unravel and constrain this link and to refine and validate model tools to improve predictions on the future evolution of biogeochemical functioning of the coastal zone and hence guide decision makers and managers.

7.6 References

Andersson A.J. and F.T. Mackenzie. 2004. Shallow-water oceans: a source or sink of atmospheric CO_2? Frontiers in Ecology and the Environment 2(7): 348-353

Billen G., Garnier J. and P. Hanset. 1994. Modelling phytoplankton development in whole drainage networks: The RIVERSTRAHLER model applied to the Seine river system. Hydrobiologia 289: 119-137

Billen G., Garnier J., Ficht A. and C. Cun. 2001. Modeling the response of water quality in the Seine river estuary to human activity in its watershed over the last 50 years. Estuaries 24 (6B): 977-993

Billen G., Garnier J. and V. Rousseau. 2005. Nutrient fluxes and water quality in the drainage network the Scheldt basin over the last 50 years. Hydrobiologia 540: 47-67

Billen G., Lancelot C. and M. Meybeck. 1991. N, P and Si retention along the Aquatic Continuum from Land to Ocean. In: Ocean Margin Processes in Global Change. R.F.C Mantoura, J-M. Martin and R. Wollast (Eds), Dahlem Worshop Reports, Wiley, pp. 19-44

Borges A.V. and M. Frankignoulle. 1999 Daily and seasonal variations of the partial pressure of CO_2 in surface seawater along the Belgian and southern Dutch coastal areas. Journal of Marine Systems 19: 251-266

Borges A.V. and M. Frankignoulle. 2002. Distribution and air-water exchange of carbon dioxide in the Scheldt plume off the Belgian coast. Biogeochemistry 59(1-): 41-67

Borges A.V. 2005. Do we have enough pieces of the jigsaw to integrate CO_2 fluxes in the Coastal Ocean ? Estuaries 28(1): 3-27

Borges A.V., Schiettecatte L.-S., Abril G., Delille B. and F. Gazeau. 2006. Carbon dioxide in European coastal waters. Estuarine, Coastal and Shelf Science 70(3): 375-387

Borges A.V., Ruddick K., Delille B. and L.-S. Schiettecatte 2008. Net ecosystem production and carbon dioxide fluxes in the Scheldt estuarine plume, BMC Ecology, in review

Breton E., Rousseau V., Parent J.-Y.,Ozer J. and C. Lancelot. 2006. Hydroclimatic modulation of diatom/*Phaeocystis* blooms in nutrient-enriched Belgian coastal waters (North Sea). Limnology and Oceanography 51(3): 1401-1409

Cloern, J.E.. 2001. Our evolving conceptual model of the coastal eutrophication problem. Marine Ecology Progress Series 210: 223-253

Daro N., Breton E., Antajan E., Gasparini S . and V. Rousseau. 2008. Do *Phaeocystis* colony blooms affect zooplankton in the Belgian coastal zone? In: Current Status of Eutrophication in the Belgian Coastal Zone. V. Rousseau, C. Lancelot and D. Cox (Eds). Presses Universitaires de Bruxelles, Bruxelles, pp. 61-72

De Haas H., Van Weering T.C.E. and H. De Stigter. 2002. Organic carbon in shelf seas: sinks or sources, processes and products. Continental Shelf Research 22: 691–717

Gattuso J.-P., Frankignoulle M. and R. Wollast. 1998. Carbon and carbonate metabolism in coastal aquatic ecosystems. Annual Review Ecology Systematics 29: 405-433

Gazeau F., Gattuso J.-P., Middelburg J.J., Brion N., Schiettecatte L.-S., Frankignoulle M. and A.V. Borges. 2005. Planktonic and whole system metabolism in a nutrient-rich estuary (the Scheldt estuary). Estuaries 28(6): 868-883

Gypens N., Lancelot C. and A.V. Borges. 2004. Carbon dynamics and CO_2 air-sea exchanges in the eutrophicated coastal waters of the southern bight of the North Sea: a modelling study. Biogeosciences 1(2): 147-157

Lancelot, C., 1995. The mucilage phenomenon in the continental coastal waters of the North Sea. Science Total Environment 165: 83-102

Lancelot C., Spitz Y., Gypens N., Ruddick K., Becquevort S., Rousseau V., Lacroix G. and G. Billen. 2005. Modelling diatom and *Phaeocystis* blooms and nutrient cycles in the Southern Bight of the North Sea: the MIRO model. Marine Ecology Progress Series 289: 63-78

Lancelot C., Gypens N., Billen G., Garnier J. and V. Roubeix. 2007. Testing an integrated river–ocean mathematical tool for linking marine eutrophication to land use: The *Phaeocystis*-dominated Belgian coastal zone (Southern North Sea) over the past 50 years. Journal of Marine Systems 64(14): 216-228

Mackenzie F.T., Andersson A.J., Lerman A. and Ver L.M. 2005. Boundary exchanges in the global coastal margin: Implications for the organic and inorganic carbon cycles. In: The Global Coastal Ocean- Multi-scale Interdisciplinary Processes. Robinson A.R. and K.H. Brink (Eds.), , Harvard University Press, Cambridge. Pp 193-225

Mackenzie F.T., Lerman A. and A.J. Andersson. 2004. Past and present of sediment and carbon biogeochemical cycling models. Biogeosciences 1(1): 11-32

Rousseau V., Leynaert A., Daoud N. and C. Lancelot. 2002. Diatom succession, silicification and silicic acid availability in Belgian coastal waters (Southern North Sea). Marine Ecology, Progress Series 236: 61–73

Rousseau V., Park Y., Ruddick K., Vyverman W., Jans S. and C. Lancelot. 2008. Phytoplankton blooms in response to nutrient enrichment. In: Current Status of Eutrophication in the Belgian Coastal Zone. Rousseau V., Lancelot C. and D. Cox (Eds). Presses Universitaires de Bruxelles, Bruxelles, pp. 45-59

Schiettecatte L.-S. 2006 The carbon cycle in the Southern North Sea Region. PhD Thesis, Université de Liège, Belgium. 130 pp

Schiettecatte L.-S., Gazeau F., Van der Zee C., Brion N. and A.V. Borges. 2006. Time series of the partial pressure of carbon dioxide (2001-2004) and preliminary inorganic carbon budget in the Scheldt plume (Belgian coast waters). Geochemistry, Geophysics, Geosystems G3, Vol. 7 Q06009. doi: 10.1029/2005GC001161

Schiettecatte L.-S., Thomas H., Bozec Y. and A.V. Borges. 2007. High temporal coverage of carbon dioxide measurements in the Southern Bight of the North Sea. Marine Chemistry 106(1-2): 161-173

Soetaert K. and P.M.J. Herman. 1995. Carbon flows in the Westerschelde estuary (The Netherlands) evaluated by means of an ecosystem model (MOSES). Hydrobiologia 311: 247-266

Vanaverbeke J., Franco M., van Oevelen D., Moodley L., Provoost P., Steyaert M., Soetaert K. and M. Vincx. 2008. Benthic responses to sedimentation of phytoplankton on the Belgian Continental Shelf. In: Current Status of Eutrophication in the Belgian Coastal Zone. Rousseau V., Lancelot C. and D. Cox (Eds). Presses Universitaires de Bruxelles, Bruxelles, pp. 73-90

Wollast R. 1976. Transport et accumulation de polluants dans l'estuaire de l'Escaut. In: Project Mer, Rapport Final. Nihoul J.C.J. and R. Wollast (Eds), Vol 10 :196-218. Services du premier Ministre Programmation de la politique scientifique, Belgium

Wollast R. 1983. Interactions in Estuaries and Coastal waters. In: The major Biogeochemical Cycles and their Interactions. Bolin B. and R.B. Cook (Eds), Wiley and Sons, London